الجمهورية الجزائرية الديمقراطية الشعبية
People's Democratic Republic of Algeria
وزارة التعليم العالي والبحث العلمي
Ministry of Higher Education and Scientific Research

جامعة زيان عاشور بالجلفة
Ziane Achour University of Djelfa

كلية العلوم و التكنولوجيا
Faculty of Science and Technology

Department: Electrical Engineering

Order N° : . …. / 2022

Defense authorization N° ……/2022

DOCTORAL THESIS

Doctor of Sciences

Presented by

ELBAR Mohamed

submitted in partial fulfilment of the requirements for the degree of Doctor of Sciences

Branch: Automatic

Specialty: Automatic

Topic

POWER QUALITY ENHANCEMENT TECHNIQUES IN SMART GRID

Supported, on 05 /05 / 2022, before the jury composed of:

Last and first name	Grade	Institution of affiliation	Designation
Benalia M'HAMDI	MCA	Djelfa University	President
Imad MERZOUK	MCA	Djelfa University	Supervisor
Mohamed Mounir REZAOUI	Professor	Djelfa University	Co-Supervisor
Belkacem TOUAL	MCA	Djelfa University	Examiner
Noureddine HANINI	MCA	Medea University	Examiner
Younes CHIBA	MCA	Medea University	Examiner
Abdelaziz RABEHI	MCA	Tissemsilt University	Examiner

Djelfa University, FST - 2022

الجمهورية الجزائرية الديمقراطية الشعبية

People's Democratic Republic of Algeria

وزارة التعليم العالي والبحث العلمي

Ministry of Higher Education and Scientific Research

POWER QUALITY ENHANCEMENT TECHNIQUES IN SMART GRID

THESIS

submitted in partial fulfilment
of the requirements for the degree of
Doctor of Sciences
in Electrical Engineering option Automatic

by

ELBAR Mohamed

Thesis Committee Members:

Benalia M'HAMDI	President
MCA, Djelfa University	
Imad MERZOUK	Supervisor
MCA, Djelfa University	
Mohamed Mounir REZAOUI	Supervisor
Professor, Djelfa University	
Belkacem TOUAL	Examiner
MCA, Djelfa University	
Noureddine HANINI	Examiner
MCA, Medea University	
Younes CHIBA	Examiner
MCA, Medea University	
Abdelaziz RABEHI	Examiner
MCA, Tissemsilt University	

Department of Electrical Engineering
Applied Automation and Industrial Diagnostics Laboratory

Djelfa University, FST - 2022

ACKNOWLEDGEMENTS

First of all, I thank ALLAH for helping me throughout my research and enabling me to finish my thesis.

I would like to thanks my parents, for their unconditional love and support during all my life, which allows me to be the man who I am now. Likewise, I want to thank to the love of my life, for her unlimited love and invaluable support, encouragement and patient throughout these years, which helped me to successfully finish this work.

I am deeply indebted to my supervisor Dr. Imad MERZOUK and Professors Mohamed Mounir REZAOUI whose help, stimulating suggestions and encouragement helped me in all the time of research and writing of this thesis.

I have furthermore to thank Professors Abdellah KOUZOU and Professors Ahmed HAFAIFA for the supervision, valuable hints and outstanding support that he gave me which truly help, progression and smoothness in this thesis. I could not have imagined having a better advisor and mentor for my study.

I also want to say thank to all members of jury. I am particularly grateful to Dr. Noureddine HANINI , Dr. Younes CHIBA, Dr. Abdelaziz RABEHI and Dr. Belkacem TOUAL for accepting to report my thesis and for their advices, comments and questions, and to Dr. Benalia M'HAMDI to participate as president to my Thesis Committee.

In general, I would like to thank all people who encouraged and supported me from both technical and human point of view during these years of intense work. I am thankful for all enriching and valuable conversions, which increased and contributed to my technical maturity and my ideas.

List of Publications

It is certified that the following publication(s) have been made out of the research work that has been carried out for this thesis:

Journal Publications:

- **ELBAR M.**, MERZOUK I., BEALDEL A., REZAOUI M.M., IRATNI A., HAFAIFA A., "Power Quality Enhancement in Four-Wire Systems Under Different Distributed Energy Resource Penetration", in Electrotehnica, Electronica, Automatica (EEA), 2021, vol. 69, no. 4, pp. 50-58, ISSN 1582-5175.
- **ELBAR Mohamed**, MERZOUK Imad, DJEDDI Ahmed Zohir, REZAOUI Mohamed Mounir, HAFAIFA Ahmed, " A PWM Current Controller for Three-Level Neural-Point-Clamped Inverter based active Power Filter for Unbalanced Current Operation", in International Journal of Advanced Studies in Computer Science & Engineering (IJASCSE),2021, vol. 10, ISSUE 10, ISSN 2278 7917
- **Mohamed ELBAR**, Imad MERZOUK, Mohamed Mounir REZAOUI, Noureddine BESSOUS, " Three-Dimensional Pulse Width Modulation Techniques for Three-Phase Four Leg Voltage Source Converters", in Algerian Journal of Signals and Systems (AJSS),Vol.5, Issue.3, September-2020, ISSN:2543-3792-EISSN: 2676-1548

Conference Publications:

- **E. Mohamed**, B. Abdelkader, K. Abdellah and H. Ahmed, "NPC three-level four-legged Shunt Active Power Filter under Non-Sinusoidal Power Supply Conditions," 2019 4th International Conference on Power Electronics and their Applications (ICPEA), 2019, pp. 1-6, doi: 10.1109/ICPEA1.2019.8911161.

ملخـص

في الشبكات الكهربائية, الاضطرابات الناتجة عن الحمولات الكهربائية غير الخطية لها أثر سلبي على التجهيزات الكهربائية. بهدف تحسين نوعية الطاقة الكهربائية, المرشحات ثلاثية الطور ذات ثلاث خطوط أثبتت كفاءتها من حيث تحسين الاضطرابات الناتجة عن الحمولات الكهربائية غير الخطية في الشبكات الكهربائية ذات ثلاث خطوط.

العمل المبين في هذه المذكرة معني خصوصا بالتحكم في المرشحات ثلاثية الطور ذات أربعة خطوط, لقد قمنا بدراسة لمختلف التركيبات ومختلف استراتيجيات التحكم في المرشحات النشيطة المتوازية والذي يسمح بتعويض الاضطرابات و الاستطاعة الردية و كذا فقدان التوازن في الشبكات الكهربائية ذات أربعة خطوط. كل طرق استخراج مراجع التيار قد درست و طبقت ثم قورنت من حيث الفعالية والكفاءة.

كلمات مفتاحية : المرشحات النشيطة,PLL, الحمولات الكهربائية غير الخطية, معوض نشيط.

Abstract

In an electrical network, the harmonic disturbances can strongly degrade customer power quality.

In order to improve power system quality, the three-phase three wire active filter showed its effectiveness in term of compensation of the harmonics generated by the nonlinear loads in a three-wire network.

The work presented in this thesis more particularly relates to the control of three phase four wire active filter, different topologies and control strategies of the parallel active power filters to compensate current harmonics and reactive power in the four-wire electrical network is studied. These references identification methods were studied simulated then, compared on the basis of their effectiveness.

Keys words: Active filter, PLL, Non-Linear load, reactive power, network pollution, Active Compensator

Résumé

Dans un réseau électrique les perturbations harmoniques ont des effets néfastes sur les équipements électriques.

Dans l'objectif d'améliorer la qualité de l'énergie électrique, Le filtre actif triphasé à trois fils a montré son efficacité en termes de compensation des harmoniques générés par les charges non linéaires et/ou déséquilibrées dans un réseau à trois fils.

Le travail présenté dans cette thèse concerne plus particulièrement la commande d'un filtre actif à quatre fils, nous avons abordé, les différentes topologies et stratégies de commande des filtres actifs parallèles en vue de compenser les harmoniques de courants et la puissance réactive susceptible d'apparaître dans les réseaux électriques à quatre fils. Ces méthodes d'identifications ont été simulées puis comparées sur leurs efficacités.

Mots clés : Filtrage actif, PLL, charges non linéaires, énergie réactive, compensateur actif.

Table of Contents

ACKNOWLEDGEMENTS **1**

List of Publications **2**

ABSTRACT **3**

ILLUSTRATIONS **8**

TABLES **10**

1 INTRODUCTION **11**

I Power Quality Problems: . . . 11

I.1 Voltage flickers: . . . 11

I.2 Transients: . . . 12

I.2.1 Impulsive transients: . . . 13

I.2.2 Oscillatory transients: . . . 13

I.3 Voltage fluctuations: . . . 14

I.4 Waveform distortion: . . . 14

I.4.1 DC offset: . . . 15

I.4.2 Harmonics: . . . 15

I.4.2.1 Harmonics Definition: . . . 15

I.4.2.2 Causes of Harmonics: . . . 15

I.4.2.3 Effects of Harmonic Distortion: . . . 16

I.4.3 Interharmonics: . . . 17

I.4.4 Notching: . . . 17

I.4.5 Noise: . . . 17

I.5 Power frequency variations: . . . 18

I.6 Long-Duration Voltage Variations: . . . 18

I.6.1 Overvoltage: . . . 19

I.6.2 Undervoltage: . . . 19

I.6.3 Sustained interruptions: . . . 20

I.7 Voltage Imbalance: . . . 20

I.8 Short-Duration Voltage Variations: . . . 21

I.8.1 Voltage sag (dips): . . . 21

I.8.2 Voltage swell: . . . 21

I.8.3 Interruption: . . . 22

II Power Quality Issues of Smart Grids: . . . 22

II.1 Smart Microgrids: . . . 22

II.2 Concept of Smart Grid: . . . 24

II.3 Driving Factors of Smart Grids: . . . 24

II.4 Challenges in Smart grid Power Quality: . . . 25

II.4.1 Power Electronic devices: . . . 26
II.4.2 Plug-In Hybrid Electrical Vehicles Integration: . . . 26
II.4.3 Renewable Energy Sources Integration: . . . 26
III Power Quality Enhancement in Smart Grid: . . . 26
III.1 Passive Compensation Approach: . . . 27
III.1.1 Potentialities of Passive Filter: . . . 28
III.1.2 Limitations of Passive Filter: . . . 28
III.2 Active Compensation Approach: . . . 29
III.2.1 Series Active Filter: . . . 29
III.2.2 Shunt Active Filter: . . . 30
III.2.3 Three-phase, Three-wire active power filter: . . . 31
III.2.4 Three-phase, Four-wire active power filter: . . . 31
III.2.4.1 Three-phase, Four-wire split capacitor APF Topology . . . 31
III.2.4.2 Three-phase, Four-wire Four-leg APF Topology: . . . 32
III.2.5 Hybrid Active Filter: . . . 33
III.2.6 Unified Power Quality Conditioner: . . . 35
IV Motivation: . . . 35
V Scope of the Thesis: . . . 35
VI Thesis Outline: . . . 36
VII Summary: . . . 36

2 Shunt Active Power Filter for Three-Phase, Four-Wire Systems 38
I Introduction: . . . 38
II Reference Current Generation: . . . 38
II.1 P-Q-O Theory: . . . 39
II.1.1 Improved P-Q-O Theory with PLL: . . . 41
II.2 Cross-Vector Theory: . . . 43
II.2.1 Improved Cross-Vector Theory: . . . 43
II.3 *pqr* Theory: . . . 44
II.4 Synchronous Reference Frame Theory: . . . 47
III Current Injection Techniques: . . . 47
III.1 Hysteresis Current Control Technique: . . . 48
III.1.1 Advantages of Hysteresis PWM: . . . 48
III.1.2 Disadvantages of Hysteresis PWM: . . . 49
III.2 3 Dimensional Hysteresis PWM Technique: . . . 49
III.2.1 Principle of the 3 dimensional hysteresis PWM techniques : 50
IV DC Link Voltage Control: . . . 52
V Summary: . . . 53

3 Simulation Results and Discussion 55
I Introduction . . . 55
II First scenario: The proposed shunt active power filter is not used. . . . 56
III Second scenario: The proposed shunt active power filter is used. . . . 57
IV Summary: . . . 64

4 Three-Level Neural-Point-Clamped Inverter Based Three-phase Four-wire active Power Filter 65
I Introduction . . . 65
II Description of the APF Topology . . . 66
III PWM technique for Four-leg three-level inverters . . . 67

IV Harmonics and reactive power calculation 67
V Simulation Results and Discussion 70
V.1 First case: The proposed shunt active power filter is not used . . . 71
V.2 Second case: The proposed shunt active power filter is used. 73
VI Summary: 76

5 Conclusion and Future Work **78**
I Conclusion 78
II Suggestions for Future Work 80

A TITLE OF APPENDIX **81**

Bibliography **83**

ILLUSTRATIONS

1.1 Power Quality issues classification . . . 11
1.2 Positive polarity impulsive transient appearing in the positive cycle. . . . 13
1.3 Oscillatory transients. . . . 14
1.4 Voltage Fluctuations. . . . 14
1.5 Sources of harmonics in power system. . . . 16
1.6 voltage notching. . . . 17
1.7 Noise. . . . 18
1.8 Frequency variations. . . . 18
1.9 Overvoltage. . . . 19
1.10 Undervoltage. . . . 19
1.11 Sustained interruptions. . . . 20
1.12 Voltage Imbalance. . . . 20
1.13 Example 60% sag with a duration of 4 cycles (Instantaneous). . . . 21
1.14 Voltage swells. . . . 22
1.15 Momentary interruption. . . . 22
1.16 Conceptual vision of smart grid. . . . 23
1.17 Harmonic passive filters (a) Single-tuned filter, (b) Double-tuned filter and, (c) High-pass filter . . . 27
1.18 Series active power filters . . . 30
1.19 Shunt Active Filter . . . 30
1.20 Three-phase, Three-wire active power filter . . . 31
1.21 Three-phase, Four-wire split capacitor APF . . . 32
1.22 Three-phase, Four-wire Four-leg APF . . . 32
1.23 Series active and shunt passive filter . . . 33
1.24 Shunt active and shunt passive filter . . . 34
1.25 Active power filter is in series with shunt passive filter . . . 34
1.26 Unified power quality conditioner (UPQC) system configuration . . . 35

2.1 Reference Current Generation Techniques . . . 39
2.2 Physical meaning of instantaneous powers. . . . 39
2.3 Phase locked loop circuit. . . . 42
2.4 Hysteresis control scheme showing the tolerance band and the resulting switching signals. . . . 48
2.5 Switching states of the three-phase four-leg inverter. . . . 49
2.6 Switching vectors in $\alpha\beta o$ coordinate . . . 50
2.7 Reference current vector representation in $\alpha\beta o$ plane . . . 50
2.8 Detection of the cube . . . 52
2.9 Control loop of the DC voltage . . . 53

3.1 Three single phase diode rectifiers feeding unbalanced load . . . 55

3.2 The current waveform of phase "a" and its harmonics spectrum under the first scenario. . . . 56
3.3 The neutral current waveform under the first case. . . . 57
3.4 The different scenarios of the power supply voltages system. . . . 58
3.5 Supply currents after filtering pqo theory. . . . 58
3.6 Filter currents after filtering pqo theory. . . . 59
3.7 Evolution of the DC-capacitor voltage using pqo theory. . . . 59
3.8 Power factor correction using pqo theory. . . . 60
3.9 Simulation Results for Cross-Vector theory THDis1= 1,8%. . . . 61
3.10 Simulation Results for Cross-Vector theory THDis1= 1,7%. . . . 62
3.11 Simulation Results for Cross-Vector theory THDis1= 1,2%. . . . 63

4.1 The Four-Legged Active Power Filter (FL-APF) based on three-level NPC inverter. . . . 66
4.2 The principle of the PWM currents control technique. . . . 67
4.3 Three single phase diode rectifiers feeding unbalanced load. . . . 71
4.4 The current waveform of phase "a" and its harmonics spectrum under the first scenario. . . . 72
4.5 The neutral current waveform under the first case. . . . 72
4.6 The different scenarios of the power supply voltages system. . . . 73
4.7 The power system currents in the three-phases and in the neutral under the use of the proposed active power filter. . . . 74
4.8 The current waveform of phase "a" in the second case under the use of the proposed shunt APF. The first scenario [0.2 0.4s], The second scenario [0.8 1s], The third scenario [1.1 1.3s]. . . . 75
4.9 Power factor correction (v_s, $10 * i_s$). . . . 75
4.10 The proposed Active power filter current (the reference current and the APF injected current) . . . 76
4.11 APF output voltage v_{fan}. . . . 76

TABLES

1.1 Sources of transients 12
1.2 Classifications of transients. 13
1.3 Long duration voltage variation 19
1.4 Short duration voltage variation. 21
1.5 Root mean square (RMS) voltage variations during the momentary interruption. 22
1.6 An Overview of main driving factors for Smart Grids 25

2.1 Different compensation objectives and their corresponding references . . . 41
2.2 Different compensation objectives and their corresponding references . . . 43
2.3 Different compensation objectives and their corresponding references . . . 46
2.4 Switch Combinations in $\alpha\beta o$ orthogonal coordinate 49
2.5 Switch Combinations all the eight cubes 52

3.1 Simulation Parameters 56
3.2 THD currents after filtering 64

4.1 Simulation Parameters 71

Chapter 1

INTRODUCTION

I Power Quality Problems:

Power Quality (PQ) is defined as the perfection of delivered electrical power in terms of wave shape, frequency, amplitude, and sustainability [1]- [2]. Current and voltage waveforms of an ideal electrical grid should be in forms of perfect sinusoidal wave in-phase to each other having constant frequency and defined constant magnitude [3]. In addition to their quantifiable parameters, the sustainability is also an important factor for PQ analysis of an electrical grid [4]. Generally, power quality problems are divided into two types:

- Voltage-related problems include sags, swells, blackouts, harmonics, etc.,
- current-related problems include electromagnetic field, leakage current, electromagnetic interference, radiofrequency interference, etc.

The main classification of the PQ issues is represented in **Figure 1.1**.

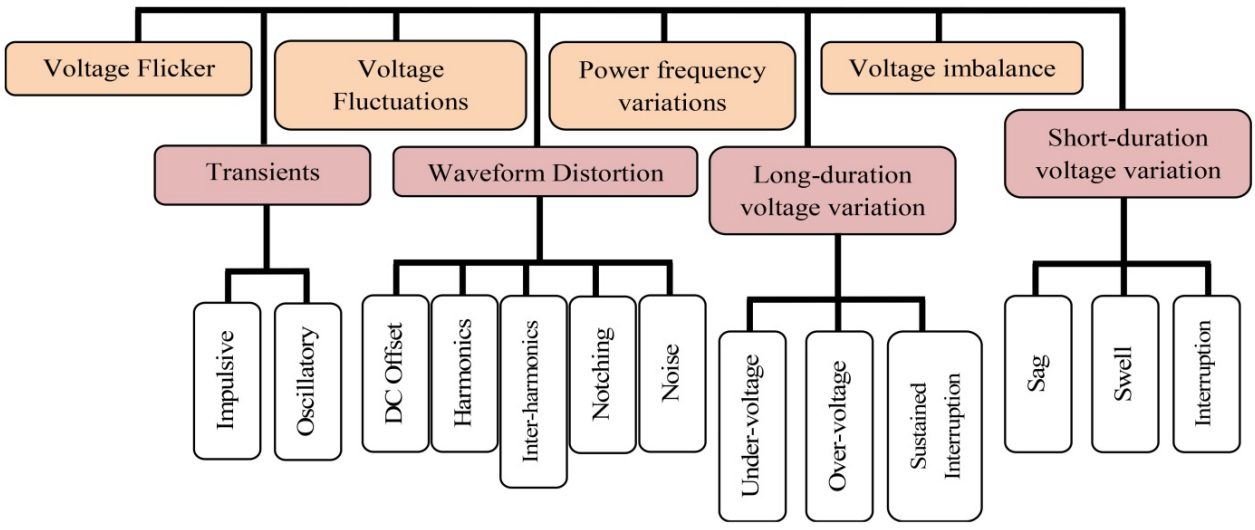

Figure 1.1: Power Quality issues classification

I.1 Voltage flickers:

Voltage flickers are defined as a continuous rapid variation of input supply voltage sustained for an appropriate period to enable visual recognition of a variation in electric

light intensity. Flicker is a power quality problem in which the magnitude of the voltage or frequency changes at a rate that is to be noticeable to the human eye [5]. The main causes of the voltage flicker are the loads that draw large starting currents during initial energization such as elevators, arc furnaces, and arc welders. If load starting cases are rapidly repeated, then light flicker effects can be quite noticeable. The severity of voltage flickers is measured using short-term and long-term flicker severity terms, where an expected flicker severity over a short duration (typically 10 minutes) is known as P_{st}, and that evaluated over a long duration (typically 2 hours) is known as P_{lt}. Thus, P_{lt} is a combination of $12 P_{st}$ values.

$$P_{st} = \sqrt{(0.0314 \times P_a) + (0.0525 \times P_b) + (0.0657 \times P_c) + (0.28 \times P_d) + (0.08 \times P_e)}$$

where P_a, P_b, P_c, P_d, and P_e are the surpassed flicker levels during 0.1, 1, 3, 10, and 50% of the surveillance period. By definition, a value of one for P_{st} expresses a visible disturbance, a level of optical severity at which 50% of persons might sense a flicker in a 60-W incandescent lamp. Excessive light flicker can cause a severe headache and can lead to the so-called 'sick building' [6].

I.2 Transients:

A transient voltage (These are also sometimes called as spikes, surges, power pulses, etc.) is a large impressed voltage with a very short duration (microseconds). Voltages may be in the magnitude of several thousands of volts, and due to the short duration, frequency components are significantly higher than the nominal frequency [7]. Although these events are of a very short duration, the high peak voltage is often sufficient to breakdown sensitive electronic components. The usual result is that the equipment stops operating with a blown fuse. Unfortunately, the fuse, being a thermal device, probably blew sometime after the transient had already passed through to damaged susceptible semiconductor components [8]. Transient overvoltage is the result of the rapid change of current in an inductive circuit. Sources of transients are listed in **Table 1.1**.

Table 1.1: Sources of transients

Category	Type	Sources of problems
Transients	External sources	Lightning strike
		Opening and closing of energized lines
		Breaker opening and closing
		Transients from other users in shared sources
	Internal sources	Switching operation
		High resistance fault
		Photocopy machines
		Welding machines
		Capacitor bank switching
		High-frequency switching in inverter or switch-mode power supply

The classifications of transients as listed in IEEE 1159-2019 [8] are shown in **Table 1.2**.

Table 1.2: Classifications of transients.

Parameter	Category	Type	Duration/Frequency
Transients	Impulsive	Nanosecond	¡50 ns
		Microsecond	50 ns - 1 ms
		Millisecond	¿1 ms
	Oscillatory	Low frequency	¡ 5 kHz
		Medium frequency	5 - 500 kHz
		High frequency	0.5 - 5 MHz

Based on the polarity change, transients are classified into two categories:

I.2.1 Impulsive transients:

Impulsive transients are sudden high peak events that raise the voltage and/or current levels in either a positive or a negative direction [9]. These types of events can be categorized further by the speed at which they occur (fast, medium or slow). Impulsive transients can be very fast events (5 ns rise time from steady state to the peak of the impulse) of short-term duration (less than 50 ns), and may reach thousands of volts, even in low voltage. **Figure 1.2** shows a positive polarity impulsive transient appearing in the positive cycle [10].

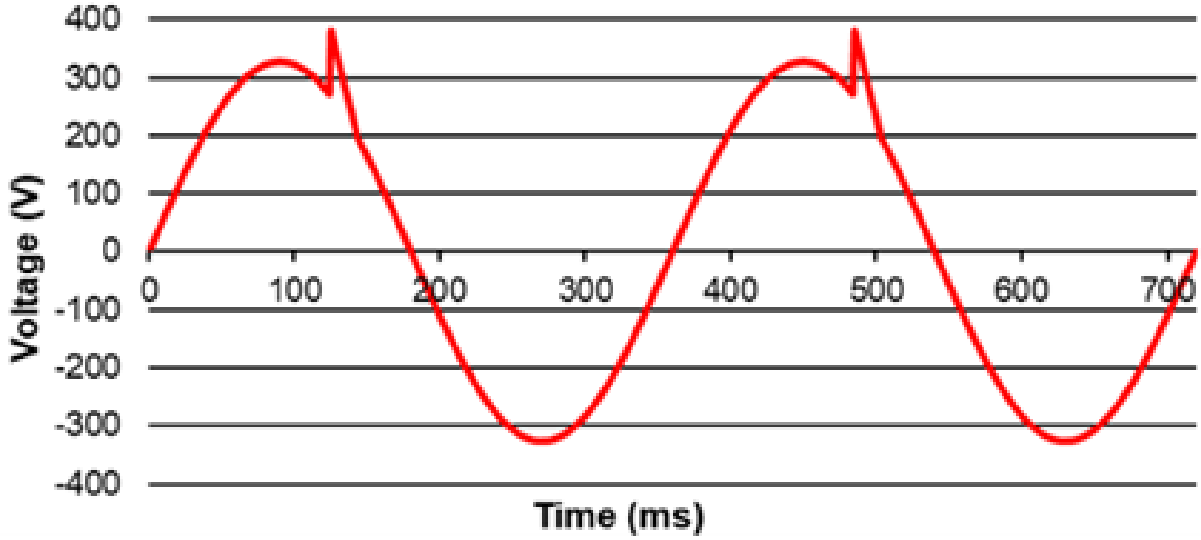

Figure 1.2: Positive polarity impulsive transient appearing in the positive cycle.

I.2.2 Oscillatory transients:

An oscillatory transient is a sudden change in the steady-state condition of a signal's voltage, current, or both, at both the positive and negative signal limits, oscillating at the natural system frequency [11]. The transient causes the power signal to alternately swell and then shrink, very rapidly. Oscillatory transients usually decay to zero within a cycle. Depending on the frequency, they can be classified in low, medium or high frequency transients. **Figure 1.3** shows the oscillatory transients in the voltage wave [12].

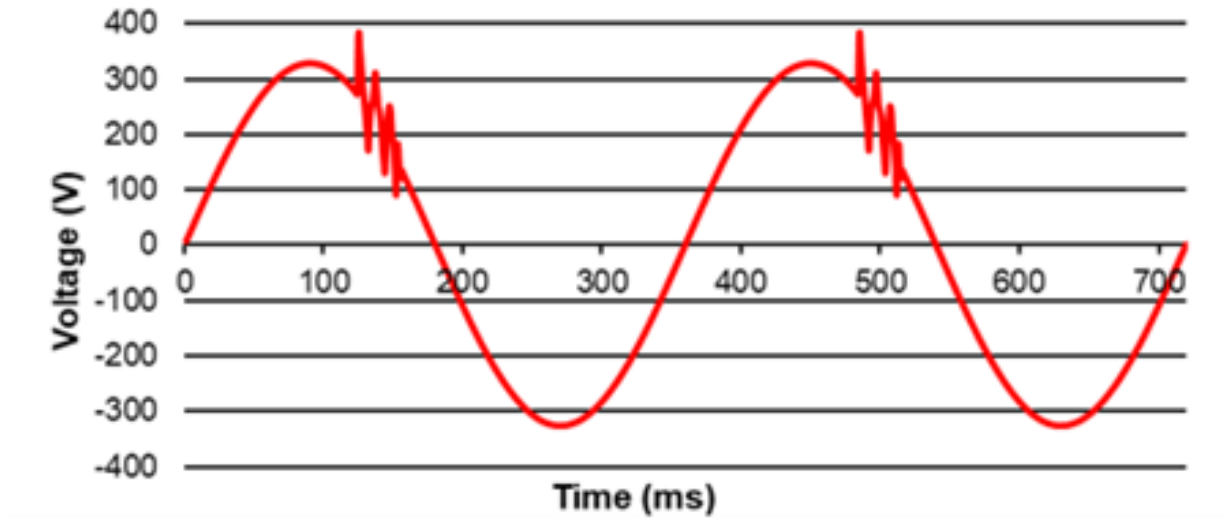

Figure 1.3: Oscillatory transients.

I.3 Voltage fluctuations:

Voltage fluctuation is a continuous change in the instantaneous voltage (cycle to cycle) due to variation in load resistance in every cycle. Continuous voltage changes are called voltage fluctuation. The definition of voltage fluctuation by IEC 61000-3-3 is a series of changes of RMS voltage evaluated as a single value for each successive half period between zero crossings of the source voltage. The major cause of voltage fluctuation is arc furnaces in industrial plant [13]. Voltage fluctuations have an impact on illumination intensity from the lamp. That is, continuous variation in voltage has an impact on illumination density resulting in a noticeable change in illumination by the normal human eye. This phenomenon is called flicker or voltage flicker.
The definition of flicker by IEC 61000-3-3 is the impression of unsteadiness of visual sensation induced by a light stimulus whose luminance or spectral distribution fluctuates with time. **Figure 1.4** shows a fluctuation in voltage.

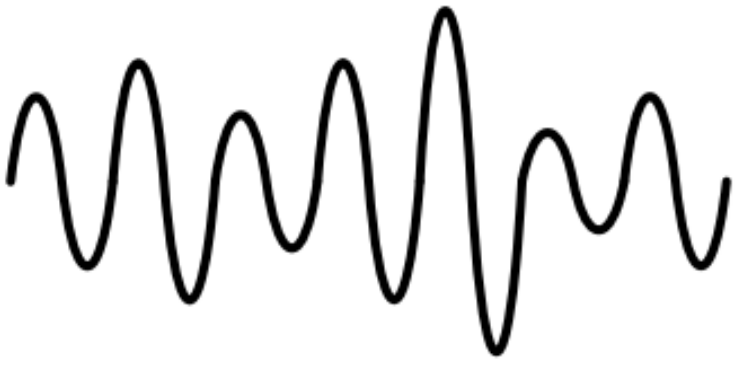

Figure 1.4: Voltage Fluctuations.

I.4 Waveform distortion:

IEEE 1159-2019 defines waveform distortion as a steady-state deviation from an ideal sine wave of power frequency principally characterized by the spectral content of the deviation

. There are five primary types of waveform distortion [14]:

I.4.1 DC offset:

The presence of a dc voltage or current in an ac power system is termed dc offset. This can occur as the result of a geomagnetic disturbance or asymmetry of electronic power converters [15].
Examples: Incandescent light bulb life extenders may consist of diodes that reduce the rms voltage supplied to the light bulb by half-wave rectification. Direct current in ac networks can have a detrimental effect by biasing transformer cores so they saturate in normal operation. This causes additional heating and loss of transformer life.

I.4.2 Harmonics:

Harmonics is considered as the major issue out of all power quality problems [16]. Recently mitigation of harmonics has gain a lot of attention due to the increased use of non-linear loads.

I.4.2.1 Harmonics Definition: Harmonics, as defined in IEEE guide for harmonic control in electrical power systems [17], are sinusoidal components of a periodical quantity having frequency components which are integer multiples of the fundamental frequency of that periodical quantity. The presence of harmonics in electrical systems means that current and voltage are distorted and deviate from sinusoidal waveforms [18]. If the fundamental frequency of an alternating current (AC) signal is represented by f then the harmonic frequencies like second harmonic and third harmonic will be represented by 2f, 3f and so on. The fundamental frequency is the frequency at which most of the energy is contained or at which the signal is defined to occur.

I.4.2.2 Causes of Harmonics: Harmonics are caused by the loads in which the current waveform does not conform to the fundamental waveform of the supply voltage. Developments in digital electronics and power semiconducting devices have led to a rapid increase in the use of nonlinear devices. The requirement of controlled power through power electronic converter for automation of processes in industries is the main source of current harmonics [19] [20]. The sources of harmonics in power system can be classified as shown in **Figure 1.5**

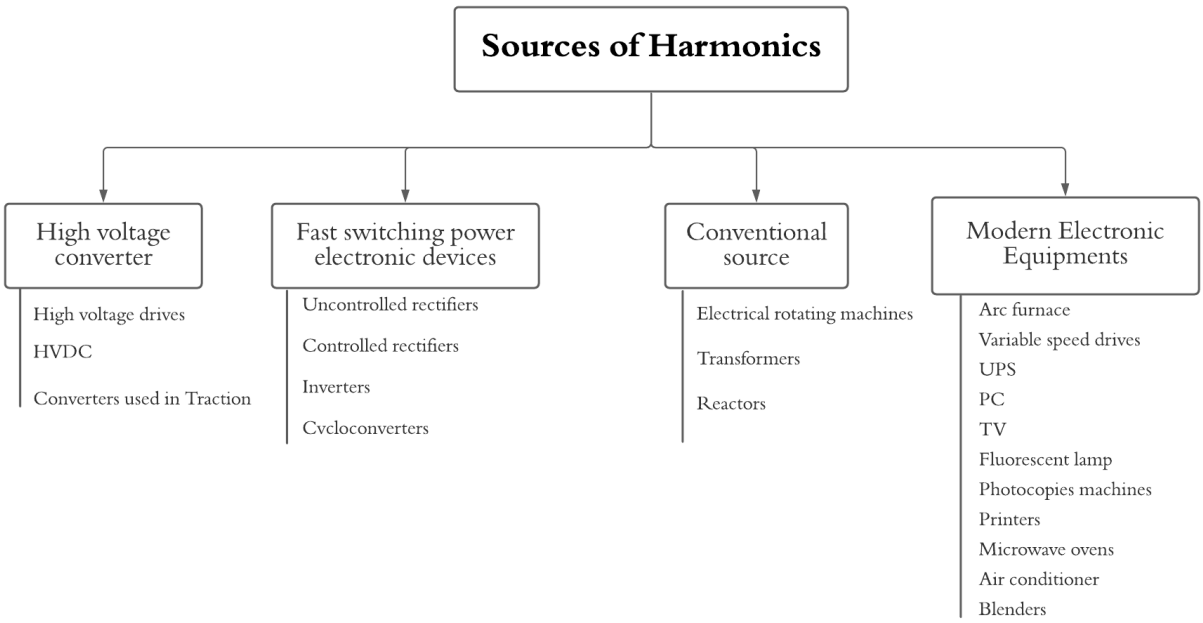

Figure 1.5: Sources of harmonics in power system.

I.4.2.3 Effects of Harmonic Distortion: Current harmonics generated by the non-linear loads propagates throughout the power network. Harmonic current passing through the system impedance causes a voltage drop for each harmonic and results in voltage harmonics appearing at the system bus and leads to power quality problem. These currents interact adversely with a wide range of power system equipment, most notably capacitors, transformers and motors causing additional losses and consequent, overheating [21] [22] [23] [24].

- Shunt capacitors which are used for power factor correction causes the harmonic resonance.
- Harmonic currents may result in the transformer rms current being higher than its capacity. The increased total rms current results in increasedconductor losses and heating. Harmonic currents in transformer also increases eddy current losses and core losses.
- The performance of motors is deteriorated by voltage harmonics. This distortion at the motor terminals is translated into harmonic fluxes within the motor causing high frequency currents in the rotor and resulting in additional losses, decreased efficiency, vibration and high pitch noises.
- Higher order harmonics cause problems of electromagnetic Interference (EMI), especially with sensitive electronic equipments (e.g. navigation, communication control and automation).
- Harmonic currents from non-linear loads affect the accuracy of watt-hour and demand meters. Conventional magnetic disk watt-hour meters tend to have negative values at harmonic frequencies. This error increases with increasing frequency.
- The digital relays and their control algorithms depend on the sampling data and zero crossing, which may be adversely affected in presence of harmonics in both voltage and current. Current harmonic distortion can also have an effect on the interruption capability of circuit breakers and fuses.

I.4.3 Interharmonics:

Interharmonics are non-integer multiples of fundamental frequency. Interharmonics add extra signals to the power system which can cause a number of effects, particularly if they are magnified by resonance. The risk of resonance increases with the presence of wider range of frequencies. Many of the effects of interharmonics are similar to those of harmonics, but some are unique as a result of their non-periodic nature.
The most common interharmonics sources are double conversion systems such as cyclo-converters, High Voltage Direct Current (HVDC) converters, variable speed AC motor drives, and the metal shaping and melting systems like ladle furnaces, Electric Arc Furnaces (EAF), and IMFs. [25], [26], [27].

I.4.4 Notching:

Notching is a periodic voltage disturbance caused by the normal operation of power electronic devices when current is commutated from one phase to another. Since notching occurs continuously, it can be characterized through the harmonic spectrum of the affected voltage. However, it is generally treated as a special case. The frequency components associated with notching can be quite high and may not be readily characterized with measurement equipment normally used for harmonic analysis [28]. **Figure 1.6** shows a voltage notching.

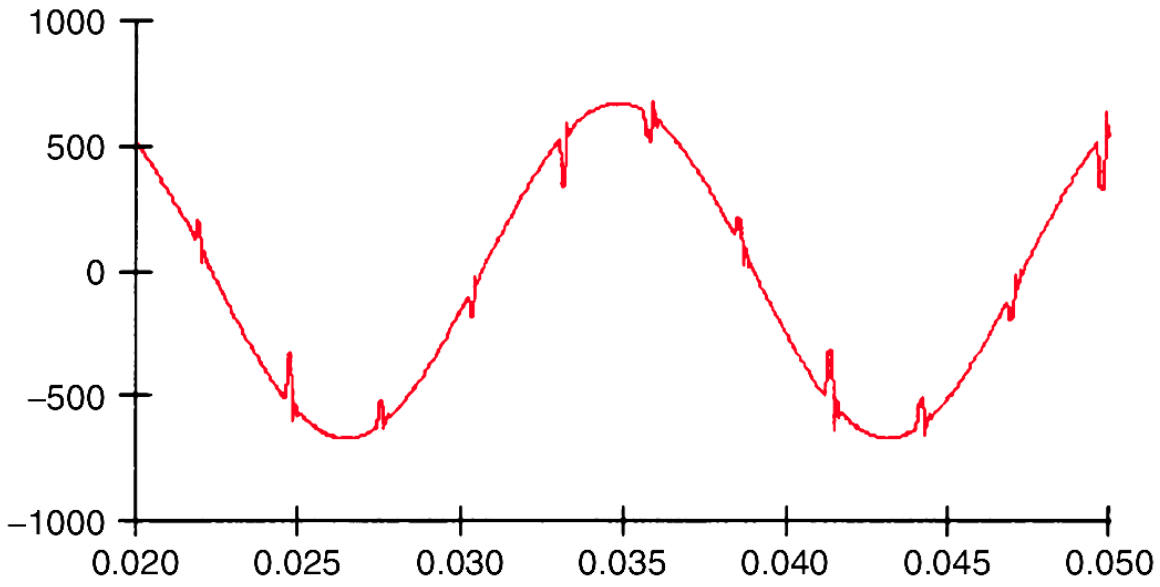

Figure 1.6: voltage notching.

I.4.5 Noise:

Any external and unwanted information that interferes with the transmission signal is known as noise. Noise is not a part of the original signal. It is caused by electromagnetic interference, radio frequency interference and ignition systems. The negative effects of noise include troubles of sensitive electronic equipment, loss of data and errors in data processing [29]. **Figure 1.7** shows a noisy signal.

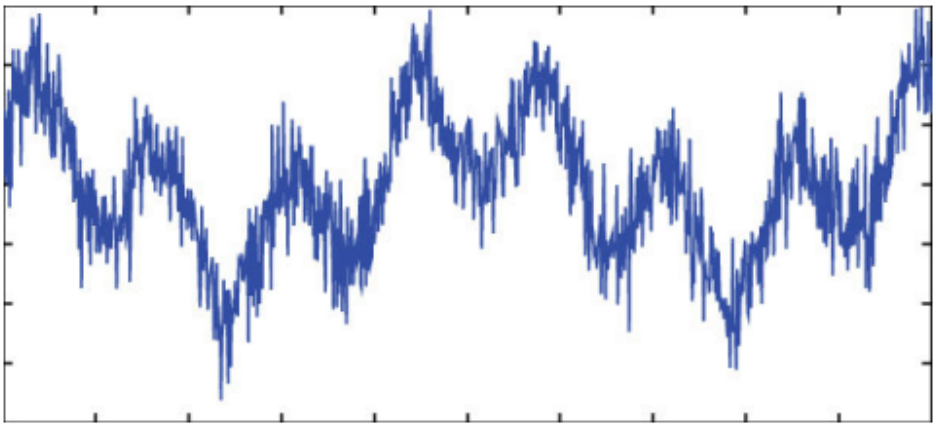

Figure 1.7: Noise.

I.5 Power frequency variations:

Power frequency variations are defined as the deviation of the power system fundamental frequency from it specified nominal value (e.g., 50 or 60 Hz). The power system frequency is directly related to the rotational speed of the generators supplying the system. There are slight variations in frequency as the dynamic balance between load and generation changes. The size of the frequency shift and its duration depend on the load characteristics and the response of the generation control system to load changes [30].
Frequency variations that go outside of accepted limits for normal steady-state operation of the power system can be caused by faults on the bulk power transmission system, a large block of load being disconnected, or a large source of generation going off-line. On modern interconnected power systems, significant frequency variations are rare. Frequency variations of consequence are much more likely to occur for loads that are supplied by a generator isolated from the utility system. In such cases, governor response to abrupt load changes may not be adequate to regulate within the narrow bandwidth required by frequency-sensitive equipment. **Figure 1.8** illustrates frequency variations for a 24-h period on a typical 13-kV substation bus [31].

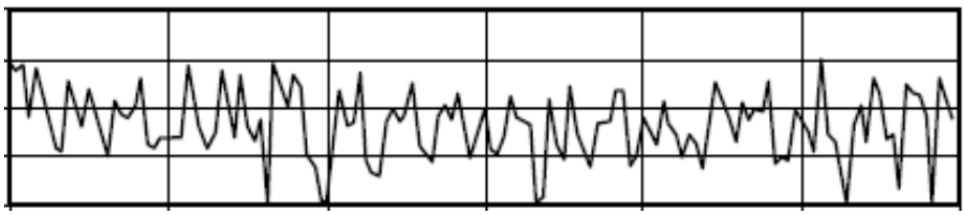

Figure 1.8: Frequency variations.

I.6 Long-Duration Voltage Variations:

Long-duration variations encompass root-mean-square (rms) deviations at power frequencies for longer than 1 min. Long-duration variations can be either overvoltages or undervoltages. Overvoltages and undervoltages generally are not the result of system faults, but are caused by load variations on the system and system switching operations. Such variations are typically displayed as plots of rms voltage versus time [32]. The different classifications of long duration voltage variations are listed in **Table 1.3**.

Table 1.3: Long duration voltage variation

Parameters	Duration	Voltage magnitude
Undervoltage	>1 min	0.8 - 0.9 pu
Overvoltage	>1 min	1.1 - 1.2 pu
Sustained interruption	>1 min	0.0 pu
Current overload	>1 min	-

I.6.1 Overvoltage:

An overvoltage **Figure 1.9** is an increase in the rms ac voltage greater than 110 percent at the power frequency for a duration longer than 1 min [33].
Causes: switching off a large load or energizing a capacitor bank, Incorrect tap settings on transformers

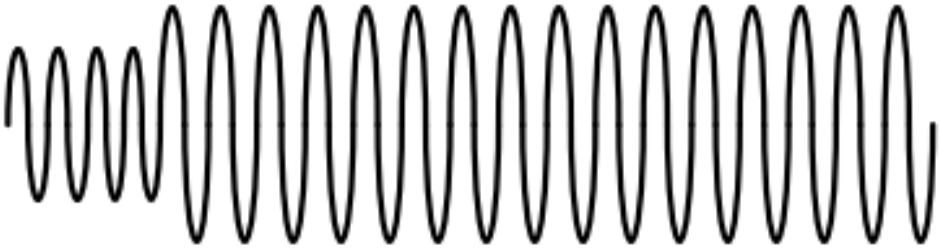

Figure 1.9: Overvoltage.

I.6.2 Undervoltage:

An undervoltage **Figure 1.10** is a decrease in the rms ac voltage to less than 90 percent at the power frequency for a duration longer than 1 min. Undervoltages are the result of switching events that are the opposite of the events that cause overvoltages.
Causes: A load switching on or a capacitor bank switching off Overloaded circuits The term brownout is often used to describe sustained periods of undervoltage initiated as a specific utility dispatch strategy to reduce power demand [34].

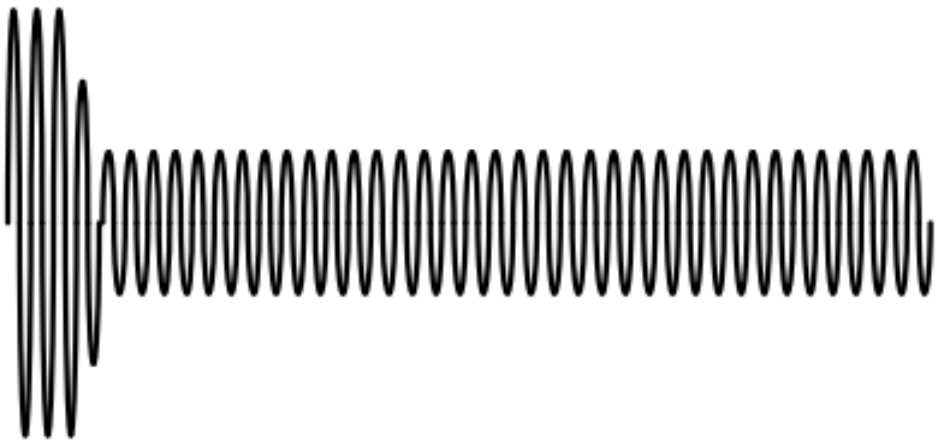

Figure 1.10: Undervoltage.

I.6.3 Sustained interruptions:

When the supply voltage has been zero for a period of time in excess of 1 min, the long-duration voltage variation is considered a sustained interruption. Voltage interruptions longer than 1 min are often permanent and require human intervention to repair the system for restoration.
The term sustained interruption **Figure 1.11** refers to specific power system phenomena and, in general, has no relation to the usage of the term outage [35].

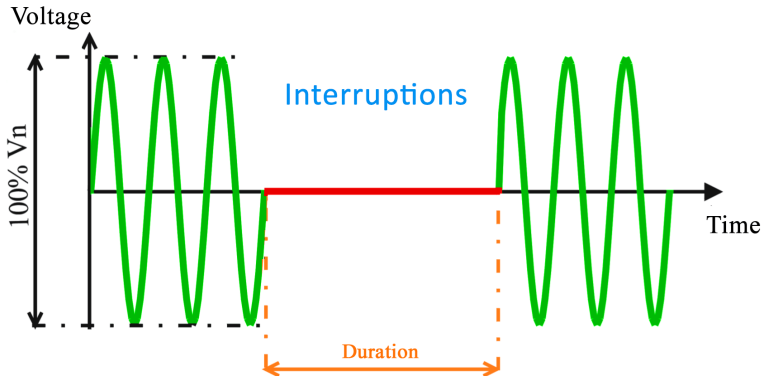

Figure 1.11: Sustained interruptions.

I.7 Voltage Imbalance:

A voltage imbalance **Figure 1.12** is not a type of waveform distortion. However, because it is essential to be aware of voltage imbalances when assessing power quality problems, Voltage imbalance (also called voltage unbalance) is sometimes defined as the maximum deviation from the average of the three-phase voltages or currents, divided by the average of the three-phase voltages or currents, expressed in percent.
Imbalance is more rigorously defined in the standards using symmetrical components. The ratio of either the negative- or zero sequence component to the positive-sequence component can be used to specify the percent unbalance [36].
Causes: The primary source of voltage unbalances of less than 2 percent is single-phase loads on a three-phase circuit. Voltage unbalance can also be the result of blown fuses in one phase of a three-phase capacitor bank. Severe voltage unbalance (greater than 5 percent) can result from single-phasing conditions.

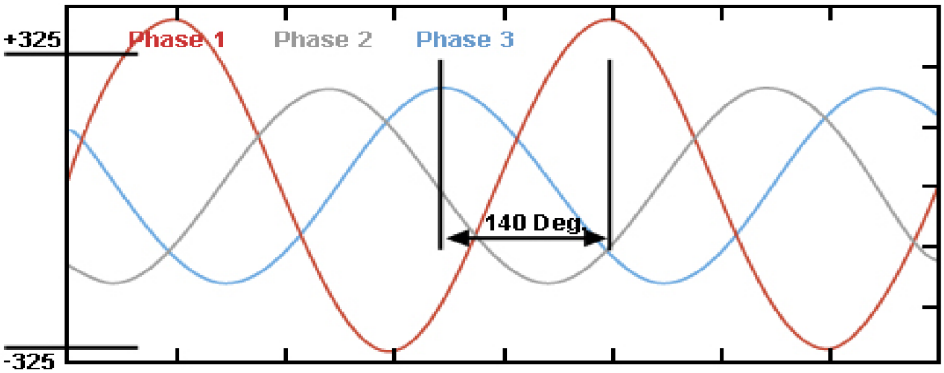

Figure 1.12: Voltage Imbalance.

I.8 Short-Duration Voltage Variations:

Variations in RMS voltage lasting from 0.5 cycles to less than or equal to 1 min are classified as short duration RMS variations as per IEEE 1159-2019. Based on the duration of the event, short duration voltage variation can be classified into three categories, namely instantaneous, momentary, and temporary. The different classifications of short duration voltage variations are listed in **Table 1.4** [37].

Table 1.4: Short duration voltage variation.

Parameters	Instantaneous		Momentary		Temporary	
	Duration	Voltage magnitude	Duration	Voltage magnitude	Duration	Voltage magnitude
Sag	0.5-30 cycles	0.1-0.9 pu	30 cycles-3s	0.1-0.9 pu	>3s - 1 min	0.1 - 0.9 pu
swell	0.5-30 cycles	1.1-1.8 pu	30 cycles-3s	1.1-1.4 pu	>3s - 1 min	1.1 - 1.2 pu
Interruption	-	-	0.5 cycles-3s	<0.1 pu	>3s - 1 min	<0.1 pu
Voltage imbalance	-	-	30 cycles-3s	2% - 15%	>3s - 1 min	2% - 15%

I.8.1 Voltage sag (dips):

Voltage sags **Figure 1.13** are short duration reductions in voltage magnitude and duration lasting typically from a few cycles to a few seconds. It is a decrease in RMS voltage between 0.1 and 0.9 pu and a time duration from 0.5 cycles to 1 min. The depth of voltage sag depends on multiple factors like network impedance, distance of the fault occurrence, voltage level at the fault location, connected loads at the time of fault, and voltage improvement due to reactive power components in the power system. The duration of voltage sag is determined by the dynamics of rotating loads, system impedance, and fault clearing time [38].

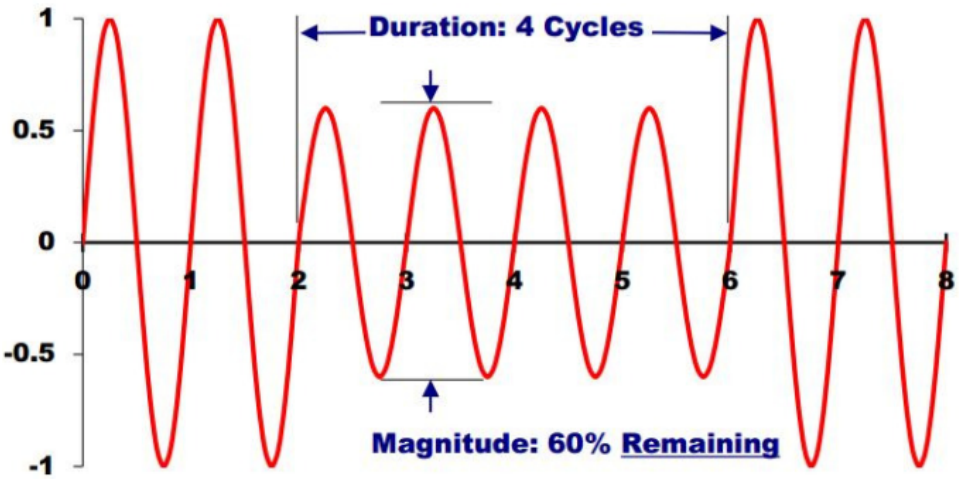

Figure 1.13: Example 60% sag with a duration of 4 cycles (Instantaneous).

I.8.2 Voltage swell:

Voltage swells **Figure 1.14** are short duration increases in voltage magnitude lasting typically from a few cycles to a few seconds. It is an increase in RMS voltage between 1.1 and 1.8 pu and a time duration from 0.5 cycles to 1 min [39]. The typical voltage magnitude is between 1.1 and 1.2 pu.

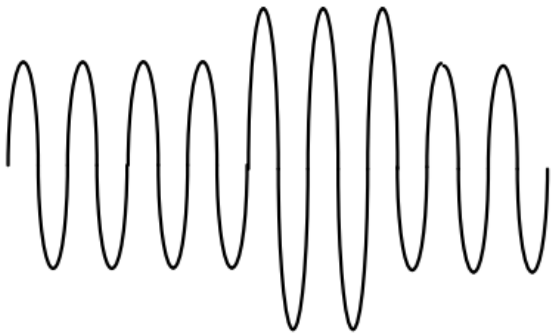

Figure 1.14: Voltage swells.

I.8.3 Interruption:

Momentary interruptions **Figure 1.15** are short duration reductions in voltage magnitude of less than 0.1 pu for less than 1 min time duration. The duration of the momentary interruption is determined by the fault clearing time and breaker closing time. Depending on its duration, an interruption is categorized as instantaneous, momentary, temporary, or sustained.**Table 1.5**. describes the RMS voltage recorded just before, during, and after the momentary interruption [40].

Table 1.5: Root mean square (RMS) voltage variations during the momentary interruption.

Parameter	Before the interruption event	During the interruption event	After interruption recovery
RMS voltage (R-Y) in V	400	4.5	400
RMS voltage (R-B) in V	402	2.8	401
RMS voltage (Y-B) in V	401	6	401

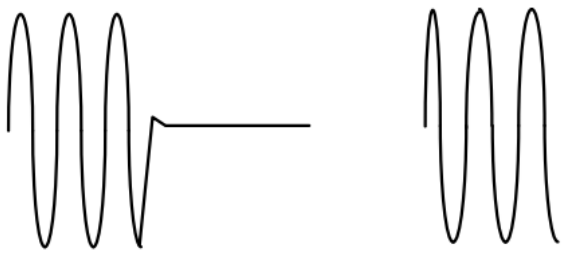

Figure 1.15: Momentary interruption.

II Power Quality Issues of Smart Grids:

II.1 Smart Microgrids:

In general, the 'Smart Grid' can be defined as 'a system of systems'. It is a platform that enables functioning of different technologies and systems. It can be viewed as a better electricity delivery infrastructure.
A Smart Grid is an electricity network that can intelligently integrate the actions of all users connected to it - generators, consumers and those that do both – in order to

efficiently deliver sustainable, economic and secure electricity supplies. See **Figure 1.16** for a visual representation of the Smart Grid concept [41].

Figure 1.16: Conceptual vision of smart grid.

Here are some other definitions of the Smart Grid [42] [43] [44] [45]:

- A power system that contains multiple automated transmission and distribution (T&D) systems, all operating in a coordinated, efficient, and reliable manner.
- A power system that serves millions of customers and has an intelligent communications infrastructure, enabling the timely, secure, and adaptable information flow, needed to provide power to the evolving digital economy.
- A power system that handles emergency conditions with 'self-healing' actions and is responsive to energy-market and utility needs.
- The smart grid is a broad collection of technologies that delivers an electricity network that is flexible, accessible, reliable and economic. Smart grid facilitates the desired actions of its users and these may include distributed generation, the deployment of demand management and energy storage systems or the optimal expansion and management of grid assets.

After analyzing the definitions stated above, the following characteristics of the Smart Grids can be distinguished:

- Optimized for best resource and equipment utilization
- Distributed by its structure (assets and information)
- Interactive (customers, retailers, markets)
- Adaptive and scalable (for changing situations)
- Proactive rather than reactive (to prevent emergencies)
- Self-healing (can predict/distinguish/bypass abnormal situations)
- Reliable and secure (from threats and external disturbance)

- Efficient and reliable
- Open for all types and sized of generation
- Environmental friendly (using renewable energy resources)
- Integrated (monitoring, control, protection, maintenance, EMS, DMS, AMI)

II.2 Concept of Smart Grid:

Among Smart Grid research and development activities, there is not currently a globally agreed the definition for "The Smart Grid". However, it has been already recognized that the Smart Grid is a new electricity network, which highly integrates the advanced sensing and measurement technologies, information and communication technologies (ICTs), analytical and decision-making technologies, automatic control technologies with energy and power technologies and infrastructure of electricity grids [46]. Some important aspects of what 'smart' are listed below:

- Observability: It enables the status of electricity grid to be observed accurately and timely by using advanced sensing and measuring technologies;
- Controllability: It enables the effective control of the power system by observing the status of the electricity grid;
- Timely analysis and decision-making: It enables the improvement of intelligent decision-making process;
- Self-adapting and self-healing: It prevents power disturbance and breakdown via self-diagnosis and fault location.
- Renewable energy integration: It enables to integrate the renewable energy such as solar and wind, as well as the electricity from micro-grid and supports efficient and safe energy delivery services for electric vehicle, smart home and others.

II.3 Driving Factors of Smart Grids:

According to the recent research, the majority of utilities consider technology as a main driver for Smart Grids. **Table 1.6**. provides an overview of the main driving factors for Smart Grids [47]:

Table 1.6: An Overview of main driving factors for Smart Grids

Technology Advancement	• Smart Grid can be seen as the convergence of IT, telecom, and energy markets. • New products and solutions through technology advancement. • Significant amounts of venture capital investment in Smart Grid technologies and solutions.
Higher Efficiency with the Help of Grid Optimization	• Multiple integration points for intelligent grid hardware and software from transmission to consumption. • Embedded sensors and monitoring capabilities. • Deployment of advanced two-way communications networks. • Growing Supply of Renewable and Distributed Power Generation and Storage. • Network and systems architecture to support many forms of distributed generation and storage. • Intelligent support for multiple forms of intermittent renewable power sources (centralized and/or distributed).
Advanced Customer Services	• Robust, simple consumer energy management platforms. • Networked devices within the "smart home". • New, efficient pricing models for electricity usage.
Infrastructure Reliability and Security	• Networks/systems tolerant of attack or natural disaster. • Ability to anticipate and automatically respond to system disturbances.
21st Century Power Quality	• Delivering power that is free of sags, spikes, disturbances and interruptions.

II.4 Challenges in Smart grid Power Quality:

Similar to all technology smart grids bring some challenges to traditional grids. Meanwhile it also brings some new tools to improve the functionalities [48]. The key challenges, and tools that smart grids will bring are categorized as [49],

II.4.1 Power Electronic devices:

The recent progress in the field of power electronics has led to increasing penetration of power electronic devices to the modern electrical grids, these devices are like a double-edged sword, improving the electrical grid performance in one side and bringing some new challenges such as injecting harmonics to the electricity grid on the other side. Nowadays most of the renewable energy sources need power electronic interfaces to connect to the main electricity grid, most of the home appliances use power electronic converters, also power electronic converters are used in industrial loads and many other applications. On the other hand, most of the power quality improvement devices that are developed to mitigate the power quality problems, are power electronic based. Power electronic based power quality improvement devices such as active power filter, dynamic voltage restorer (DVR), static synchronous compensator (STATCOM), uninterruptible power supply (UPS) systems, smart impedances, electrical springs and multifunctional DGs are of this category [50] [51].

II.4.2 Plug-In Hybrid Electrical Vehicles Integration:

As it is known, smart grid is a green grid, meaning that it has the biggest potential to deliver carbon saving. By growing tendency to use of environment-friendly vehicles, the future of the electricity grid will face a power quality challenge. Integration of a huge amount of storage units which use rectifiers to charge the batteries with different charge rates will greatly affect the power quality of the electricity grid. Also, the peak demand will increase significantly while injecting different orders of harmonic to the electrical grid. On the other hand, this challenge could become an opportunity to improve the reliability of the electrical system, if these storage units could be used as an active demand-side management tool. This needs the enactment of ownership and utilization legislations for electrical vehicles storage units. Also distributed demand-side management and smart charging methods could be used to improve the overall quality of the system [52] [53].

II.4.3 Renewable Energy Sources Integration:

Renewable energy sources (RES) have changed the nature of the electricity generation from bulk generation units to distributed generation units (DGs). This has helped to improve the reliability of the system, voltage profile, decreased the transmission line costs, losses and dependency on the main grid. These are the benefits of using renewable energy sources, while on the other hand these energy sources are not fully reliable, because of the probabilistic nature of the energy sources such as solar or wind power. Another drawback of RES integration is that most of these sources have power electronic based interfaces to convert the power, as mentioned before over-using of power electronic converters in the electricity grid will cause lots of harmonic pollution. Recently researchers are working on methods to make these RES multifunctional, so that the integrated power electronic converters could improve the power quality of the grid [54] [55].

III Power Quality Enhancement in Smart Grid:

Multiple methods to overcome power quality issues exist, especially those related to harmonic pollutions [56] [57]. Load conditioning which is well documented in the literature consisted of changing the load's configuration in order to improve its behavior by reducing

harmonic content of its consumed current. External solutions consisted of adding a compensator to address such issues. In this category two principal configuration are available; Passive Filters and Active Filters.

III.1 Passive Compensation Approach:

The first and traditionally installed over the power systems are the conventional passive filters. These filters are built up from passive components; resistors (R), Capacitors (C), and inductors (L) [58]. They are designed to form a tuned circuit. The tuning frequency is matched to the harmonics in question. Conventionally, to overcome current issues and correct the power factor, passive filters were the primary solution. These large preset filters are able to improve the power factor and reduce current harmonics. After installation, they are not able to behave as a dynamic compensator during a change in conditions of the system. If not properly designed, they could give rise to resonance phenomena in the system. As well, the distorted current drawn by nonlinear loads could distort the PCC voltage which may then give rise to harmonic currents, even if at these locations, no harmonic generating equipment are present. Furthermore, voltage unbalance, sags, and swells are other power quality issues related to the supply voltage required to be considered for compensations that passive filters are unable to solve.

The high-pass filter is a single-tuned filter where the L and R elements are connected in parallel instead of series. This connection results in a wide-band filter having impedance at high frequencies limited by the resistance R. The three types of passive filters are shown in **Figure 1.17**.

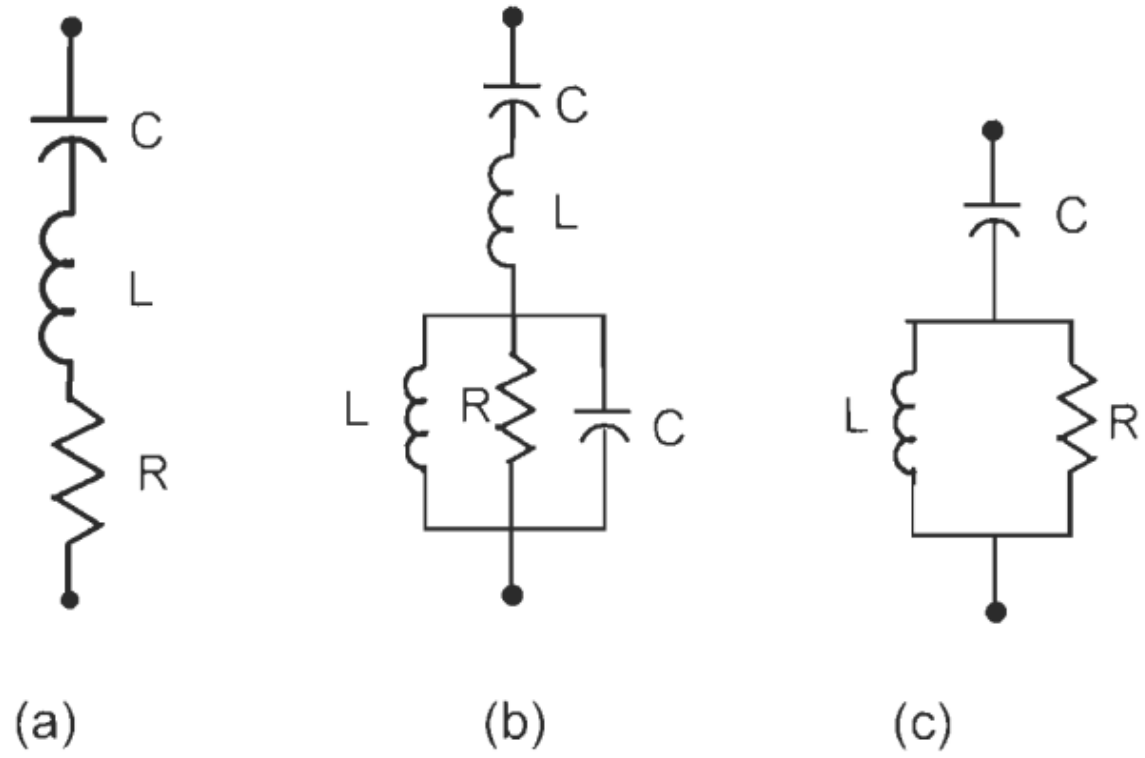

Figure 1.17: Harmonic passive filters (a) Single-tuned filter, (b) Double-tuned filter and, (c) High-pass filter

The potentialities and limitations of passive filter can be summarized as under [59]

[60] [61].

III.1.1 Potentialities of Passive Filter:

- Well-designed passive filters can be implemented in large sizes of Mvars of ratings and provide almost maintenance-free service (there are no rotating parts).
- These are more economical to implement than their rotating counterparts, i.e., synchronous condensers.
- A fast response time of the order of one cycle or less (i.e., with SVC) can be obtained, which is important for correction of flickering voltage dips due to arc furnace loads.
- Unlike rotating machines (i.e., synchronous motors or condensers) power capacitors do not contribute to the short-circuit currents.
- A single installation can serve many purposes, i.e., reactive power compensation and power-factor improvement, reducing TDD to acceptable limits, voltage support on critical buses in case of a source outage, and reducing the starting impact and voltage drop of a large motor.
- When a choice is available between active and passive filters, the passive filters are more economical.

III.1.2 Limitations of Passive Filter:

- Passive filters are not suitable for changing system conditions. Once installed, these are rigidly in place. Neither the tuned frequency nor the size of the filter can be changed so easily. The passive elements in the filter are close-tolerance components.
- A change in the system operating conditions can result in some detuning, although a filter design should consider operation with varying loads and utility's source impedance.
- The system impedance largely affects the design. To be effective, the filter impedance must be less than the system impedance, and the design can become a problem for stiff systems.
- Outage of a parallel branch can totally alter the resonant frequency, resulting in over stressing of filter components and increased harmonic distortion.
- The parallel resonance between the system and filter (shifted resonance frequency) for single tuned (ST) or double tuned (DT) filters can cause an amplification of the current at characteristics and non characteristics harmonics. A designer has limited choice in selecting tuned frequencies and ensuring adequate bandwidth between shifted frequencies and even and odd harmonics.
- The aging, deterioration, and temperature effects may increase the designed tolerances and bring about detuning, although these effects can be considered in the design stage.
- Definite-purpose circuit breakers are required. To control switching surges, resistor switching and synchronous closing may be required, although the filter reactors will reduce the magnitude of the switching inrush current and its frequency.

- The grounded neutrals of wye-connected banks provide a low-impedance path for third harmonics. Third harmonic amplification can occur in some cases. (For industrial systems, the three-phase capacitor banks are, generally, connected in ungrounded wye configuration.)
- Special protective and monitoring devices are required.
- ST or DT filters are not possible to employ for certain loads like cycloconverters or when the power system has interharmonics.
- The design may require increasing the size of the filters to control TDD. This may give rise to over voltages when the banks are switched in and under voltage when these are switched out.
- A detuning may be brought into play when consumers on the same utility's service add power capacitors or filters in their distribution systems.

III.2 Active Compensation Approach:

With the advances in power electronics, the active filtering is gaining in popularity in recent decades. The shunt active filters are among the first AFs been commercially available for small and medium voltage applications. They have numerous advantages over conventional passive filters [62] [63]. They do not require tuning and are independent of the state of the systems parameters. They respond instantaneously to load variations without any difficulties. And their compensation efficiency is much less susceptible to external parameters. The operator has instantaneous control over the device and could perform all kind of desired modification without the necessity of modifying the hardware. In this way, there exists numerous types of active filters; Shunt AFs, Series AFs, Hybrid AFs, and Unified power quality conditioner (UPQC) are among popular active compensators [64] [65].
With the technological advances in manufacturing and the decrease in production cost of power electronic converters the application of Active compensators seems inevitable. The introduction of Smart grids has promoted application of these alternative compensators to enhance power quality over traditional passive filters. Having similar topology to FACTS devices, the industry is convinced on their reliability during critical operating states [66]. Thus, in this section a brief overview of these various categories of active compensators are presented [67].

III.2.1 Series Active Filter:

The series APF act as a controlled voltage source illustrated in **Figure 1.18**. The series APF is mainly used to compensate for utility problems such as voltage disturbances (sags, swells etc.), voltage unbalances and/or voltage distortion. To compensate for harmonic currents a shunt passive filter must be connected as shown in **Figure 1.18**, providing a low impedance path [68].

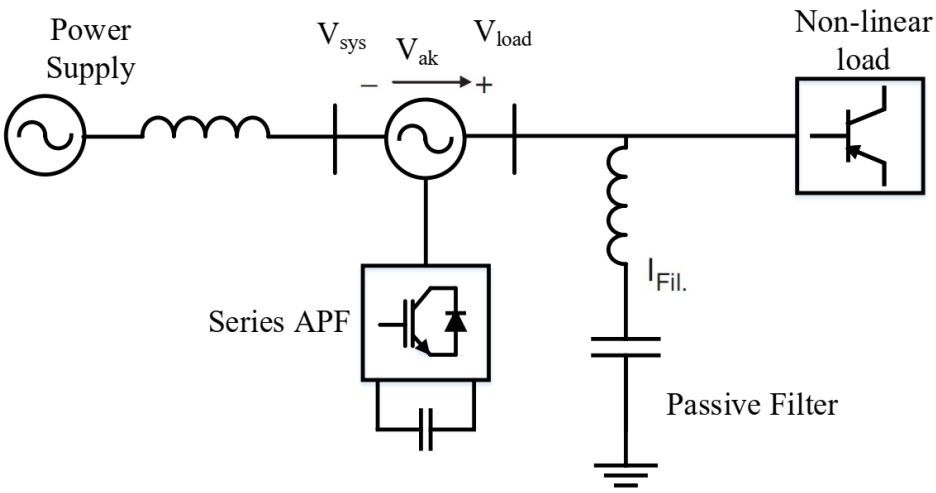

Figure 1.18: Series active power filters

III.2.2 Shunt Active Filter:

From **Figure 1.19**, the source current is equal to the load current before connecting the shunt APF and can be written as

$$i_s = i_L = i_f + i_h$$

where i_s and i_L are the source and load current respectively, the load current can be decomposed to a fundamental current i_f and harmonic currents i_h. Identifying the harmonic currents from the load [69], the shunt APF can be controlled in such a way to inject the inverse of the harmonic currents at the PCC, resulting in sinusoidal source currents

$$i_s = i_f + i_h - i_{filtre} = i_f$$

Essentially the filter act as a controllable current source injecting currents at the PCC.

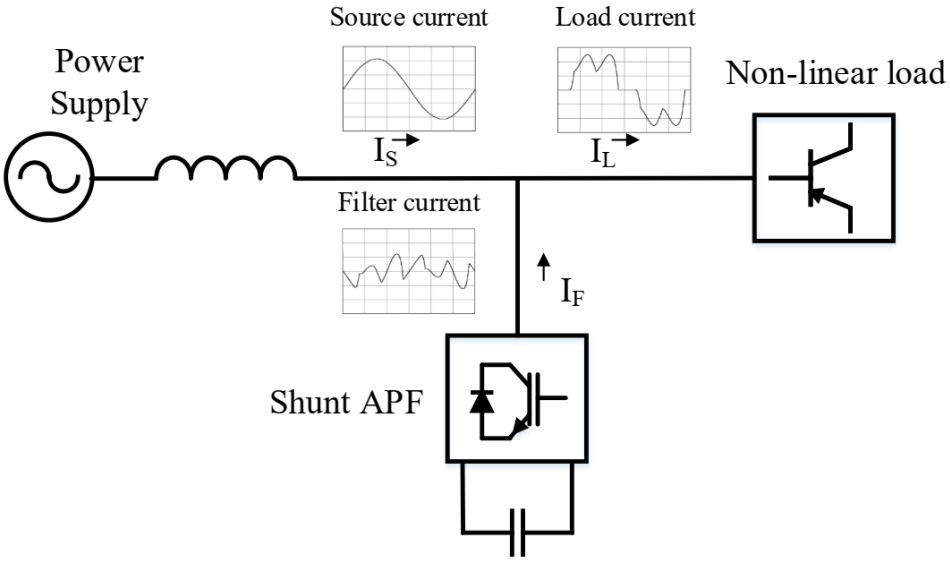

Figure 1.19: Shunt Active Filter

The classification of APF can also be based on the supply and/or the load system having three-phase three-wire (3P3W) or three-phase four-wire (3P4W) systems [70] [71] [72] [73] [74].

III.2.3 Three-phase, Three-wire active power filter:

In three-phase, three-wire (3P3W) distribution systems without neutral wire are used to provide supply for high-power loads such as adjustable speed drives, transactions, arc furnaces, and other industrial applications [75] [76]. For compensation of harmonics and reactive power in these systems, a 3P3W APF is used. **Figure 1.20** shows the connection of APF for reactive and harmonic current compensation in 3P3W distribution system

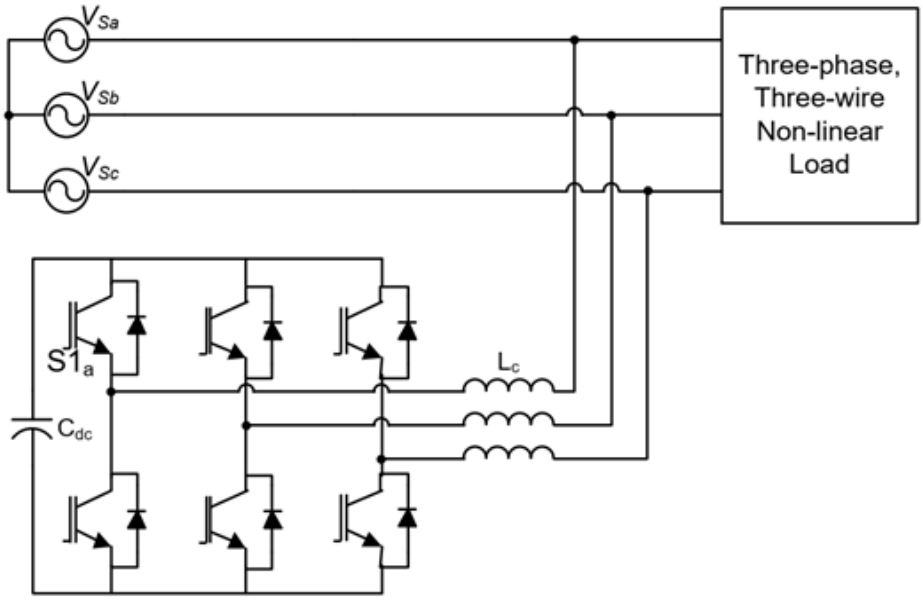

Figure 1.20: Three-phase, Three-wire active power filter

III.2.4 Three-phase, Four-wire active power filter:

APFs are specially designed to 3P4W systems for compensating neutral current along with the necessary compensation features of the 3P3W APFs. Three different topologies are available for 3P4W systems and are given below:

III.2.4.1 Three-phase, Four-wire split capacitor APF Topology The three-leg split capacitor APF topology utilizes the standard three-phase conventional inverter where the dc side capacitor is split and the neutral wire is directly connected to the electrical midpoint of the capacitors through an inductance. **Figure 1.21** shows the split capacitor APF topology used in 3P4W system and also known as midpoint clamped topology [77]. The split capacitors allow load neutral current to flow through one of the dc capacitors C_{dc1}, C_{dc2} and return to the ac neural wire. The split capacitor topology suffers from voltage balancing, control complexity and two large dc capacitors [78].

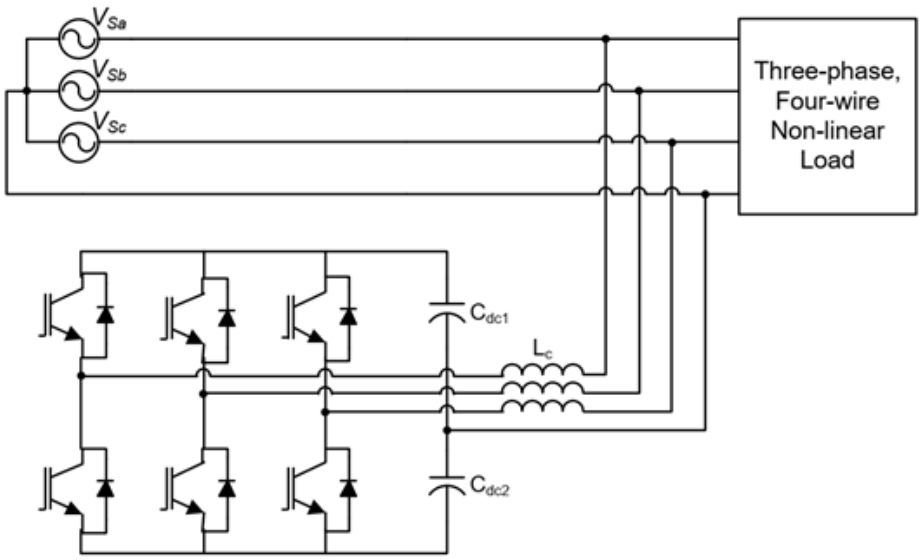

Figure 1.21: Three-phase, Four-wire split capacitor APF

III.2.4.2 Three-phase, Four-wire Four-leg APF Topology: **Figure 1.22** shows the four-leg or four pole APF topologies used in 3P4W system. In this topology, three of the switch legs are connected to the three phase conductors through a series inductance while the fourth leg is exclusively connected to the neutral conductor with an inductor [79] [80]. This topology is most suitable for compensation of high neutral currents. Despite having higher number of switching devices this topology, outweighed the split capacitor topology by number of factors [81]:

- Better controllability: In this topology only one dc-bus voltage needs to be regulated, as opposed to two in the capacitor midpoint topology. This significantly simplifies the control circuitry with better controllability.
- Lower dc voltage and current requirement: This topology requires a lower dc-bus voltage and capacitor current.

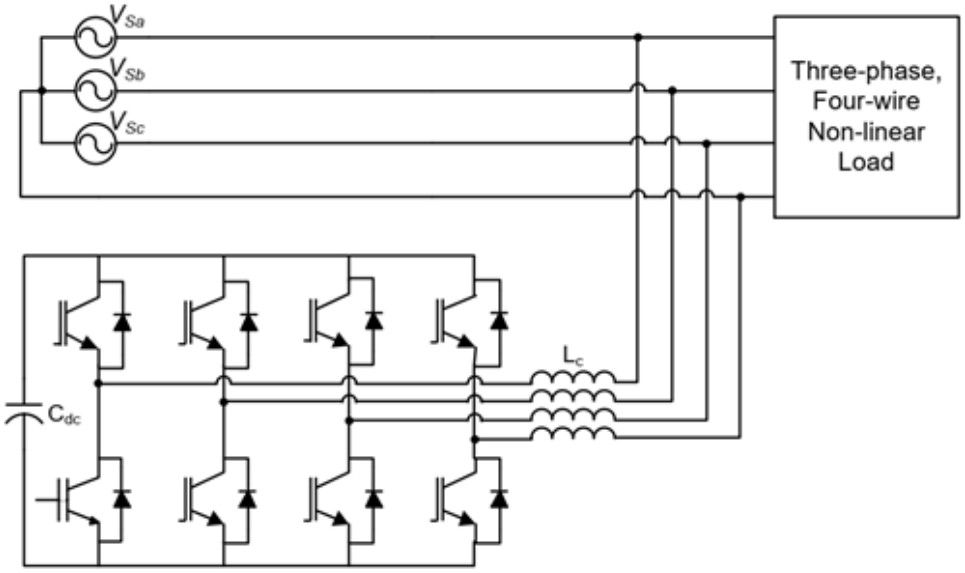

Figure 1.22: Three-phase, Four-wire Four-leg APF

III.2.5 Hybrid Active Filter:

Hybrid filter topologies are generally classified as series active filter & shunt passive filter, shunt active filter & shunt passive filter and active power filter is in series with shunt passive filter [66]. In HAPF topology 1 **Figure 1.23** active power filter is connected in series with distribution power system through filtering inductor & capacitor . In this APF acts as a harmonic isolator and forces all the harmonic current to flow through PPF [64].

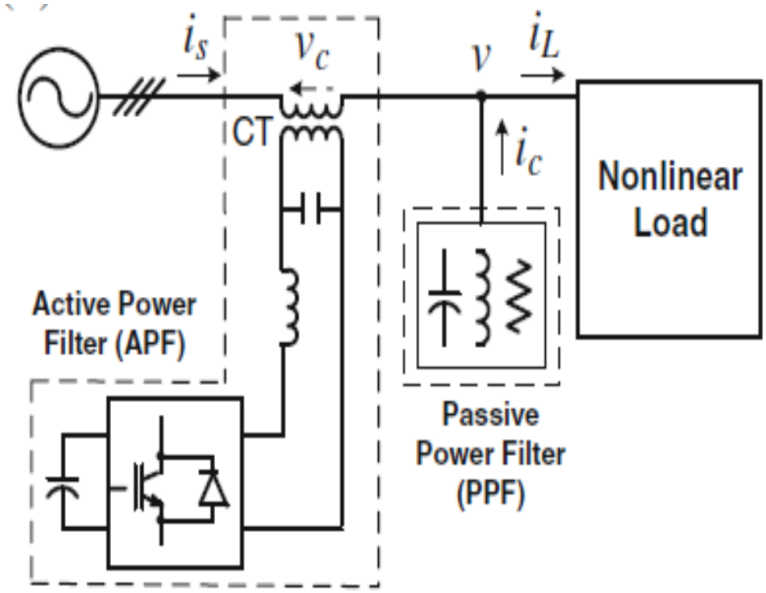

Figure 1.23: Series active and shunt passive filter

In topology 2 **Figure 1.24** PPF acts as main harmonic compensator and active power filter is used for compensating the remaining harmonic currents. Another advantage of this system is shunt active filter is applicable if shunt passive filter is existing and reactive power is controllable [82].

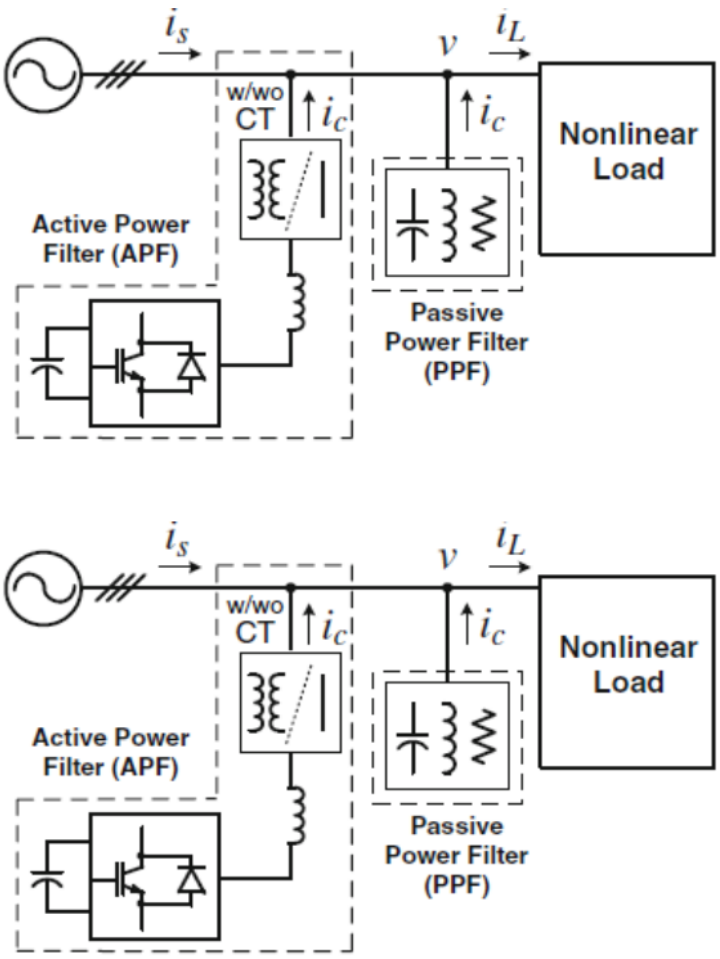

Figure 1.24: Shunt active and shunt passive filter

In the third topology **Figure 1.25** APF and PPF connected in series then shunted to distribution power system . When APF and PPF connected in series the fundamental system voltage dropped across the capacitor of PPF . So this topology aims to reduce the voltage rating of APF.

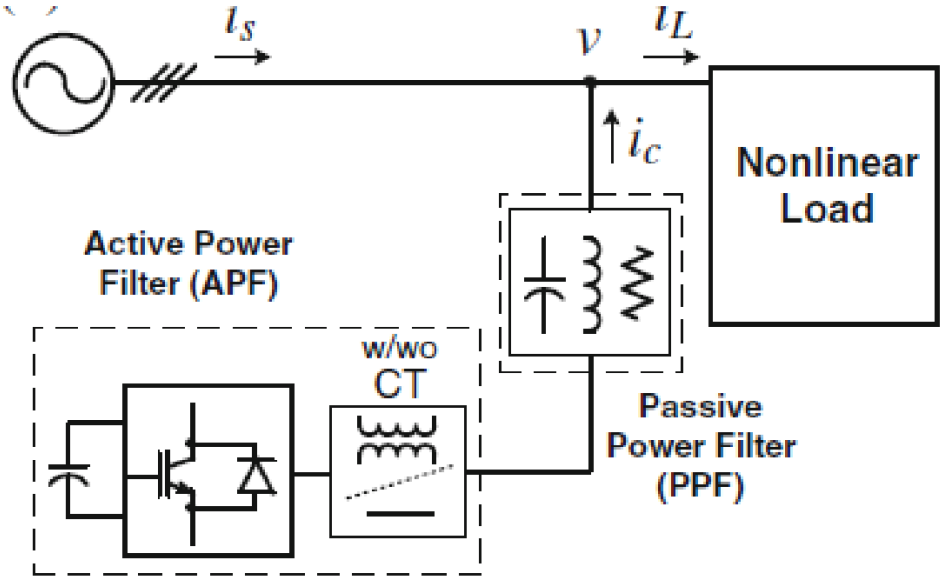

Figure 1.25: Active power filter is in series with shunt passive filter

III.2.6 Unified Power Quality Conditioner:

Combining the functionalites of both the shunt- and series APF, two systems can be connected back to back sharing the same DC bus [83]. The combination of shunt- and series APFs shown in **Figure 1.26** is often referred to as unified power quality conditioner (UPQC) [84].

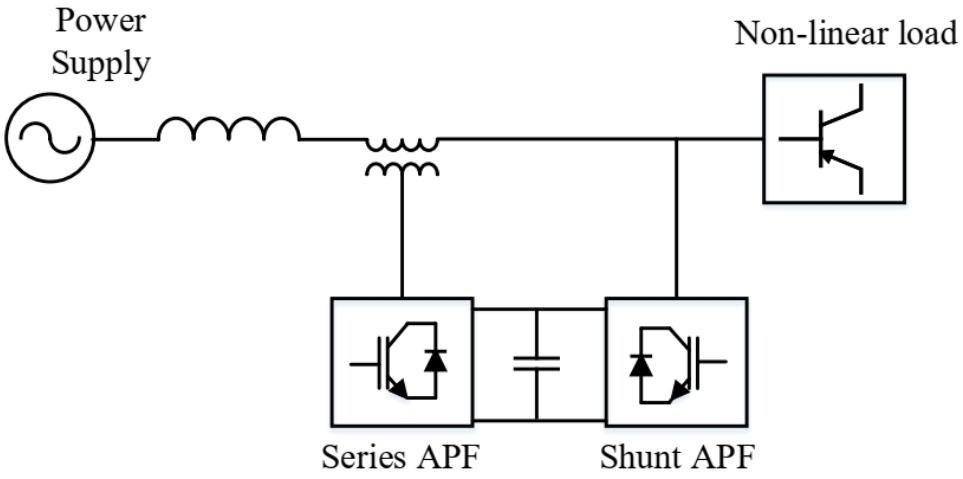

Figure 1.26: Unified power quality conditioner (UPQC) system configuration

IV Motivation:

In recent times the use of non-linear load by electric power consumers has increased to a large extent. Such loads introduce harmonics and other power quality problems thus affecting the power quality. Furthermore, the demand of energy saving appliances in recent years has also increased. The use of such smart appliances also adds harmonics to the power system. The polluted grid will result in more energy losses and cost of electric supply will considerably increase. Power quality is affected mainly by the current harmonics that gives a motivation for this research. The harmonics free supply will result in high efficiency and improved power factor thus energy saving and reduced cost objectives will be achieved.

V Scope of the Thesis:

The scope of this thesis covers the following points.

- Assessment of the impact of harmonics on power and need for harmonic compensation.
- Identification of problems affecting the power quality and harmonics mitigation techniques.
- Analysis of the impact of non-ideal grid conditions on the performance of SAPF.
- Analysis of the performance of phase locked loop techniques under various grid disturbances.
- Development of an improved reference current generation technique with added synchronization feature.

- Identification of the importance of DC link voltage regulation in the current injection process.
- Analysis of the effects of synchronization techniques on the performance of SAPF.
- Identification of the constraints of using APF without synchronizing it with the grid voltage under adverse grid conditions.
- Conclusion of the research work accomplished in this thesis and giving recommendations for future work

VI Thesis Outline:

- **Chapter 1:** In this chapter power quality is defined and its importance in modern power distribution system is explained. Different issues affecting the power quality are briefly overviewed. Harmonics issue and the existing techniques for its mitigation are also briefly discussed. SAPF which is the research aim of this thesis is explained in detail. Motivation of the research and objectives and scope are also stated in this chapter.
- **Chapter 2:** This chapter discusses the techniques used for reference current generation. Mathematical model of SAPF is also developed here. Time domain and frequency domain techniques are studied and are evaluated in simulation by adding the reference current to the distorted source current to get a sinusoidal waveform. A low value of THD of the compensated source current will show the accuracy of the observed technique. This chapter deals with the current injection part of active power filters. An overview of four control techniques is presented which are used to generate gating signals for voltage source inverter in order to inject the reference current at the point of common coupling. The regulation of DC link capacitor voltage is briefly studied too in this chapter.
- **Chapter 3:** In this chapter, The simulation results of four control methods, are performed using Matlab—Simulink Power Blockset ToolBox. They are realised in the same conditions, with the same parameters for the system and control so as the obtained results can be compared with each other.
- **Chapter 4:** In this chapter, a three-level four-legged active power filter based on a neutral-point-clamped (NPC) inverter is presented. To fulfill the requirement of the active power filtering function under balanced, unbalanced, and distorted (including 3rd and 5th harmonics) power supply voltages, a control method based on the instantaneous power theory has been used and discussed. On the other side, the inverter switching state control has been achieved based on PWM current controller. The performance of the proposed topology under the control approach has been finally discussed through the obtained simulation results.
- **Chapter 5:** This chapter concludes the research work and few recommendations for future work are also stated.

VII Summary:

In this chapter the importance of power quality has been highlighted and various power quality problems are explained. Impact of these problems on power qulaity is stud-

ied. Among the various problems, harmonics and its drawbacks are discussed in detail. Furthermore, a brief overview of both passive and active techniques used for harmonics mitigation is presented. A detailed discussion on the working of shunt active power filter, highlighting its different parts is presented. In summary, shunt active power filter is being recognized as the best solution for mitigation of current harmonics. Furthermore, the control techniques used for reference current generation and current injection have a vital role to play in the performance enhancement of SAPF.
The following chapter presents the review of contributions made by different researchers in developing control techniques for active power filters.

Chapter 2

Shunt Active Power Filter for Three-Phase, Four-Wire Systems

I Introduction:

A large number of residential and industrial single-phase loads are supplied from three phase mains with neutral conductor where single-phase load is connected between phase to neutral. Although single phase loads try to be distributed equally between phases, however, they cause excessive neutral current, harmonic and reactive power burden, and unbalance that sum up in neutral conductor and produce high neutral current with harmonics in system. Three-phase three wires STATCOMs and APFs are not able to deal with this problem then, three-phase four wires scheme was investigated and well-designed to accompany with neutral current [85].
This chapter presents three-phase, four-wire voltage source shunt active power filter for the compensation of current harmonics and reactive power present in a non-ideal supply voltage distribution system. The control scheme is based on sensing supply voltage, load and supply current. Balanced and sinusoidal component of supply voltage is derived using symmetrical component theory and fundamental tuned filter control algorithm, respectively. Average power is calculated to compute desired component of supply. A PI controller is used to control DC link voltage. PWM current controller is used for generating switching signals for VSI. The performance of control algorithm is validated with simulation results for different loading conditions [86].

II Reference Current Generation:

The reference current has a vital role to play in active power filtering. The accurate generation of reference current is the first main target in active power filtering and is a key to attain superior performance of the filter in reducing harmonic distortion [87]. In this section a brief overview of various reference current generation techniques is presented **Figure 2.1**.

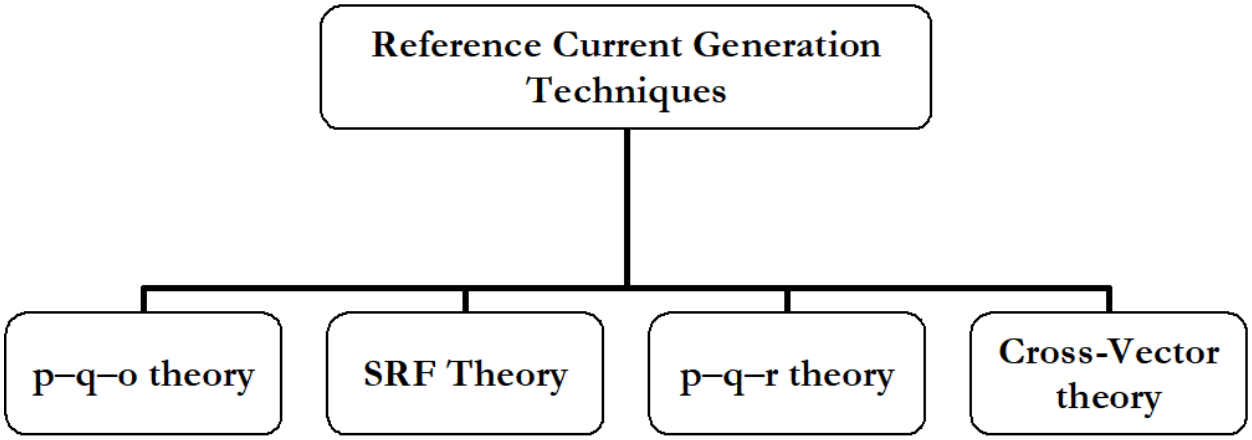

Figure 2.1: Reference Current Generation Techniques

II.1 P-Q-O Theory:

The clearly knowing about the physical meaning of all instantaneous powers is an important key to develop control circuits for current or voltage compensation used in active power filters. **Figure 2.2** summarizes the concepts involved in these powers [88]. Three concepts are necessary to understand the physical meaning of the instantaneous powers defined in the $\alpha\beta o$ reference frame.

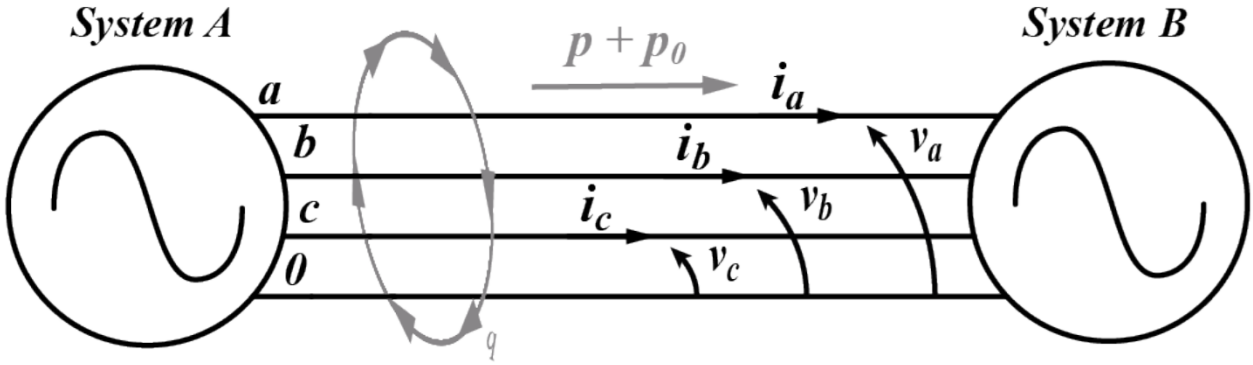

Figure 2.2: Physical meaning of instantaneous powers.

Zero-sequence components in the fundamental voltage and current and/or in the harmonics do not contribute to the real power p or the imaginary power q.
Total instantaneous energy flow per time unit (three phases instantaneous active power), even in a distorted and unbalanced system, is always equal to the sum of the real power and the zero-sequence power ($P_{3\phi} = P + P_0$), and may contain average and oscillating parts.
The imaginary power q , independent of the presence of harmonic or unbalance, represents the energy quantity that is being exchanged between the phases of the system. This means that the imaginary power does not contribute to energy transfer between the source and the load at any time [89].
The $\alpha\beta o$ transformation also called Clarke transformation is used to deal properly with zero-sequence voltage and current components that are separated from the $\alpha\beta$ components, and treated as" single-phase variables" [90]. The Clarke transformation and the inverse Clarke transformation for currents components are given by

$$\begin{bmatrix} i_\alpha \\ i_\beta \\ i_o \end{bmatrix} = \sqrt{\frac{2}{3}} \begin{bmatrix} 1 & -\frac{1}{2} & -\frac{1}{2} \\ 0 & \frac{\sqrt{3}}{2} & -\frac{\sqrt{3}}{2} \\ \sqrt{\frac{1}{2}} & \sqrt{\frac{1}{2}} & \sqrt{\frac{1}{2}} \end{bmatrix} \begin{bmatrix} i_a \\ i_b \\ i_c \end{bmatrix} \tag{2.1}$$

$$\begin{bmatrix} i_a \\ i_b \\ i_c \end{bmatrix} = \sqrt{\frac{2}{3}} \begin{bmatrix} 1 & 0 & \sqrt{\frac{1}{2}} \\ -\frac{1}{2} & \sqrt{\frac{3}{2}} & \sqrt{\frac{1}{2}} \\ -\frac{1}{2} & -\sqrt{\frac{3}{2}} & \sqrt{\frac{1}{2}} \end{bmatrix} \begin{bmatrix} i_\alpha \\ i_\beta \\ i_o \end{bmatrix} \tag{2.2}$$

Similarly, voltages are obtained

$$\begin{bmatrix} v_\alpha \\ v_\beta \\ v_o \end{bmatrix} = \sqrt{\frac{2}{3}} \begin{bmatrix} 1 & -\frac{1}{2} & -\frac{1}{2} \\ 0 & \frac{\sqrt{3}}{2} & -\frac{\sqrt{3}}{2} \\ \sqrt{\frac{1}{2}} & \sqrt{\frac{1}{2}} & \sqrt{\frac{1}{2}} \end{bmatrix} \begin{bmatrix} v_a \\ v_b \\ v_c \end{bmatrix} \tag{2.3}$$

$$\begin{bmatrix} v_a \\ v_b \\ v_c \end{bmatrix} = \sqrt{\frac{2}{3}} \begin{bmatrix} 1 & 0 & \sqrt{\frac{1}{2}} \\ -\frac{1}{2} & \sqrt{\frac{3}{2}} & \sqrt{\frac{1}{2}} \\ -\frac{1}{2} & -\sqrt{\frac{3}{2}} & \sqrt{\frac{1}{2}} \end{bmatrix} \begin{bmatrix} v_\alpha \\ v_\beta \\ v_o \end{bmatrix} \tag{2.4}$$

And the neutral current is equal to:

$$\begin{aligned} i_n &= i_a + i_b + i_c \\ i_o &= \tfrac{1}{\sqrt{3}}(i_a + i_b + i_c) = \tfrac{1}{\sqrt{3}} i_n \end{aligned}$$

The zero-sequence instantaneous real power p_o, the $\alpha\beta$ instantaneous real and imaginary power, p and q, are defined as follows:

$$\begin{bmatrix} p \\ q \\ p_o \end{bmatrix} = \begin{bmatrix} v_\alpha & v_\beta & 0 \\ -v_\beta & v_\alpha & 0 \\ 0 & 0 & v_o \end{bmatrix} \begin{bmatrix} i_\alpha \\ i_\beta \\ i_o \end{bmatrix} \tag{2.5}$$

Both the instantaneous powers p , q and p_o include an average component ($\overline{p}$, $\overline{q}$, $\overline{p_o}$) and an oscillating component ($\widetilde{p}$, $\widetilde{q}$, $\widetilde{p_o}$), which can be described as

$$\begin{bmatrix} p \\ q \\ p_o \end{bmatrix} = \begin{bmatrix} \bar{p} + \tilde{p} \\ \bar{q} + \tilde{q} \\ \bar{p_o} + \tilde{p_o} \end{bmatrix} \tag{2.6}$$

From equation (**2.5**), we can deduce the corresponding current components:

$$\begin{bmatrix} i_\alpha \\ i_\beta \\ i_o \end{bmatrix} = \begin{bmatrix} v_\alpha & v_\beta & 0 \\ -v_\beta & v_\alpha & 0 \\ 0 & 0 & v_o \end{bmatrix}^{-1} \begin{bmatrix} p \\ q \\ p_o \end{bmatrix} \tag{2.7}$$

the currents in $\alpha\beta o$ co-ordinates will become:

$$\begin{bmatrix} i_\alpha \\ i_\beta \\ i_o \end{bmatrix} = \frac{1}{v_o\left(v_\alpha^2 + v_\beta^2\right)} \begin{bmatrix} v_o v_\alpha & -v_o v_\beta & 0 \\ v_o v_\beta & v_o v_\alpha & 0 \\ 0 & 0 & \left(v_\alpha^2 + v_\beta^2\right) \end{bmatrix} \begin{bmatrix} p \\ q \\ p_o \end{bmatrix} \tag{2.8}$$

Depending on the function you want to give to the active filter, you can compensate the harmonic current and /or reactive power. **Table 2.1** gives different compensation objectives and their corresponding references.

Table 2.1: Different compensation objectives and their corresponding references

Compensation Objectives	p_{ref}	q_{ref}	Features and Considerations
Harmonic Current	$\widetilde{p}$	$\widetilde{q}$	Source current will become sinusoidal and positive- sequence if the voltage is relatively sinusoidal. Energy storage is needed and the required storage capacity is determined by $\widetilde{p}$
Instantaneous Reactive Power	0	q	No need of energy storage for a compensator consisting of PWM converter under any (balanced or unbalanced, distorted or sine-wave) conditions.
Reactive Power & Harmonics	$\widetilde{p}$	q	Source current will become instantaneously unity power-factor. In addition it will become sine wave for a relatively low distorted voltage.

In order to extract the Reactive Power & Harmonics currents, which will be injected by the APF, the continuous component, $\bar{p}$, should be eliminated. Thus, the currents in $\alpha\beta o$ co-ordinates equation (**2.8**) will become:

$$\begin{bmatrix} i_\alpha \\ i_\beta \\ i_o \end{bmatrix} = \frac{1}{v_o\left(v_\alpha^2 + v_\beta^2\right)} \begin{bmatrix} v_o v_\alpha & -v_o v_\beta & 0 \\ v_o v_\beta & v_o v_\alpha & 0 \\ 0 & 0 & \left(v_\alpha^2 + v_\beta^2\right) \end{bmatrix} \begin{bmatrix} \widetilde{p} \\ q \\ p_o \end{bmatrix} \tag{2.9}$$

II.1.1 Improved P-Q-O Theory with PLL:

The main drawback of the proposed theories is when the voltages in the electrical network are disturbed by harmonics and/or unbalanced. To overcome this problem, a PLL in the control loop is used [91].
PLL systems are used in different industrial fields such as motor drives, induction heating and power supplies. Also, in the field of renewable energy integration, PLL systems have been used for synchronization process between grid-interfaced converters and the utility network even under unbalanced harmonic grid voltage [92]. When the network has high distorted current and unbalanced loads, A phase-locked loop is used to calculate the reference current. A PLL consists of three control units that individually control

frequency, load current and voltage source. In control frequency unit, the fundamental frequency of the pure sinusoidal signal is extracted as shown in **Figure 2.3**. [93].

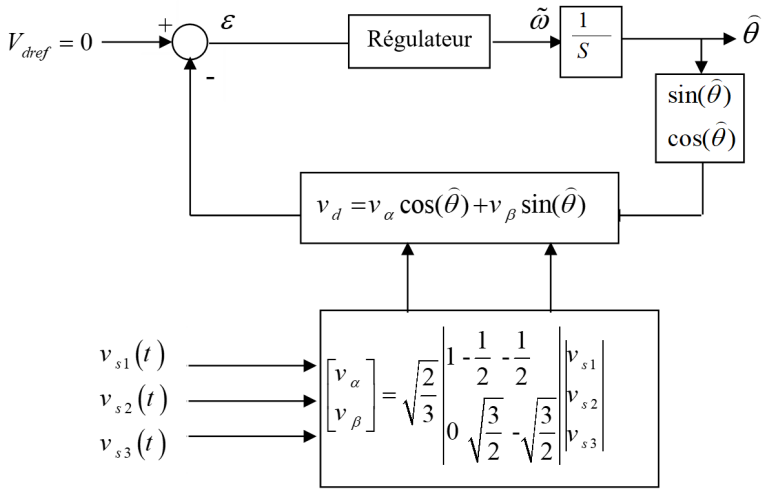

Figure 2.3: Phase locked loop circuit.

The PLL generates balanced and sinusoidal signals, perfectly in phase with the electrical network voltages. They will be directly generated in the $\alpha\beta$ co-ordinates illustrated by the following expressions:

$$\begin{cases} v_\alpha = \sqrt{3} V_s \sin(\omega t) \\ v_\beta = \sqrt{3} V_s \cos(\omega t) \end{cases} \tag{2.10}$$

The $\alpha\beta$ instantaneous real and imaginary powers are:

$$\begin{bmatrix} p \\ q \end{bmatrix} = \begin{bmatrix} v_\alpha & v_\beta \\ -v_\beta & v_\alpha \end{bmatrix} \begin{vmatrix} i_\alpha \\ i_\beta \end{vmatrix} \tag{2.11}$$

It should be remarked that the zero-sequence instantaneous real power $p_\emptyset$ is equal to zero in this case because the voltage $v_\emptyset$ is equal to zero.
To obtain the current harmonics, which will be injected by the active power filter, the continuous component of the instantaneous active power is filtered:

$$\begin{bmatrix} i_\alpha \\ i_\beta \\ i_0 \end{bmatrix} = \begin{bmatrix} v_\alpha & -v_\beta & 0 \\ v_\beta & v_\alpha & 0 \\ 0 & 0 & 1 \end{bmatrix} \begin{bmatrix} \tilde{p} \\ q \\ i_0 \end{bmatrix} \tag{2.12}$$

By retransforming from $\alpha\beta o$ co-ordinates to abc coordinates, one obtains:

$$\begin{bmatrix} i_{aref} \\ i_{bref} \\ i_{cref} \end{bmatrix} = \sqrt{\frac{2}{3}} \begin{bmatrix} 1 & 0 & \frac{1}{\sqrt{2}} \\ -\frac{1}{2} & \frac{\sqrt{3}}{2} & \frac{1}{\sqrt{2}} \\ -\frac{1}{2} & -\frac{\sqrt{3}}{2} & \frac{1}{\sqrt{2}} \end{bmatrix} \begin{bmatrix} i_\alpha \\ i_\beta \\ i_0 \end{bmatrix} \tag{2.13}$$

and the neutral current is equal to:

$$i_n = -(i_{aref} + i_{bref} + i_{cref}) \tag{2.14}$$

II.2 Cross-Vector Theory:

The Cross-Vector theory is a modified *pqo* theory, and differs from only in the mapping matrices [94]. Consider a three-phase four-wire system including zero-sequence voltage and zero-sequence current. The instantaneous powers will be defined as follows:

$$\begin{vmatrix} p \\ q_o \\ q_\alpha \\ q_\beta \end{vmatrix} = \begin{vmatrix} v_o & v_\alpha & v_\beta \\ 0 & -v_\beta & v_\alpha \\ v_\beta & 0 & -v_o \\ -v_\alpha & v_o & 0 \end{vmatrix} \begin{vmatrix} i_o \\ i_\beta \\ i_\alpha \end{vmatrix} \tag{2.15}$$

the currents in $\alpha\beta o$ co-ordinates will become:

$$\begin{vmatrix} i_0 \\ i_\alpha \\ i_\beta \end{vmatrix} = \frac{1}{\sqrt{v_\alpha^2 + v_\beta^2 + v_o^2}} \begin{vmatrix} v_o & 0 & v_\beta & v_\alpha \\ v_\alpha & -v_\beta & 0 & v_o \\ v_\beta & v_\alpha & -v_o & 0 \end{vmatrix} \begin{vmatrix} p \\ q_o \\ q_\alpha \\ q_\beta \end{vmatrix} \tag{2.16}$$

Depending on the function you want to give to the active filter, you can compensate the harmonic current and /or reactive power. **Table 2.2** gives different compensation objectives and their corresponding references.

Table 2.2: Different compensation objectives and their corresponding references

Compensation Objectives	p_{ref}	$q_{\alpha ref}$	$q_{\beta ref}$	$q_{o ref}$
Harmonic Current	$\widetilde{p}$	$\widetilde{q}_\alpha$	$\widetilde{q}_\beta$	$\widetilde{q}_o$
Instantaneous Reactive Power	0	$\bar{q}_o$		
Reactive Power & Harmonics	$\widetilde{p}$	q_α	q_β	q_o

In order to extract the Reactive Power & Harmonics currents, which will be injected by the APF, the continuous component, $\bar{p}$, should be eliminated. Thus, the currents in $\alpha\beta o$ co-ordinates equation (**2.17**) will become:

$$\begin{vmatrix} i_0 \\ i_\alpha \\ i_\beta \end{vmatrix} = \frac{1}{\sqrt{v_\alpha^2 + v_\beta^2 + v_o^2}} \begin{vmatrix} v_o & 0 & v_\beta & v_\alpha \\ v_\alpha & -v_\beta & 0 & v_o \\ v_\beta & v_\alpha & -v_o & 0 \end{vmatrix} \begin{vmatrix} \widetilde{p} \\ q_o \\ q_\alpha \\ q_\beta \end{vmatrix} \tag{2.17}$$

II.2.1 Improved Cross-Vector Theory:

For the cross-vector theory, the new approach gives:

$$\begin{bmatrix} p \\ q_0 \\ q_\alpha \\ q_\beta \end{bmatrix} = \sqrt{3}V \begin{bmatrix} 0 & \sin(\omega t) & -\cos(\omega t) \\ 0 & \cos(\omega t) & \sin(\omega t) \\ -\cos(\omega t) & 0 & 0 \\ -\sin(\omega t) & 0 & 0 \end{bmatrix} \begin{bmatrix} i_0 \\ i_\alpha \\ i_\beta \end{bmatrix} \tag{2.18}$$

the currents in $\alpha\beta o$ co-ordinates will become:

$$\begin{vmatrix} i_o \\ i_\alpha \\ i_\beta \end{vmatrix} = \frac{1}{\sqrt{3}V} \begin{bmatrix} 0 & 0 & -\cos(\omega t) & -\sin(\omega t) \\ \sin(\omega t) & \cos(\omega t) & 0 & 0 \\ -\cos(\omega t) & \sin(\omega t) & 0 & 0 \end{bmatrix} \begin{bmatrix} \tilde{p} \\ q_0 \\ q_\alpha \\ q_\beta \end{bmatrix} \tag{2.19}$$

By retransforming from $\alpha\beta o$ co-ordinates to *abc* coordinates, one obtains:

$$\begin{bmatrix} i_{aref} \\ i_{bref} \\ i_{cref} \end{bmatrix} = \sqrt{\frac{2}{3}} \begin{bmatrix} 1 & 0 & \frac{1}{\sqrt{2}} \\ -\frac{1}{2} & \frac{\sqrt{3}}{2} & \frac{1}{\sqrt{2}} \\ -\frac{1}{2} & -\frac{\sqrt{3}}{2} & \frac{1}{\sqrt{2}} \end{bmatrix} \begin{bmatrix} i_\alpha \\ i_\beta \\ i_0 \end{bmatrix} \tag{2.20}$$

and the neutral current is equal to:

$$i_n = -(i_{aref} + i_{bref} + i_{cref}) \tag{2.21}$$

II.3 *pqr* Theory:

This identification strategy is based on double transformation, where, a set of voltages (v_a, v_b, v_c) and a set of currents (i_a, i_b, i_c) that are obtained from the three-phase four-wire system are firstly transformed into a three-axis representation $\alpha\beta o$ based on Clark transformation [95].
Here, i_o is the zero-sequence current which is equal to $\frac{1}{3}$ of the neutral current i_n.
The second transformation is achieved by rotating the o-axis of the $\alpha\beta o$ frame by θ_1, aligning the α-axis with the projection line of the voltage space vector to the $\alpha\beta$ plane. The new components of voltage and current in the resulting frame $\alpha'\beta' o$ can be obtained as follows:

$$\begin{bmatrix} i_{\alpha\prime} \\ i_{\beta\prime} \\ i_o \end{bmatrix} = \begin{bmatrix} \cos\theta_1 & \sin\theta_1 & 0 \\ -\sin\theta_1 & \cos\theta_1 & 0 \\ 0 & 0 & 1 \end{bmatrix} \begin{bmatrix} i_\alpha \\ i_\beta \\ i_o \end{bmatrix} \tag{2.22}$$

Which can be expressed in function of voltages components of $\alpha\beta o$ frame

$$\begin{bmatrix} i_{\alpha\prime} \\ i_{\beta\prime} \\ i_o \end{bmatrix} = \begin{bmatrix} \frac{v_\alpha}{v_{\alpha\beta}} & \frac{v_\beta}{v_{\alpha\beta}} & 0 \\ \frac{-v_\beta}{v_{\alpha\beta}} & \frac{v_\alpha}{v_{\alpha\beta}} & 0 \\ 0 & 0 & 1 \end{bmatrix} \begin{bmatrix} i_\alpha \\ i_\beta \\ i_o \end{bmatrix} \tag{2.23}$$

Where:

$$\begin{aligned} v_{\alpha\beta o} &= \sqrt{v_\alpha^2 + v_\beta^2 + v_o^2} \\ v_{\alpha\beta} &= \sqrt{v_\alpha^2 + v_\beta^2} \end{aligned} \tag{2.24}$$

The new frame *pqr* can be obtained by the third transformation by rotating the β-axis of the $\beta'\alpha' o$ frame by θ_2 , aligning the α'-axis with the voltage space vector.
The new components of voltage and current in the new frame *pqr* can be obtained as follows:

$$\begin{bmatrix} i_p \\ i_q \\ i_r \end{bmatrix} = \begin{bmatrix} \cos\theta_2 & 0 & \sin\theta_2 \\ 0 & 1 & 0 \\ -\sin\theta_2 & 0 & \cos\theta_2 \end{bmatrix} \begin{bmatrix} i_{\alpha\prime} \\ i_{\beta\prime} \\ i_o \end{bmatrix} \tag{2.25}$$

Which can once be expressed in function of voltages components of $\alpha\beta o$ frame

$$\begin{bmatrix} i_p \\ i_q \\ i_r \end{bmatrix} = \begin{bmatrix} \frac{v_\alpha}{v_{\alpha\beta o}} & 0 & \frac{v_o}{v_{\alpha\beta o}} \\ 0 & 1 & 0 \\ \frac{-v_\beta}{v_{\alpha\beta o}} & 0 & \frac{v_{\alpha\beta}}{v_{\alpha\beta o}} \end{bmatrix} \begin{bmatrix} i_{\alpha\prime} \\ i_{\beta\prime} \\ i_o \end{bmatrix} \tag{2.26}$$

Where:

$$v_{\alpha\beta o} = \sqrt{v_\alpha^2 + v_\beta^2 + v_o^2} \tag{2.27}$$

It is important to note that the β'-axis and the p-axis are identical. On the other side, the three axes are mutually perpendicular to each other. The p-axis is always aligned with the system voltage space vector. The q-axis is located on the surface of $\alpha\beta$ plane. The r-axis is perpendicular to the p-axis and q-axis and it oscillates with an angle= $\tan^{-1}(e_o/e_{\alpha\beta})$ from the o-axis. The rotating speed of pqr coordinates vary according to the voltage space vector system [96]. the second and the third transformation applied to the voltages and currents can be combined to one transformation from the $\alpha\beta o$ frame to the pqr frame as follows:

$$\begin{bmatrix} i_p \\ i_q \\ i_r \end{bmatrix} = \begin{bmatrix} \frac{v_\alpha}{v_{\alpha\beta o}} & \frac{v_\beta}{v_{\alpha\beta o}} & \frac{v_o}{v_{\alpha\beta o}} \\ \frac{-v_\beta}{v_{\alpha\beta}} & \frac{v_\alpha}{v_{\alpha\beta}} & 0 \\ \frac{-v_\alpha v_o}{v_{\alpha\beta} v_{\alpha\beta o}} & \frac{-v_\beta v_o}{v_{\alpha\beta} v_{\alpha\beta o}} & \frac{v_{\alpha\beta}}{v_{\alpha\beta o}} \end{bmatrix} \begin{bmatrix} i_\alpha \\ i_\beta \\ i_o \end{bmatrix} \tag{2.28}$$

$$\begin{bmatrix} v_p \\ v_q \\ v_r \end{bmatrix} = \begin{bmatrix} \frac{v_\alpha}{v_{\alpha\beta o}} & \frac{v_\beta}{v_{\alpha\beta o}} & \frac{v_o}{v_{\alpha\beta o}} \\ \frac{-v_\beta}{v_{\alpha\beta}} & \frac{v_\alpha}{v_{\alpha\beta}} & 0 \\ \frac{-v_{\alpha\alpha} v_o}{v_{\alpha\beta} v_{\alpha\beta o}} & \frac{-v_\beta v_o}{v_{\alpha\beta} v_{\alpha\beta o}} & \frac{v_{\alpha\beta}}{v_{\alpha\beta o}} \end{bmatrix} \begin{bmatrix} v_{a\beta o} \\ 0 \\ 0 \end{bmatrix} \tag{2.29}$$

Where:

$$v_{a\beta o} = \sqrt{v_a^2 + v_\beta^2 + v_o^2} \tag{2.30}$$

From equation (2.29), it is obvious that the only existing voltage is along the p-axis, the other two components along q-axis and r-axis are equal to zero [97], [98]. The p-axis voltage is expressed as follows:

$$v_p = v_{\alpha\beta o} = \sqrt{v_\alpha^2 + v_\beta^2 + v_o^2} \tag{2.31}$$

The instantaneous power $p(t)$ is a scalar presenting the scalar product of the voltage and current vectors in pqr coordinates and the instantaneous reactive power $q(t)$ is a vector presenting the vector product of the same components. These are expressed as follows:

$$p = \overrightarrow{v_{pqr}} \cdot \overrightarrow{i_{pqr}} = v_p i_p \tag{2.32}$$

$$q = \overrightarrow{v_{pqr}} \times \overrightarrow{i_{pqr}} = \begin{vmatrix} 0 \\ -v_p i_r \\ v_p i_q \end{vmatrix} \tag{2.33}$$

Three components are obtained for the instantaneous power, one component is corresponding to the active power $p(t)$, where as the two other components are corresponding to the reactive power $q_q(t)$ and $q_r(t)$:

$$\begin{bmatrix} p \\ q_q \\ q_r \end{bmatrix} = \begin{bmatrix} v_p i_p \\ -v_p i_r \\ v_p i_q \end{bmatrix} \tag{2.34}$$

From the above equation, it is clear that the three instantaneous powers are linearly independent. Thus, the three current components following the three axes p, q and r can be controlled independently based on the corresponding instantaneous power respectively. Moreover, it is clear that each instantaneous power is defined in the same way as a single-phase system. The current i_p is used for the control of the instantaneous active power present in the power system. The current i_r is used to control the reactive power associated with zero sequence current or the neutral current present in the three-phase

four-wire system [99]. The current i_q is used to control the instantaneous reactive power associated with conventional reactive power as well as the power associated with the negative sequence component and the harmonics presented in the power system [100].

Depending on the function you want to give to the active filter, you can compensate the harmonic current and /or reactive power. **Table 2.3** gives different compensation objectives and their corresponding references.

Table 2.3: Different compensation objectives and their corresponding references

Compensation Objectives	p_{ref}	q_{refr}	q_{refq}
Harmonic Current	$\widetilde{p}$	$\widetilde{q}_r$	$\widetilde{q}_q$
Reactive Power & Harmonics	$\widetilde{p}$	q_r	q_q

In order to extract the Reactive Power & Harmonics currents, which will be injected by the APF, the continuous component of the three instantaneous powers should not be taken into account. Thus, the reference currents in $\alpha\beta o$ coordinates can be obtained as follows:

$$\begin{bmatrix} i_\alpha^{ref} \\ i_\beta^{ref} \\ i_o^{ref} \end{bmatrix} = \frac{1}{v_{\alpha\beta o}} \begin{bmatrix} \frac{v_\alpha}{v_{\alpha\beta o}} & \frac{v_\beta}{v_{\alpha\beta o}} & \frac{v_o}{v_{\alpha\beta o}} \\ \frac{-v_\beta}{v_{\alpha\beta}} & \frac{v_\alpha}{v_{\alpha\beta}} & 0 \\ \frac{v_\alpha v_o}{v_{\alpha\beta} v_{\alpha\beta o}} & \frac{-v_\beta v_o}{v_{\alpha\beta} v_{\alpha\beta o}} & \frac{v_{\alpha\beta}}{v_{\alpha\beta o}} \end{bmatrix} \begin{bmatrix} \tilde{p} \\ \tilde{q}_q \\ q_r \end{bmatrix} \tag{2.35}$$

Whereas, in order to identify the reference current which has to be injected by the APF to ensure the compensation of the current harmonics, the reactive current components and the negative current component the following expression is used:

$$\begin{bmatrix} i_\alpha^{ref} \\ i_\beta^{ref} \\ i_o^{ref} \end{bmatrix} = \frac{1}{v_{\alpha\beta o}} \begin{bmatrix} \frac{v_\alpha}{v_{\alpha\beta o}} & \frac{v_\beta}{v_{\alpha\beta o}} & \frac{v_o}{v_{\alpha\beta o}} \\ \frac{-v_\beta}{v_{\alpha\beta}} & \frac{v_\alpha}{v_{\alpha\beta}} & 0 \\ \frac{-v_\alpha v_o}{v_{\alpha\beta} v_{\alpha\beta o}} & \frac{-v_\beta v_o}{v_{\alpha\beta} v_{\alpha\beta o}} & \frac{v_{\alpha\beta}}{v_{\alpha\beta o}} \end{bmatrix} \begin{bmatrix} \beta \\ q_q \\ q_r \end{bmatrix} \tag{2.36}$$

The main drawback of this theory is that when the voltages of the power system are disturbed by harmonics and/or unbalances the identification of the right reference current is not possible. Therefore, to overcome this problem, a PLL is used within the control loop [101].
The main aim of the PLL is to generate a balanced sine waveform three phase system, perfectly in phase with the fundamental positive component of the power system voltages. Using equation (2.10 and 2.28), it yields to:

$$\begin{bmatrix} i_p \\ i_q \\ i_r \end{bmatrix} = \begin{bmatrix} \sin(\omega t) & -\cos(\omega t) & 0 \\ \cos(\omega t) & \sin(\omega t) & 0 \\ 0 & 0 & 1 \end{bmatrix} \begin{bmatrix} i_\alpha \\ i_\beta \\ i_o \end{bmatrix} \tag{2.37}$$

Under this case, the three instantaneous powers can be expressed as follows:

$$\begin{bmatrix} p \\ q_q \\ q_r \end{bmatrix} = \sqrt{3} V_s \begin{bmatrix} 1 & 0 & 0 \\ 0 & 1 & 0 \\ 0 & 0 & 1 \end{bmatrix} \begin{bmatrix} i_p \\ i_q \\ i_r \end{bmatrix} \tag{2.38}$$

The reference currents in $\alpha\beta o$ coordinates can be identified by the following expression:

$$\begin{bmatrix} i_\alpha^{ref} \\ i_\beta^{ref} \\ i_o^{ref} \end{bmatrix} = \begin{bmatrix} \sin(\omega t) & -\cos(\omega t) & 0 \\ \cos(\omega t) & \sin(\omega t) & 0 \\ 0 & 0 & 1 \end{bmatrix} \begin{bmatrix} \tilde{p} \\ q_q \\ q_r \end{bmatrix} \tag{2.39}$$

Whereas, the reference neutral current is:

$$i_n^{ref} = i_a^{ref} + i_b^{ref} + i_c^{ref} \tag{2.40}$$

This reference neutral current can be existed only if the phases currents are unbalanced and/or are containing the third order harmonics and their multiplies components.

II.4 Synchronous Reference Frame Theory:

In general, the synchronous reference frame is used for three-phase three-wire active filter's control. In this case, the instantaneous real and imaginary power theory introduced by Akagi is used. But the voltages are replaced by two "sine and cosine" signals, with unity magnitude, generated by a PLL. So, the influence of the disturbances of the electrical network is eliminated [102].
For four-wire electrical active power filters, the sine and cosine signals will be also generated by a PLL. The question will be to select one of the previous control theories to be applied.
Indeed, a comparison of simulation results of the three improved control theories gives that the improved *pqr* theory provides better results in term of rms neutral current and THD. But, with regard to the complexity of the control strategy "number of sums and products used in each control", the *pqr* control theory is much more complex than cross vector control theory. Considering these remarks, the improved cross-vector theory has been chosen to be introduced synchronous reference frame theory for three-phase four-wire APF control. Let the sine and cosine signals, with unity magnitude, generated by a robust PLL [103], then the cross-vector theory gives:

$$\begin{bmatrix} i_d \\ i_q \\ i_{q\alpha} \\ i_{q\beta} \end{bmatrix} = \begin{bmatrix} 0 & \sin(\omega t) & -\cos(\omega t) \\ 0 & \cos(\omega t) & \sin(\omega t) \\ -\cos(\omega t) & 0 & 0 \\ -\sin(\omega t) & 0 & 0 \mid \end{bmatrix} \begin{bmatrix} i_0 \\ i_\alpha \\ i_\beta \end{bmatrix} \tag{2.41}$$

As before, by filtering the continuous component of i_d, one can obtain the currents in $\alpha\beta o$ axis first:

$$\begin{bmatrix} i_0 \\ i_\alpha \\ i_\beta \end{bmatrix} = \begin{bmatrix} 0 & 0 & -\cos(\omega t) & -\sin(\omega t) \\ \sin(\omega t) & \cos(\omega t) & 0 & 0 \\ -\cos(\omega t) & \sin(\omega t) & 0 & 0 \end{bmatrix} \begin{bmatrix} \tilde{i}_d \\ i_q \\ i_{q\alpha} \\ i_{q\beta} \end{bmatrix} \tag{2.42}$$

By retransforming from $\alpha\beta o$ co-ordinates to *abc* coordinates, one obtains:

$$\begin{bmatrix} i_{aref} \\ i_{bref} \\ i_{cref} \end{bmatrix} = \sqrt{\frac{2}{3}} \begin{bmatrix} 1 & 0 & \frac{1}{\sqrt{2}} \\ -\frac{1}{2} & \frac{\sqrt{3}}{2} & \frac{1}{\sqrt{2}} \\ -\frac{1}{2} & -\frac{\sqrt{3}}{2} & \frac{1}{\sqrt{2}} \end{bmatrix} \begin{bmatrix} i_\alpha \\ i_\beta \\ i_0 \end{bmatrix} \tag{2.43}$$

and the neutral current is equal to:

$$i_n = -(i_{aref} + i_{bref} + i_{cref}) \tag{2.44}$$

III Current Injection Techniques:

The aim of the control of the VSC is to force the output currents of the inverter to follow their predefined reference currents. The main principle is based on the comparison

between the actual current of the filter with the reference currents generated by the different extraction methods. This section describes two of the most commonly applied control techniques for APF [104].

III.1 Hysteresis Current Control Technique:

With hysteresis control, upper and lower tolerance limits are defined, to include the reference signal in a tolerance band with a width of H. When the current output of the VSC reaches the upper tolerance limit, the switching signal is set to zero, for the output current to decrease. As long as the output current stays within the tolerance band, no switching action is taken, but when the lower limit is reached, the switching signal is set to one accordingly. In **Figure 2.4** this control scheme is shown. To obtain currents with small switching ripples, smaller values of H can be chosen. While this controller is simple in design and provides small reference errors with appropriate tolerance bands, the main drawback of this scheme is a variable switching frequency, which could lead to unwanted resonances [105].

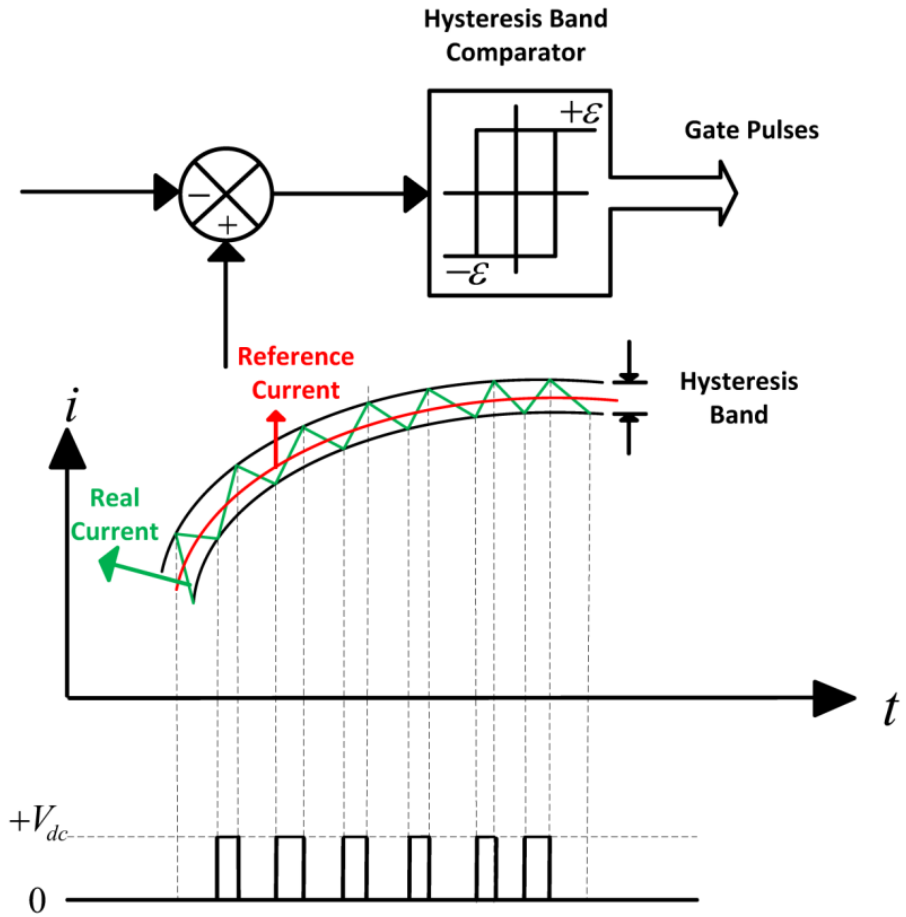

Figure 2.4: Hysteresis control scheme showing the tolerance band and the resulting switching signals.

III.1.1 Advantages of Hysteresis PWM:

- Excellent dynamic response [106].
- Low cost and easy implementation.

III.1.2 Disadvantages of Hysteresis PWM:

- Large current ripple in steady-state [107].
- Variation of switching frequency.
- The modulation process generates sub-harmonic components.

III.2 3 Dimensional Hysteresis PWM Technique:

In a three-legged inverter, there are eight possible switch combinations. With the fourth neutral leg, the total number of switch combinations increases to sixteen, as shown in **Figure 2.5**. Each switching state is specified as the space vector for the output voltage of inverter [108] [109].
The switch combinations are represented by ordered sets $[S_a, S_b, S_c, S_{\mathrm{n}}]$, where $S_a = p$ denotes that the upper switch in phase A, S_{ap}, is closed, and $S_a = n$ denotes that the bottom switch in phase A, S_{an} , is closed. The same notation applies to phase legs B and C and the fourth neutral leg [110] [111].

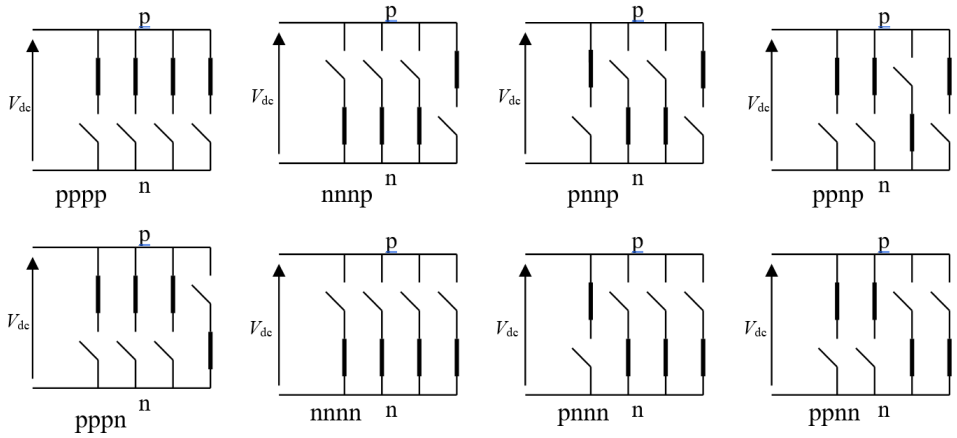

Figure 2.5: Switching states of the three-phase four-leg inverter.

The terminal voltages $[v_{an}, v_{bn}, v_{cn}]^T$ in abc coordinate can be transformed into $[v_\alpha, v_\beta, v_o]^T$ in $\alpha\beta o$ orthogonal coordinate. The results of the transformation are shown in **Table 2.4**. There are fourteen non-zero space voltage vectors **(NZSVV)** and two zero space voltage vectors **(ZSVV)** as shown in **Figure 2.6** [112].

Table 2.4: Switch Combinations in $\alpha\beta o$ orthogonal coordinate

	pppp	nnnp	pnnp	ppnp	npnp	nppp	nnpp	pnpp
$v\alpha$	0	0	$\frac{2v_c}{3}$	$\frac{v_c}{3}$	$\frac{-v_c}{3}$	$\frac{-2v_c}{3}$	$\frac{-v_c}{3}$	$\frac{v_c}{3}$
$v\beta$	0	0	0	$\frac{v_c}{\sqrt{3}}$	$\frac{v_c}{\sqrt{3}}$	0	$\frac{-v_c}{\sqrt{3}}$	$\frac{-v_c}{\sqrt{3}}$
vo	0	$-v_c$	$\frac{-2v_c}{3}$	$\frac{-v_c}{3}$	$\frac{-2v_c}{3}$	$\frac{-v_c}{3}$	$\frac{-2v_c}{3}$	$\frac{-v_c}{3}$
	pppn	nnnn	pnnn	ppnn	npnn	nppn	nnpn	pnpn
$v\alpha$	0	0	$\frac{2v_c}{3}$	$\frac{v_c}{3}$	$\frac{-v_c}{3}$	$\frac{-2v_c}{3}$	$\frac{-v_c}{3}$	$\frac{v_c}{3}$
$v\beta$	0	0	0	$\frac{v_c}{\sqrt{3}}$	$\frac{v_c}{\sqrt{3}}$	0	$\frac{-v_c}{\sqrt{3}}$	$\frac{-v_c}{\sqrt{3}}$
vo	v_c	0	$\frac{v_c}{3}$	$\frac{2v_c}{3}$	$\frac{v_c}{3}$	$\frac{2v_c}{3}$	$\frac{v_c}{3}$	$\frac{2v_c}{3}$

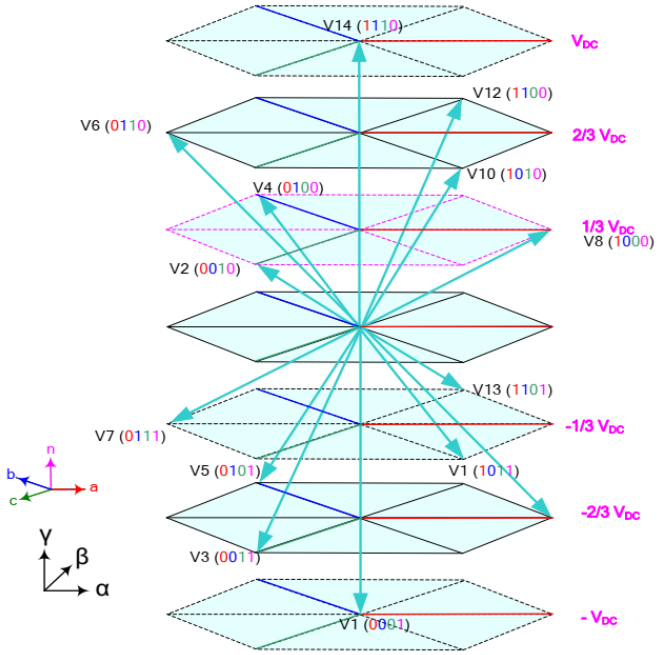

Figure 2.6: Switching vectors in $\alpha\beta o$ coordinate

III.2.1 Principle of the 3 dimensional hysteresis PWM techniques :

The reference current be written with the space vector representation as follows:

$$\vec{i}_f^{ref} = i_{f_\alpha}^{ref}\vec{i} + i_{f_\beta}^{ref}\vec{j} + i_{fo}^{ref}\vec{k} \tag{2.45}$$

The same representation can be given to the measured active filter current:

$$\vec{i}_f = i_{f_\alpha}\vec{i} + i_{f_\beta}\vec{j} + i_{fo}\vec{k} \tag{2.46}$$

The reference current is represented in space voltage vector as shown in **Figure 2.6**, the tip of the reference current $\vec{i}_f^{ref}$ is located at the centre of a three dimensional cube, while the tip of the measured active filter current $\vec{i}_f$ can be located in any cube of the eight small cubes as illustrated in **Figure 2.7**.

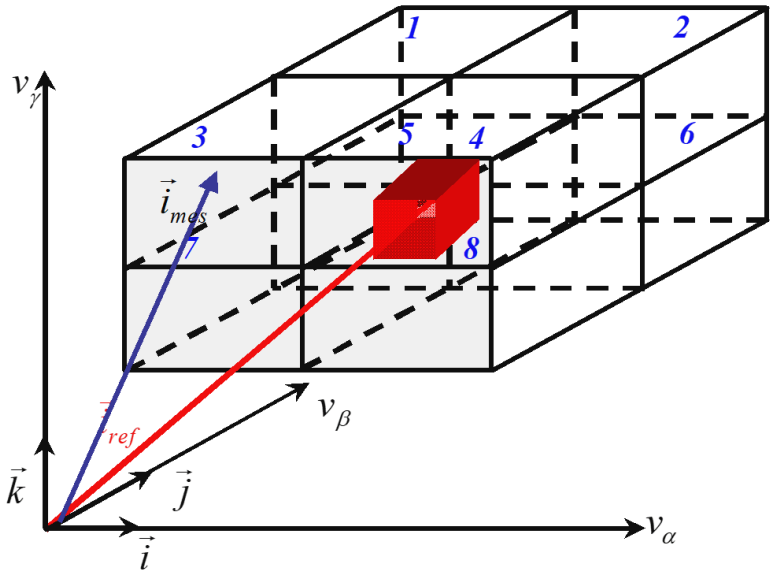

Figure 2.7: Reference current vector representation in $\alpha\beta o$ plane

The error between the reference current and the active filter current, at any sampling time t can be expressed as follows:

$$\begin{bmatrix} \varepsilon_\alpha \\ \varepsilon_\beta \\ \varepsilon_o \end{bmatrix} = \begin{bmatrix} i_{f\alpha}^{ref}(k) - i_{f\alpha}(k) \\ i_{f\beta}^{ref}(k) - i_{f\beta}(k) \\ i_{fo}^{ref}(k) - i_{fo}(k) \end{bmatrix} \tag{2.47}$$

The eight cubes can be determined according to the sign of the calculated error as shown in **Figure 2.8**.
In order to minimise the error, a suitable space voltage vector among the sixteen space voltage vectors should be applied to force the measured vector to be as close as possible to coincide with the reference vector within the hysteresis boundary.
To reduce the switching frequency, the ZSVV $\vec{v}$ (nnnn) and $\vec{v}$ (pppp) must be chosen only when the error vector has the natural tendency to converge toward the hysteresis boundary. This can be verified by satisfying the following conditions:

$$(\varepsilon_\alpha(k).\frac{d\varepsilon_\alpha(k)}{dt} < 0, \varepsilon_\beta(k).\frac{d\varepsilon_\beta(k)}{dt} < 0, \varepsilon_o(k).\frac{d\varepsilon_o(k)}{dt} < 0) \tag{2.48}$$

Moreover the two space voltage vectors $\vec{v}$ (nnnp) and $\vec{v}$ (pppn), which can be considered as a ZSVV regarding to their influence on $\varepsilon_\alpha(k)$ and $\varepsilon_\beta(k)$, can be applied when it is certain that only the errors $\varepsilon_\alpha(k)$ and $\varepsilon_\beta(k)$ have the tendency to converge toward the hysteresis boundary and the $\varepsilon_o(k)$ has the tendency to diverge from the hysteresis boundary. Similarly, this case can be verified by satisfying the following condition:

$$(\varepsilon_\alpha(k).\frac{d\varepsilon_\alpha(k)}{dt} < 0, \varepsilon_\beta(k).\frac{d\varepsilon_\beta(k)}{dt} < 0, \varepsilon_o(k).\frac{d\varepsilon_o(k)}{dt} > 0) \tag{2.49}$$

However; when the conditions (2.48) and (2.49) are both not verified, in other words when the current error components and their respective derivative in $\alpha\beta o$ reference frame have the same sign. It is necessary to apply the suitable non-zero space voltage vector to force the measured active filter current to forward the right trajectory towards the hysteresis boundary.
For each of the eight possible locations, there are eight space voltage vectors which can be applied, among them: one of either ZSVV, which can be chosen as $\vec{v}$ (nnnn) or $\vec{v}$ (pppp) in the case when condition (2.48) is verified. Similarly one ZSVV which can be applied as $\vec{v}$ (nnnp) or $\vec{v}$ (pppn) in the case when condition (2.49) is verified, and six active NZSVV. In the same cube, the eight space voltage vectors can drive the measured active filter current vector towards the reference current vector with reducing the switching frequency. Sixty four (64) possible configurations can be distinguished, summarising the eight cubes. **Table 2.5** shows the complete look up table implemented to control the filter current in three phase four wires active filter.

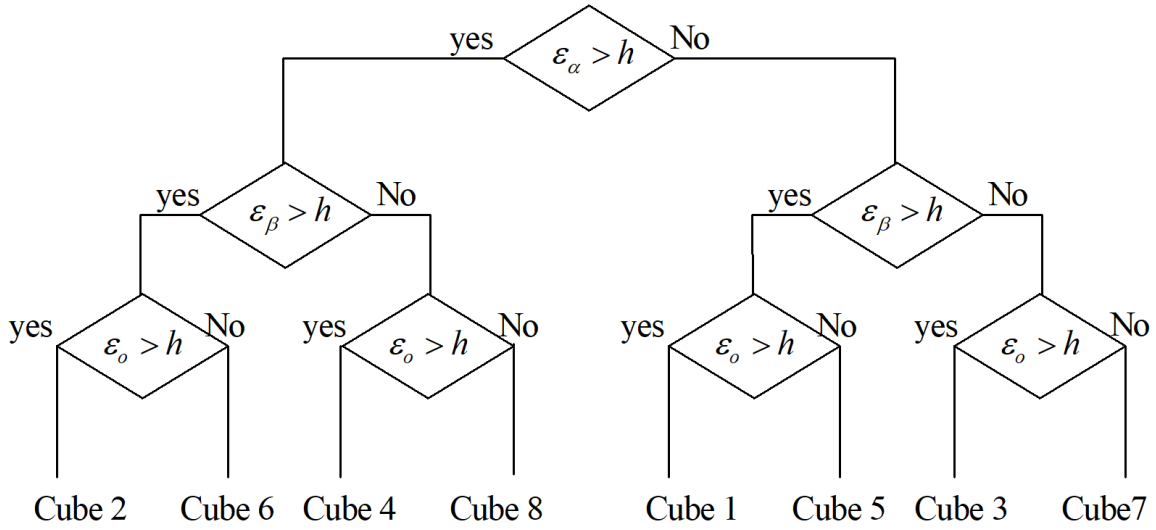

Figure 2.8: Detection of the cube

Table 2.5: Switch Combinations all the eight cubes

			Cube 01	**Cube 02**	**Cube 03**	**Cube 04**	**Cube 05**	**Cube 06**	**Cube 07**	**Cube 08**
$\varepsilon_o < h$	$\varepsilon_\beta < h$	$\varepsilon_\alpha < h$	npnn	ppnn	nnpn	pnpn	npnp	ppnp	nnpp	pnpp
		$\varepsilon_\alpha > h$	npnn	ppnn	nnpn	pnpn	npnp	ppnp	nnpp	pnpp
	$\varepsilon_\beta > h$	$\varepsilon_\alpha < h$	npnn	ppnn	nnpn	pnpn	npnp	ppnp	nnpp	pnpp
		$\varepsilon_\alpha > h$	npnn	ppnn	nnpn	pnpn	npnp	ppnp	nnpp	pnpp
$\varepsilon_o > h$	$\varepsilon_\beta < h$	$\varepsilon_\alpha < h$	npnn	ppnn	nnpn	pnpn	npnp	ppnp	nnpp	pnpp
		$\varepsilon_\alpha > h$	npnn	ppnn	nnpn	pnpn	npnp	ppnp	nnpp	pnpp
	$\varepsilon_\beta > h$	$\varepsilon_\alpha < h$	npnn	ppnn	nnpn	pnpn	npnp	ppnp	nnpp	pnpp
		$\varepsilon_\alpha > h$	npnn	ppnn	nnpn	pnpn	npnp	ppnp	nnpp	pnpp

IV DC Link Voltage Control:

The DC voltage around the capacitor of the VSI must be kept constant [4, 6, and 63]. The cause of its variation is the power exchange between the grid and the capacitor [6], In addition to the losses in the switches and the filter inductance. The variations of this voltage must be small in order not to exceed the voltage limits of the semi-conductors from the one hand, and in order not to affect the performance of the filter from the other hand [63]. To ensure the regulation of the dc capacitor voltage, a PI controller can be used. If we neglect the losses in the inverter and the output filter, the relation between the absorbed power by the filter and the voltage around the capacitor can be given by:

$$P_c = \frac{d}{dt}W = \frac{d}{dt}\left(\frac{1}{2}Cv_{dc}^2\right) \tag{2.50}$$

Applying the Laplace transform, we can achieve:

$$P_c(s) = \frac{1}{2}C.s.v_{dc}^2(s) \tag{2.51}$$

The voltage of the capacitor is then given by:

$$V_{dc}^2(S) = \frac{2p_{dc}(S)}{C_{dc}S} \tag{2.52}$$

From Eqn.(2.52) and considering the use of PI controller, the control loop of the dc voltage can be represented by **Figure 2.9**. The choice of the PI parameters is restrained by a minimal response time and a stable dynamic behavior that doesn't affect the performance of the APF. It is important to notice at this stage that high cut-off frequency ameliorates the control of the direct voltage and minimize the response time of the system. But it leads to errors in the generation of APF's reference currents and then reduces the filtering efficiency.

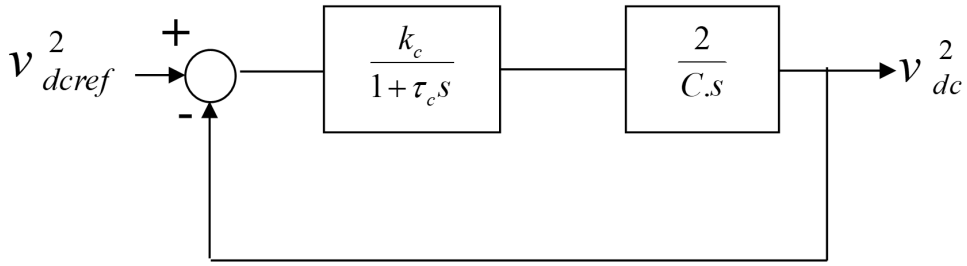

Figure 2.9: Control loop of the DC voltage

From **Figure 2.9**, the closed loop transfer function of the system with the controller can be given by:

$$F(s) = \frac{\omega_c^2}{s^2 + 2\zeta\omega_c s + \omega_c^2} \tag{2.53}$$

From where we can find the different parameters of the controller as:

$$\omega_c = \sqrt{\frac{2k_c}{C\tau_c}} \tag{2.54}$$

$$\zeta = \frac{1}{2\sqrt{2}}\sqrt{\frac{C}{k_c\tau_c}} \tag{2.55}$$

In order to obtain sufficient damping, the product $k_c\tau_c$ must be limited. A value of ζ between 0.5 and 0.707 achieves a good compromise between dynamic and static performance. As for the cut-off frequency f_c, it must be chosen as a function of the harmonics of the loop voltage.

V Summary:

In the first part of this chapter, three classical APF controls which are *pqo* theory, cross-vector control and *pqr* theory will be presented. The THD's of the lines current and the rms value of the neutral current are the quality criteria chosen all over this chapter. Then, improvements for these controls to minimise the influence of unbalanced and eventually voltage harmonics on the filtering and neutral current results are suggested. Finally, synchronous reference frame is introduced in improved cross-vector control method. Among three approaches. For the Current Injection Techniques The main principle is based on the comparison between the actual current of the filter with the reference currents generated by the different extraction methods. This chapter describes two of the most

commonly applied control techniques for APF Hysteresis Current Control Technique and 3 Dimensional Hysteresis PWM Technique. To ensure the regulation of the dc capacitor voltage, a PI controller can be used. The new approach is then applied to the control of a three-phase four-wire APF and its effectiveness is validated through simulations in the next chapter.

Chapter 3

Simulation Results and Discussion

I Introduction

In order to demonstrate the effectiveness of the complete system with the proposed shunt active power filer (SAPF) topology, simulation tests have been carried out under two scenarios. In the first scenario, the proposed shunt active power filter is not used and the power supply voltages system is supposed to be balanced and with pure sine waveform. Whereas, in the second scenario the proposed shunt active power filter is used under three cases of the power supply voltages system, which are presenting three intervals. The main aim within the second scenario is to prove that the proposed SAPF can achieve at the same time the compensation of the current harmonics generated by the non-linear load in the three phases, the compensation of the reactive current components in the three phases and the elimination of the current circulating through the neutral wire by ensuring a balanced currents in the power system. The power system in the first case is characterized by a voltage RMS and a frequency of 220V, 50 Hz respectively. The load is presented by three single phase rectifiers bridge diodes-based feeding three unbalanced loads; hence three unbalanced currents are absorbed from the power system **Figure 3.1**. The three inputs rectifiers are connected to the three phases of the power supply respectively and to the same neutral of the power system. **Table 3.1** present the parameters of the power supply system, the loads characteristics and the output filter of the APF that have been used in the second scenario.

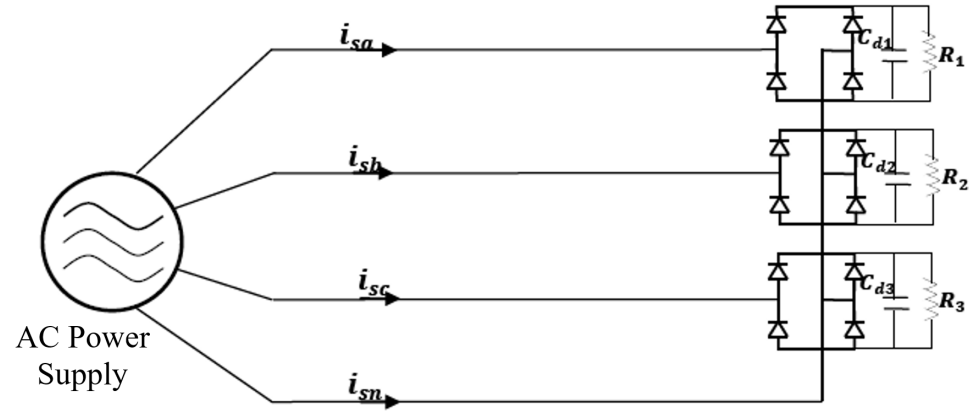

Figure 3.1: Three single phase diode rectifiers feeding unbalanced load

Table 3.1: Simulation Parameters

Power Supply	v_s	$220V$
	f_s	$50Hz$
	r_s	0.1Ω
	l_s	$0.6mH$
DC Load	R_1	20Ω
	R_2	40Ω
	R_3	40Ω
	C_{d1}= C_{d2}= C_{d3}	$5\mu F$
Active Filter	v_{dc}	$700V$
	l_f	$0.1mH$

II First scenario: The proposed shunt active power filter is not used.

The power supply current waveform before the use of the APF in phase "a" is shown in **Figure 3.2**.

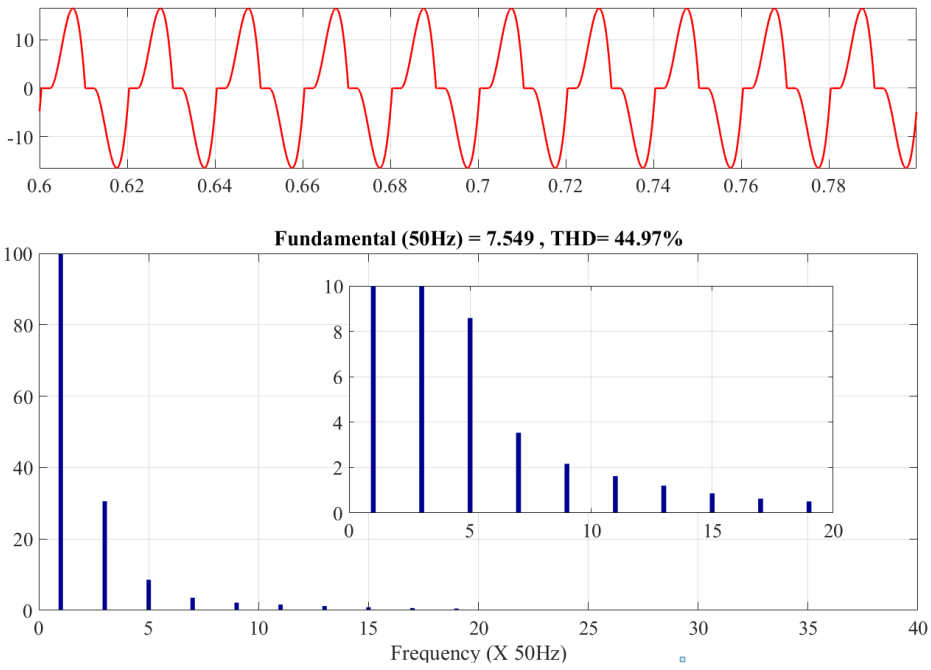

Figure 3.2: The current waveform of phase "a" and its harmonics spectrum under the first scenario.

It is clear that this current is stogngly distorted due to the dynamic nature behaviour of the single phase bridge diode rectifier connected to this phase, its harmonics spectrum is presented in the same figure. The currents waveforms of the other two phases have the smae waveforme with difference of scale due to the difference of the output loads of the three signle phase rectifiers, this difference of the scale causes the unabalnce of the three phases currents abosorbed from the power syplly. It is clear that the presence of the 3rd ,5th and 7th harmonics are very dominant where the Total Harmonic Distortion (THD)

is 44.97 % as it can be clearly observed in the zoom window of **Figure 3.2**.

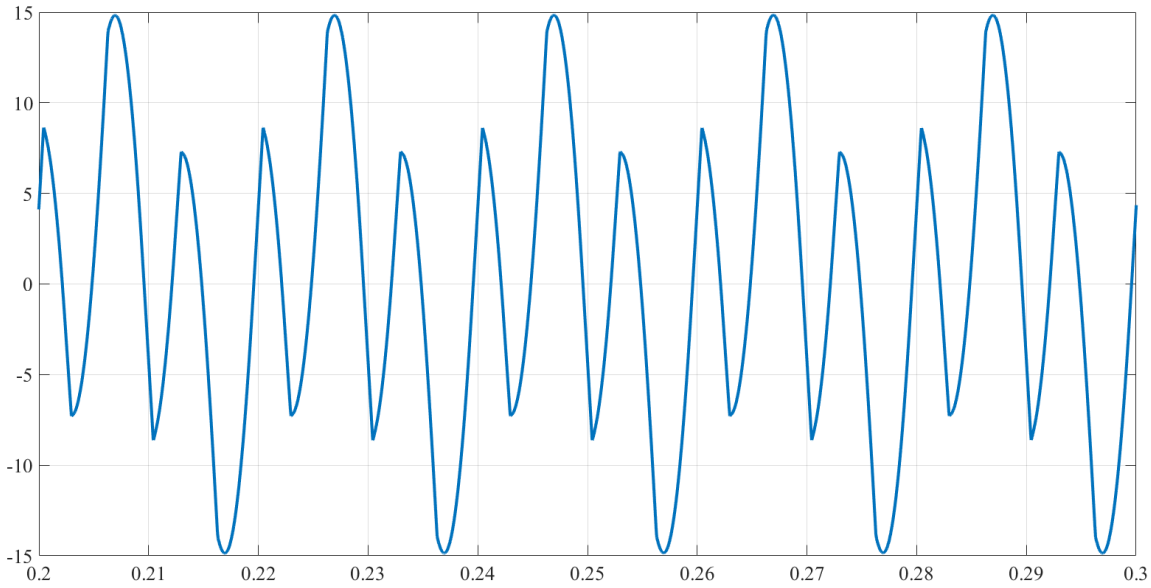

Figure 3.3: The neutral current waveform under the first case.

On the other side, the unbalnce of the three phase currents has led to the appearance of an important neutral current that is following along the path of the neutral conductor of the power system. The waveform of this current is presented in **Figure 3.3** where it can be observed that its magnitude is important compared to the currents in the three phases, where as an example, the maximum value of the current in phase "a" is 15 A, whereas the maximum value of the neutral current is 15 A as shown in **Figure 3.2** and **Figure 3.3** respectively. It is mainly generated by the unbalanced phase currents of the fundamental and the harmonics compoenents of the third harmonics and the multiplies of the third harmonics. Indeed, many researchers have studied the compensation of such current, besides the compensation of the phases' harmonics and the reactive compoenents, especially in industrila plants where the power supply current in the main three phase power system in very important.

III Second scenario: The proposed shunt active power filter is used.

In this scenario, the power supply voltages system behaves differently within the three intervals. As it can be observed clearly from the waveform presented in **Figure 3.4**.

- The first interval takes place before the instant 0.6s, where the system voltages is unbalanced with pure sine waveform which mean that there are no harmonics content, this unbalance is due to the decrease of the maximum voltage values in phases "b" and "c" to 200 V and 180 V respectively, whereas the voltage at phase "a" is kept at its rated value as shown in **Figure 3.4**.

- The second interval takes place within the interval of [0.6s 1.0s], where the voltage waveform of phase "a" contains a third harmonics component which leads to the deformation of its waveform.

- The third interval that takes place after the instant 1.0s, where furthermore the voltage of phase "a" contains the third and the fifth harmonics components which leads to more deformation of its waveform. The unbalance in the two phases of "b" and "c" remains the same along the three intervals as shown in **Figure 3.4**.

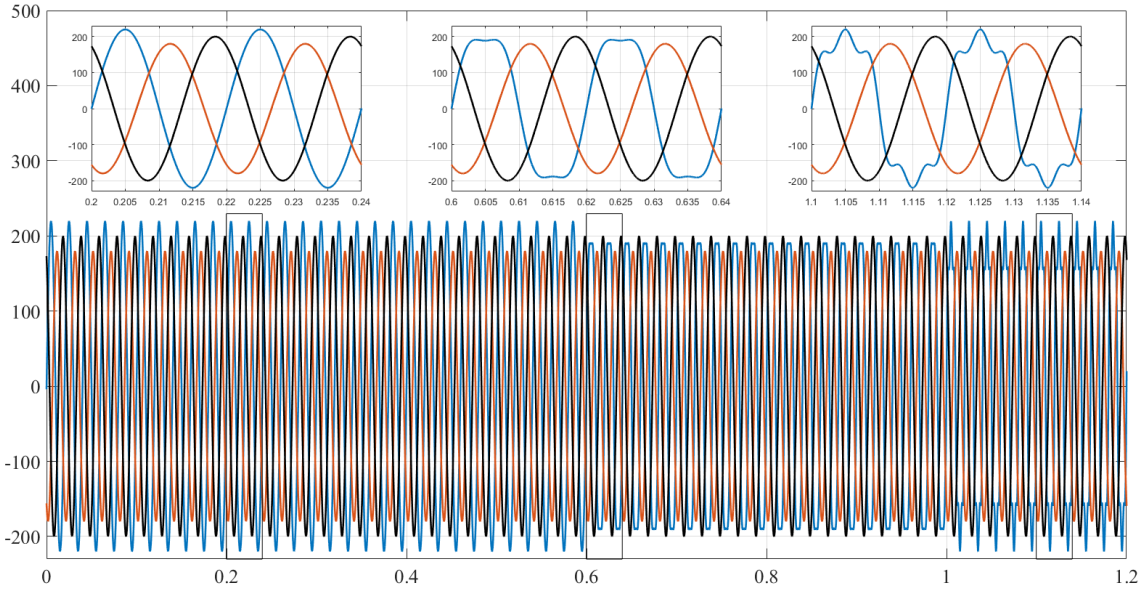

Figure 3.4: The different scenarios of the power supply voltages system.

The simulation has been carried out under the three aforementioned scenarios respectively. Figures 3.5-3.7 give respectively the simulated performance of source current, APF current, dc-bus capacitor voltage after compensation for pqo theory, within the three intervals of power system voltage variation as shown in **Figure 3.4**.

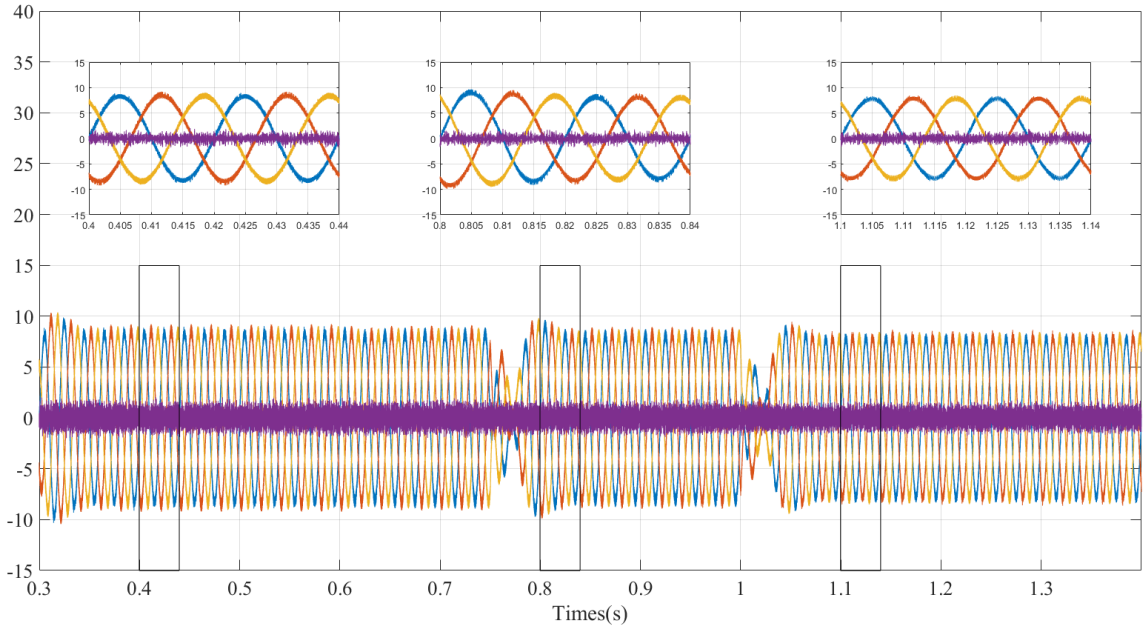

Figure 3.5: Supply currents after filtering pqo theory.

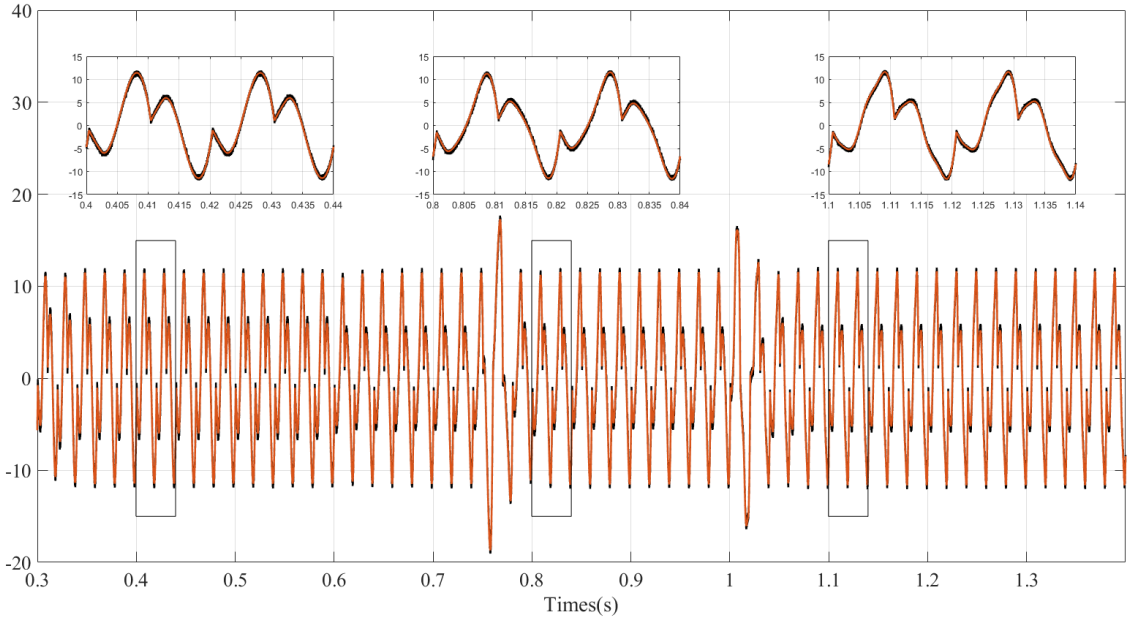

Figure 3.6: Filter currents after filtering pqo theory.

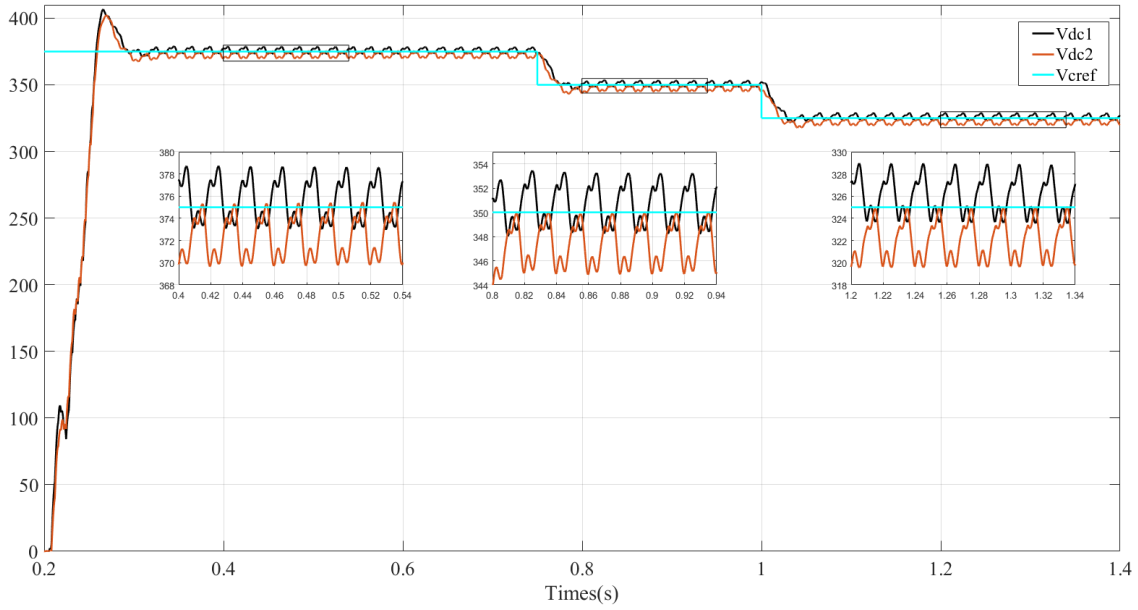

Figure 3.7: Evolution of the DC-capacitor voltage using pqo theory.

It can be clearly noted that the currents of the power supply during the three intervals are keeping nearly their balanced sinusoidal waveforms with a THD less than 5%, in the same time the current circulating in the neutral wire is nearly equal to zero with very limited ripples as shown in **Figure 3.5**, especially within the zoom windows. These simulation results prove that the use of the APF allows the compensation of the load current harmonics, the load current unbalance and the neutral current simultaneously. Where it has been proved that the source current obtained after the use of the proposed SAPF possesses nearly a sinusoidal waveform with a THD which falls within the limits of the standards.

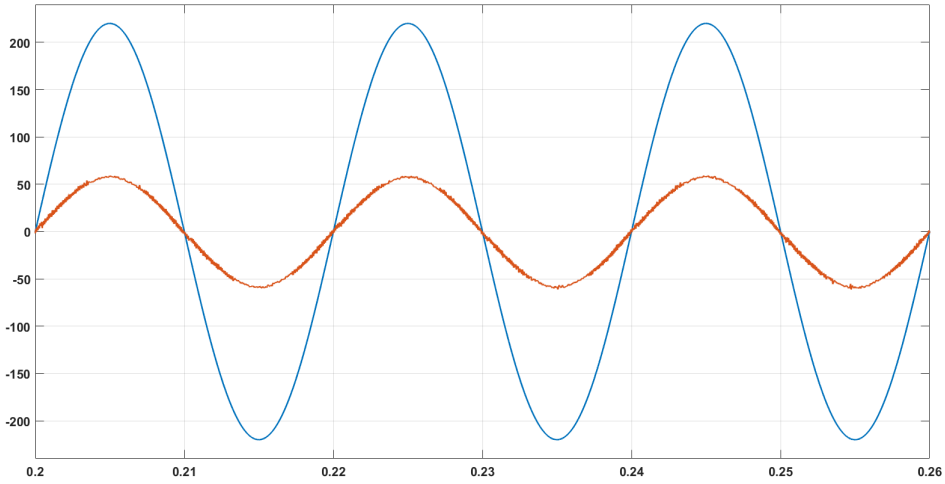

Figure 3.8: Power factor correction using pqo theory.

Figure 3.6 illustrates a Zoom of the evolution of active power filter current such as the reference current i_{ref} and the SAPF injected current i_f in phase "a". It can be clearly observed that the proposed shunt active power filter follows the reference current with a neglected error between i_{ref} and i_f and with a fast dynamic response which proves its higher performance and effectiveness. the dc capacitor voltage **Figure 3.7** reaches steady-state value of its reference in few cycles, On the other side, it can be remarked that the phase current in phase "a" is practically in phase with its corresponding voltage at the PCC which means that the power factor seen at the source side is nearly increased to the unity as shown in **Figure 3.8**.

For all control methods, the APF compensates not only current harmonics, but also unbalanced and reactive current components.

Figure 3.9-3.11 give respectively the simulation results for cross-vector theory, p–q-r theory and SRF theory for RC load.

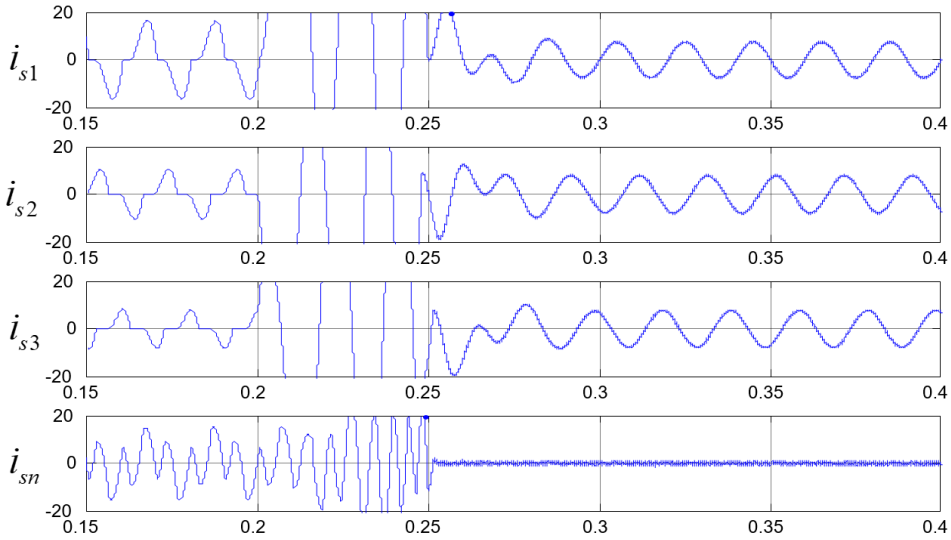

(a) Supply currents after filtering.

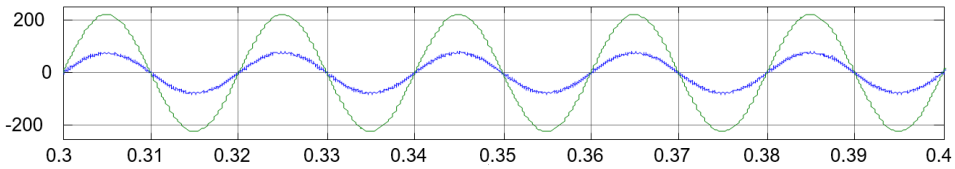

(b) Power factor correction.

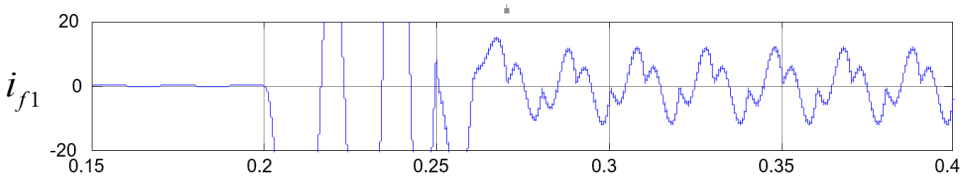

(c) Filter currents after filtering.

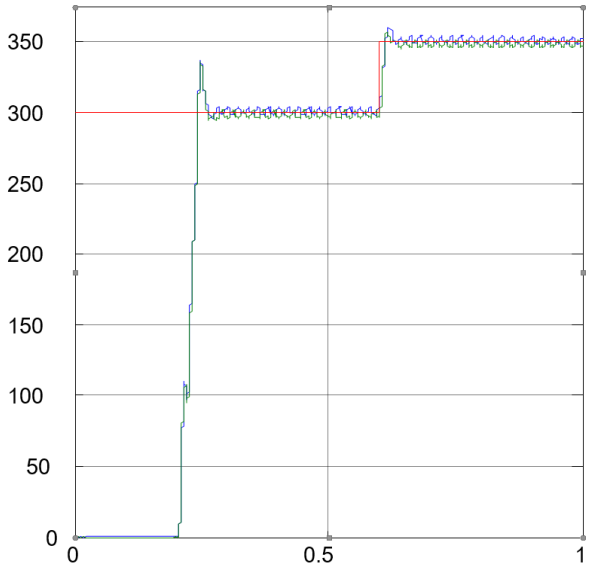

(d) Evolution of the DC-capacitor voltage.

Figure 3.9: Simulation Results for Cross-Vector theory THDis1= 1,8%.

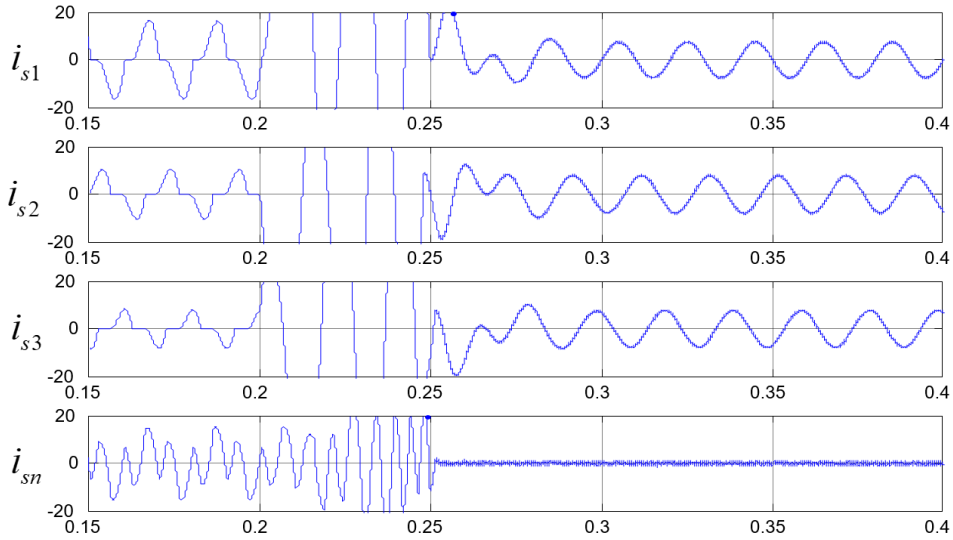

(a) Supply currents after filtering.

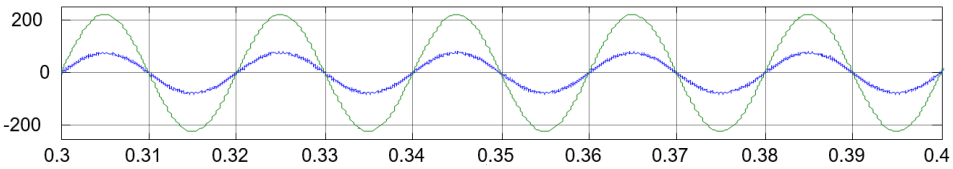

(b) Power factor correction.

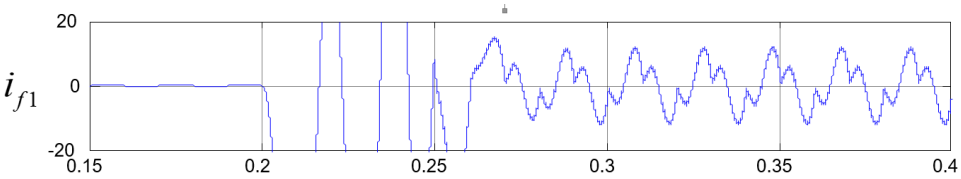

(c) Filter currents after filtering.

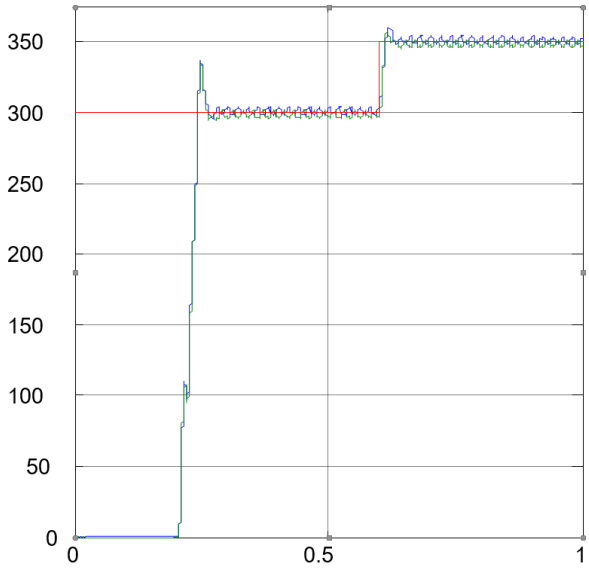

(d) Evolution of the DC-capacitor voltage.

Figure 3.10: Simulation Results for Cross-Vector theory THDis1= 1,7%.

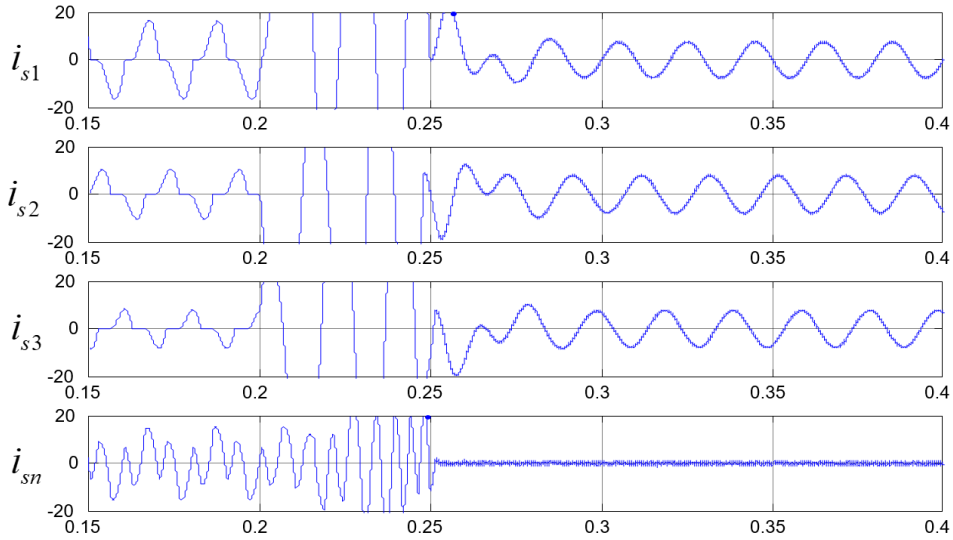

(a) Supply currents after filtering.

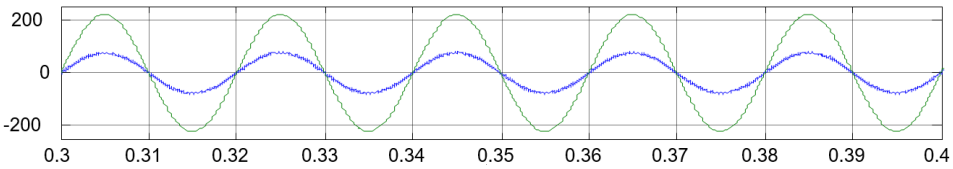

(b) Power factor correction.

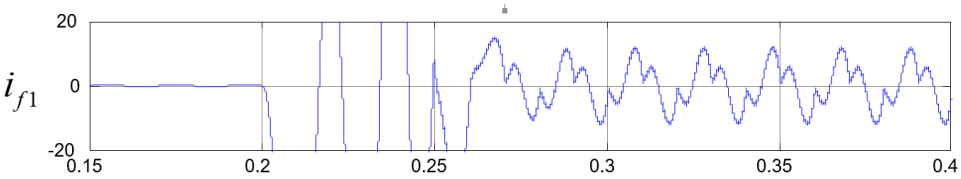

(c) Filter currents after filtering.

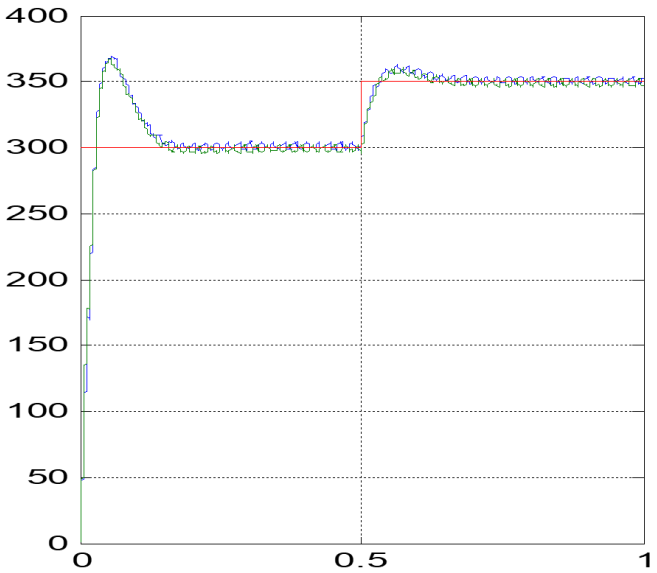

(d) Evolution of the DC-capacitor voltage.

Figure 3.11: Simulation Results for Cross-Vector theory THDis1= 1,2%.

It could be deduced that the THD's are generally well reduced with respect **Table 3.2**. Once again all methods are comparable, may be could be noticed that SRF theory provides better results than the other methods.

Moreover, all THD's are less than 5% (IEC norm).

Table 3.2: THD currents after filtering

Control Method	pqo	Cross-Vector	pqr	SFR
THD	2,9%.	1,8%.	1.7%.	1,2%.

IV Summary:

With the recent improvements in control and topology, the active power filters are capable to better compensate the currents harmonics, unbalanced and reactive power in threephase three-wire or four-wire electrical networks. This chapter deals with only control aspects but topology should not be ignored.
For the very specific case intended in this chapter, which is four-wire distribution system with unbalanced three singlephase loads, the voltage disturbances (especially unbalanced and even harmonics) are very common. In this case, the usual control approaches for APF, such as p–q–o, cross-vector and p–q–r theories, which are studied in this chapter, or DFT do not provide satisfactory results in term of currents THD's.
At first, this chapter proposes some improvements for these controls, by introducing a classical PLL in their loops. The obtained results, are better. Note that only unbalanced voltages are considered in this chapter, but this study can be extended to the voltage harmonics too. Secondly and in order to improve again the results, a new approach is introduced for one of the three control methods. The selected method is cross-vector control theory, but the others could also be tested. The new approach named synchronous reference frame, which is to use a PLL with unity magnitude sine and cosine voltages gives better results.
All APF controls studied in this chapter compensate harmonics as well as unbalanced and reactive current components. The residual neutral current is then very low and this will be really appreciated by the distribution systems.

Chapter 4

Three-Level Neural-Point-Clamped Inverter Based Three-phase Four-wire active Power Filter

I Introduction

the present chapter proposes the use of the Four-Legged Active Power Filter (FL-APF) in four-wires power distribution system to solve the problems related to the harmonics, the low power factor and the harmful neutral current. Indeed, the three phase four wire system is now being widely used in different areas including industrial facilities, service facilities, office buildings, power generation, distributed energy systems, uninterruptible power supplies, special control motors configurations, medical equipment, rural electrification based on renewable energy sources. and even in our homes. Actually, there are several four-wires APF topologies based on four-leg voltage source inverter (FL-VSI) such as; a single phase VSI topology for each leg, a three-leg topology and a special four leg topology. In the present paper, the four-wires VSI topology used is based on the classical three-level NPC inverter; where a similar leg to the original three legs is added to be as a four leg.
The use of the 4-Leg 3L-NPC topology when associated with an adapted control strategy in a microgrid context presents itself as a promising solution due to its ability to combine the following characteristics.

- Increase the efficiency of renewable energy sources (RES) and a hybrid energy storage system (HESS) integration to the microgrid through a unique power electronics interface acting as an active power compensator able to smooth the RES by acting on the HESS.
- Reduce ac-side current harmonics (for the same switching frequency and ac filter components when compared to a two-level inverter).
- Reduce HESS current harmonics caused by the floating middle point inherent to the NPC topology and move the ripples involved by unbalanced ac loads to the high specific power energy storage system (ESS).
- Compensation of ac-side microgrid disturbances produced by unbalanced/nonlinear loads thanks to the fourth leg.

Unfortunately, three level VSI has a critical disadvantage which is a greater number of power semiconductor switches are needed and therefore, more complicated control and additional costs are required. In order to ensure the control of the four-Legged active power filter based four-legs VSI, many control strategies have been proposed.

The control strategy used in the present work to ensure the generation of the switching patters of the FL-APF is the PWM technique. On the other side, for the harmonic current, reactive current components and the neutral current identification, a control approaches based on the instantaneous power theory have been used.It should also be noted that these methods are only valid if the network voltage is pure (sinusoidal and balanced). This is usually not the case in practice. To make these methods, universal and for any form of voltage, we use the direct network voltage (PLL) detection system. For the validation of the performances of the APF proposed topology, simulation results have been carried out under the use of the proposed control strategy and the identification approach.

II Description of the APF Topology

For three-phase four-wire shunt APFs, two topologies have been used, the four-leg full bridge (FLFB) and the three-leg split-up capacitor (TLSC) topologies. The FLFB which is based on a two-level VSI is presented at early 1990s and several controls with the topology have appeared. The FLFB converter has a better controllability thanks to its additional leg. However, for the three-level NPC VSI, to add one more leg, four additional switches are required, and hence they will increase the costs more compared with the two-level VSI case. Although the TLSC topology requires bigger capacitors than the FLFB topology, eliminating four switches (three-level VSI case) may compensate the cost for the bigger DC-bus capacitors. In this chapter the FLFB topology with a three-level NPC inverter for the three-phase four-wire APF is presented. The simplified circuit diagram of three-level NPC inverter is shown in **Figure 4.1**.

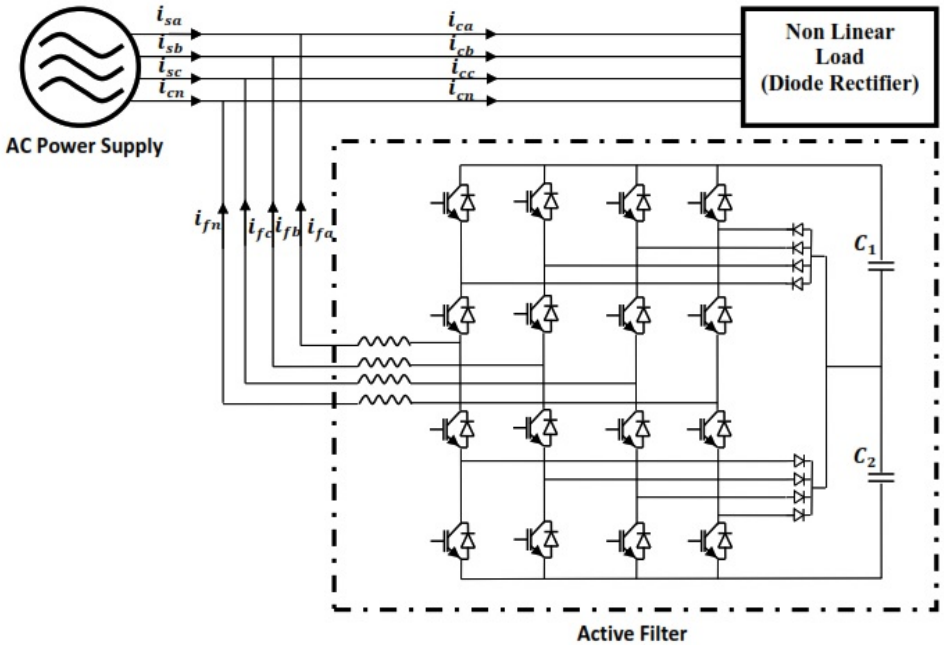

Figure 4.1: The Four-Legged Active Power Filter (FL-APF) based on three-level NPC inverter.

In this topology, each inverter leg contains four switches and four anti parallel diodes.

The input DC side of inverter in connected to a splitted DC capacitor creating a neutral point. The diodes connected to the neutral point, are called the clamping diodes that allow to clamp the inverter terminal voltage to neutral potential point NPP.
The voltages across the two DC capacitors are the same VC1=VC2, that are normally equal to the half of the total applied DC voltage. It is clear that the capacitors C1 and C2 can be charged or discharged by neutral current which can cause an NPP deviation. In the case of nonlinear loads, zero sequence current flows through the fourth leg.

III PWM technique for Four-leg three-level inverters

This control is based initially on the use of a proportional controller which input is presenting the difference between the injected current by the active filter to the common connection point (CCP) and the identified reference current. Whereas the output of the controller is presenting the reference output voltage of the inverter. This reference voltage is compared with two carrying triangular identical waves shifted by a half period.

The control of the inverter legs is summarized in two steps as follows.

Step1: Determination of the intermediate signals V_{i1} and V_{i2}.
If error $\geq V_{car1} \Rightarrow V_{i1} = 1$
else $V_i1 = 0$
If error $\geq V_{car2} \Rightarrow V_{i2} = 1$

Step2: Determination of the switches control signals T_{ij} $(j = 1, 2, 3, 4)$.
If V_{i1}+V_{i1}=1 $\Rightarrow$ T_{i1}=1, T_{i2}, T_{i3}=0, T_{i4}=0
If V_{i1}+V_{i1}=0 $\Rightarrow$ T_{i1}=1, T_{i2}, T_{i3}=1, T_{i4}=0
If V_{i1}+V_{i1}=-1 $\Rightarrow$ T_{i1}=0, T_{i2}, T_{i3}=0, T_{i4}=1

The general block diagram of the currents control is illustrated in **Figure 4.2**.

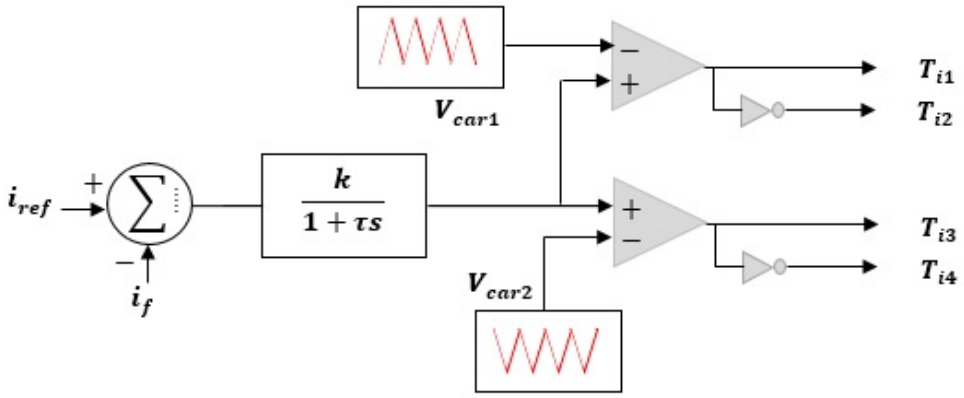

Figure 4.2: The principle of the PWM currents control technique.

IV Harmonics and reactive power calculation

This identification strategy is based on double transformation, where, a set of voltages(v_a,v_b,v_c) and a set of currents (i_a,i_b,i_c) that are obtained from the three-phase four-wire system are firstly transformed into a three-axis representation $\alpha\beta o$ based on Clark transformation under invariant power as follows:

$$V_{\alpha\beta o} = Tv\alpha\beta c;\ i_{\alpha\beta o} = Ti_{abc} \tag{4.1}$$

where

$$T = \sqrt{\frac{2}{3}} \begin{bmatrix} \frac{1}{\sqrt{2}} & \frac{1}{\sqrt{2}} & \frac{1}{\sqrt{2}} \\ 1 & -\frac{1}{2} & -\frac{1}{2} \\ 0 & \frac{\sqrt{3}}{2} & -\frac{\sqrt{3}}{2} \end{bmatrix}$$

Here, i_0 is the zero sequence current which is equal to 1/3 of the neutral current i_n.
The second transformation is achieved by rotating the $o-axis$ of the $\alpha\beta o$ frame by θ_1, aligning the $\alpha-axis$ with the projection line of the voltage space vector to the $\alpha\beta$ plane. The new components of voltage and current in the resulting frame $\alpha'\beta'o'$ can be obtained as follows:

$$\begin{bmatrix} i_{\alpha'} \\ i_{\beta'} \\ i_o \end{bmatrix} = \begin{bmatrix} \cos\theta_1 & \sin\theta_1 & 0 \\ -\sin\theta_1 & \cos\theta_1 & 0 \\ 0 & 0 & 1 \end{bmatrix} \begin{bmatrix} i_\alpha \\ i_\beta \\ i_o \end{bmatrix} \tag{4.2}$$

Which can be expressed in function of voltages components of $\alpha\beta o$ frame

$$\begin{bmatrix} i_{\alpha'} \\ i_{\beta'} \\ i_o \end{bmatrix} = \begin{bmatrix} \frac{v_\alpha}{v_{\alpha\beta}} & \frac{v_\beta}{v_{\alpha\beta}} & 0 \\ \frac{-v_\beta}{v_{\alpha\beta}} & \frac{v_\alpha}{v_{\alpha\beta}} & 0 \\ 0 & 0 & 1 \end{bmatrix} \begin{bmatrix} i_\alpha \\ i_\beta \\ i_o \end{bmatrix} \tag{4.3}$$

Where: $v_{\alpha\beta} = \sqrt{v_\alpha^2 + v_\beta^2}$
The new frame pqr can be obtained by a the third transformation by rotating the $\beta-axis$ of the $\alpha\beta o$ frame by θ_2 , aligning the $\alpha'-axis$ with the voltage space vector. The new components of voltage and current in the new frame pqr can be obtained as follows:

$$\begin{bmatrix} i_p \\ i_q \\ i_r \end{bmatrix} = \begin{bmatrix} \cos\theta_2 & 0 & \sin\theta_2 \\ 0 & 1 & 0 \\ -\sin\theta_2 & 0 & \cos\theta_2 \end{bmatrix} \begin{bmatrix} i_{\alpha'} \\ i_{\beta'} \\ i_o \end{bmatrix} \tag{4.4}$$

Which can once be expressed in function of voltages components of $\alpha\beta o$ frame

$$\begin{bmatrix} i_p \\ i_q \\ i_r \end{bmatrix} = \begin{bmatrix} \frac{v_\alpha}{v_{\alpha\beta}} & \frac{v_\beta}{v_{\alpha\beta}} & 0 \\ \frac{-v_\beta}{v_{\alpha\beta}} & \frac{v_\alpha}{v_{\alpha\beta}} & 0 \\ 0 & 0 & 1 \end{bmatrix} \begin{bmatrix} i_{\alpha'} \\ i_{\beta'} \\ i_o \end{bmatrix} \tag{4.5}$$

where: $v_{\alpha\beta o} = \sqrt{v_\alpha^2 + v_\beta^2 + v_o^2}$

It is important to note that the $\beta'-axis$ and the $p-axis$ are identical. On the other side, the three axes are mutually perpendicular to each other. The $p-axis$ is always aligned with the system voltage space vector. The $q-axis$ is located on the surface of $\alpha\beta$ plane. The $r-axis$ is perpendicular to the $p-axis$ and $q-axis$ and it oscillates with an angle=$\tan^{-1}(\frac{e_0}{e_{\alpha\beta}})$ from the $o-axis$. The rotating speed of pqr coordinates varies according to the voltage space vector system. the second and the third transformation applied to the voltages and currents can be combined to one transformation from the $\alpha\beta o$ frame to the pqr frame as follows:

$$\begin{bmatrix} i_p \\ i_q \\ i_r \end{bmatrix} = \begin{bmatrix} \frac{v_\alpha}{v_{\alpha\beta o}} & \frac{v_\beta}{v_{\alpha\beta o}} & \frac{v_o}{v_{\alpha\beta o}} \\ \frac{-v_\beta}{v_{\alpha\beta}} & \frac{v_\alpha}{v_{\alpha\beta}} & 0 \\ \frac{-v_\alpha v_o}{v_{\alpha\beta} v_{\alpha\beta o}} & \frac{-v_\beta v_o}{v_{\alpha\beta} v_{\alpha\beta o}} & \frac{v_{\alpha\beta}}{v_{\alpha\beta o}} \end{bmatrix} \begin{bmatrix} i_\alpha \\ i_\beta \\ i_o \end{bmatrix} \tag{4.6}$$

$$\begin{bmatrix} v_p \\ v_q \\ v_r \end{bmatrix} = \begin{bmatrix} \frac{v_\alpha}{v_{\alpha\beta o}} & \frac{v_\beta}{v_{\alpha\beta o}} & \frac{v_o}{v_{\alpha\beta o}} \\ \frac{-v_\beta}{v_{\alpha\beta}} & \frac{v_\alpha}{v_{\alpha\beta}} & 0 \\ \frac{-v_\alpha v_o}{v_{\alpha\beta} v_{\alpha\beta o}} & \frac{-v_\beta v_o}{v_{\alpha\beta} v_{\alpha\beta o}} & \frac{v_{\alpha\beta}}{v_{\alpha\beta o}} \end{bmatrix} \begin{bmatrix} v_{\alpha\beta o} \\ 0 \\ 0 \end{bmatrix} \tag{4.7}$$

Where: $v_{\alpha\beta o} = \sqrt{v_\alpha^2 + v_\beta^2 + v_o^2}$ and $v_{\alpha\beta} = \sqrt{v_\alpha^2 + v_\beta^2}$

From equation (7), it is obvious that the only existing voltage is along the $p - axis$ the other two components along $q - axis$ and $r - axis$ are equal to zero.. The $q - axis$ voltage is expressed as follows:

$$v_p = v_{\alpha\beta o} = \sqrt{v_\alpha^2 + v_\beta^2 + v_o^2} \tag{4.8}$$

The instantaneous power $p(t)$ is a scalar presenting the scalar product of the voltage and current vectors in pqr coordinates and the instantaneous reactive power $q(t)$ is a vector presenting the vector product of the same components. These are expressed as follows:

$$p = \vec{v}_{pqr}.\vec{i}_{pqr} = v_p.i_p \tag{4.9}$$

$$q = \vec{v}_{pqr} \times \vec{i}_{pqr} = \begin{bmatrix} 0 \\ -v_p.i_r \\ v_p.i_q \end{bmatrix} \tag{4.10}$$

Three components are obtained for the instantaneous power, one components is corresponding to the active power $p(t)$, where as the two other components are corresponding to the reactive power $q_q(t)$ and $q_r(t)$:

$$\begin{bmatrix} p \\ q_q \\ q_r \end{bmatrix} = \begin{bmatrix} v_p.i_p \\ -v_p.i_r \\ v_p.i_q \end{bmatrix} \tag{4.11}$$

From the above equation, it is clear that the three instantaneous powers are linearly independent. Thus, the three current components following the three axis p , q and r can be controlled independently based on the corresponding instantaneous power respectively. Moreover, it is clear that each instantaneous power is defined in the same way as a single-phase system. The current i_p is used for the control of the instantaneous active power present in the power system. The current i_r is used to control the reactive power associated with zero sequence current or the neutral current present in the three-phase four-wire system. The current i_q is used to control the instantaneous reactive power associated with conventional reactive power as well as the power associated with the negative sequence component and the harmonics presented in the power system.
In order to identify only the current harmonics, which has to be injected by the APF, the continuous component of the three instantaneous powers should not be taken into account. Thus, the reference currents in $\alpha\beta o$ coordinates can be obtained as follows:

$$\begin{bmatrix} i_\alpha^{ref} \\ i_\beta^{ref} \\ i_o^{ref} \end{bmatrix} = \frac{1}{v_{\alpha\beta o}} \begin{bmatrix} \frac{v_\alpha}{v_{\alpha\beta o}} & \frac{v_\beta}{v_{\alpha\beta o}} & \frac{v_o}{v_{\alpha\beta o}} \\ -\frac{v_\beta}{v_{\alpha\beta}} & \frac{v_\alpha}{v_{\alpha\beta}} & 0 \\ \frac{-v_\alpha v_o}{v_{\alpha\beta} v_{\alpha\beta o}} & \frac{-v_\beta v_o}{v_{\alpha\beta} v_{\alpha\beta o}} & \frac{v_{\alpha\beta}}{v_{\alpha\beta o}} \end{bmatrix} \begin{bmatrix} \tilde{p} \\ \tilde{q}_q \\ \tilde{q}_r \end{bmatrix} \tag{4.12}$$

Whereas, In order to identify the reference current which has to be injected by the APF to ensure the compensation of the current harmonics, the reactive current components

and the negative current component the following expression is used:

$$\begin{bmatrix} i_{\alpha}^{ref} \\ i_{\beta}^{ref} \\ i_{o}^{ref} \end{bmatrix} = \frac{1}{v_{\alpha\beta o}} \begin{bmatrix} \frac{v_{\alpha}}{v_{\alpha\beta o}} & \frac{v_{\beta}}{v_{\alpha\beta o}} & \frac{v_{o}}{v_{\alpha\beta o}} \\ -\frac{v_{\beta}}{v_{\alpha\beta}} & \frac{v_{\alpha}}{v_{\alpha\beta}} & 0 \\ \frac{-v_{\alpha}v_{o}}{v_{\alpha\beta}v_{\alpha\beta o}} & \frac{-v_{\beta}v_{o}}{v_{\alpha\beta}v_{\alpha\beta o}} & \frac{v_{\alpha\beta}}{v_{\alpha\beta o}} \end{bmatrix} \begin{bmatrix} \tilde{p} \\ q_q \\ q_r \end{bmatrix} \tag{4.13}$$

The main drawback of this theory is that when the voltages of the power system are disturbed by harmonics and/or unbalances the identification of the right reference current is not possible. Therefore, to overcome this problem, a PLL is used within the control loop. The main aim of the PLL is to generate a balanced sine waveform three phase system, perfectly in phase with the fundamental positive component of the power system voltages. the components of the obtained system in the $\alpha\beta$ co-ordinates are expressed as follows:

$$\begin{cases} v_{\alpha} = \sqrt{3}V_s \sin(wt) \\ v_{\beta} = \sqrt{3}V_s \cos(wt) \end{cases} \tag{4.14}$$

Using equation (06) and (14), it yields to:

$$\begin{bmatrix} i_p \\ i_q \\ i_r \end{bmatrix} = \begin{bmatrix} \sin(wt) & -\cos(wt) & 0 \\ \cos(wt) & \sin(wt) & 0 \\ 0 & 0 & 1 \end{bmatrix} \begin{bmatrix} i_{\alpha} \\ i_{\beta} \\ i_o \end{bmatrix} \tag{4.15}$$

Under this case, the three instantaneous power can be expressed as follows:

$$\begin{bmatrix} p \\ q_q \\ q_r \end{bmatrix} = \sqrt{3}V_s \begin{bmatrix} 1 & 0 & 0 \\ 0 & 1 & 0 \\ 0 & 0 & 1 \end{bmatrix} \begin{bmatrix} i_p \\ i_q \\ i_r \end{bmatrix} \tag{4.16}$$

The reference currents in $\alpha\beta o$ coordinates can be identified by the following expression:

$$\begin{bmatrix} i_{\alpha}^{ref} \\ i_{\beta}^{ref} \\ i_{o}^{ref} \end{bmatrix} = \begin{bmatrix} \sin(wt) & -\cos(wt) & 0 \\ \cos(wt) & \sin(wt) & 0 \\ 0 & 0 & 1 \end{bmatrix} \begin{bmatrix} \tilde{p} \\ q_q \\ q_r \end{bmatrix} \tag{4.17}$$

Whereas, the reference neutral current is:

$$i_n^{ref} = i_a^{ref} + i_b^{ref} + i_c^{ref} \tag{4.18}$$

This reference neutral current can be exist only if the phases currents are unbalanced and/or are containing the third order harmonics and its multiplies components.

V Simulation Results and Discussion

in order to demonstrate the effectiveness of the complete system with the proposed APF topology based on four-legs three-level NPC inverter, simulation validation have been performed under two cases. In the first case, the proposed shunt active power filter is not used and the power supply voltages system is supposed to be balanced and with pure sine waveform, in the second case the proposed shunt active power filter is used under three scenarios of the power supply voltages system. The main aim within the second case is to achieve the compensation of the current harmonics generated by the non-linear load, the compensation of the current reactive component and the elimination of the current circulating through the neutral wire. The power system used in the first case is

characterized by a voltage RMS and a frequency of 220V, 50 Hz respectively. The load is presented by three single phase rectifiers bridge diodes based feeding three unbalanced loads. The three inputs rectifiers are connected to the three phases of the power supply respectively, and to the same neutral of the power system as shown in in **Figure 4.3**.. **Table 4.1**. presents the parameters of the power supply system, the loads and the output filter of the APF that have been used.

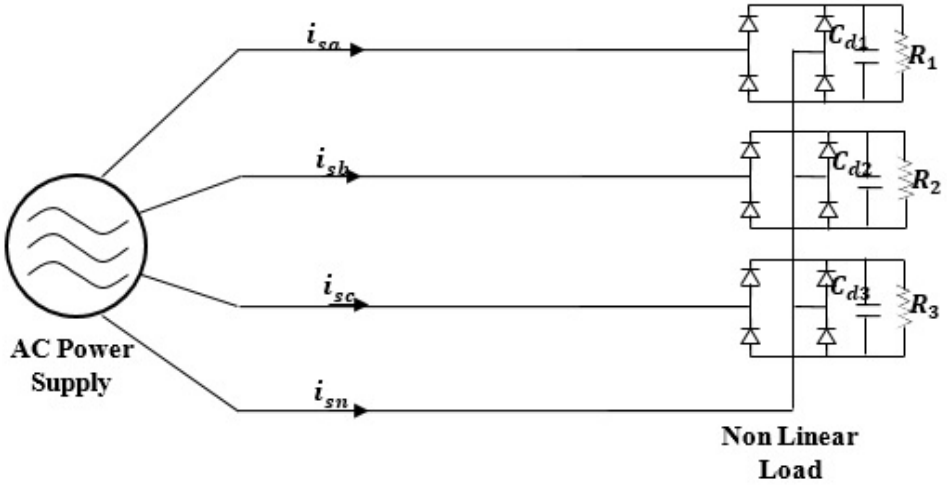

Figure 4.3: Three single phase diode rectifiers feeding unbalanced load.

Table 4.1: Simulation Parameters

Power Supply	v_s	$220V$
	f_s	$50Hz$
	r_s	0.1Ω
	l_s	$0.6mH$
DC Load	R_1	20Ω
	R_2	40Ω
	R_3	40Ω
	C_{d1}= C_{d2}= C_{d3}	$5\mu F$
Active Filter	v_{dc}	$700V$
	l_f	$0.1mH$

V.1 First case: The proposed shunt active power filter is not used

The power supply current waveform before the use of the APF in phase "a" is shown in Figure 2. It is clear that this current is stogngly distorted due to the dynamic nature behaviour of the single phase bridge diode rectifier connected to this phase, its harmonics spectrum is presented in the same figure. The currents waveforms of the other two phases have the smae waveforme with difference of scale due to the difference of the output loads of the three signle phase rectifiers, this difference of the scale causes the unabalnce of the three phases currents abosorbed from the power syplly. It is clear that the presence of the 3rd ,5th and 7th harmonics are very dominant where the Total Harmonic Distortion (THD) is 44.97 % as it can be clearly observed in the zoom window of **Figure 4.4**. On the other side, the unbalnce of the three phase currents has led to the appearance of an

important neutral current that is following along the path of the neutral conductor of the power system. The waveform of this current is presented in Figure 3 where it can be observed that its magnitude is important compared to the currents in the three phases, where as an example, the maximum value of the current in phase "a" is 10 A, whereas the maximum value of the neutral current is 15 A as shown in **Figure 4.4,4.5** respectively. It is mainly generated by the unbalanced phase currents of the fundamental and the harmonics compoenents of the third harmonics and the multiplies of the third harmonics. Indeed, many researchers have studied the compensation of such current, besides the compensation of the phases' harmonics and the reactive compoenents, especially in industrila plants where the power supply current in the main three phase power system in very important.

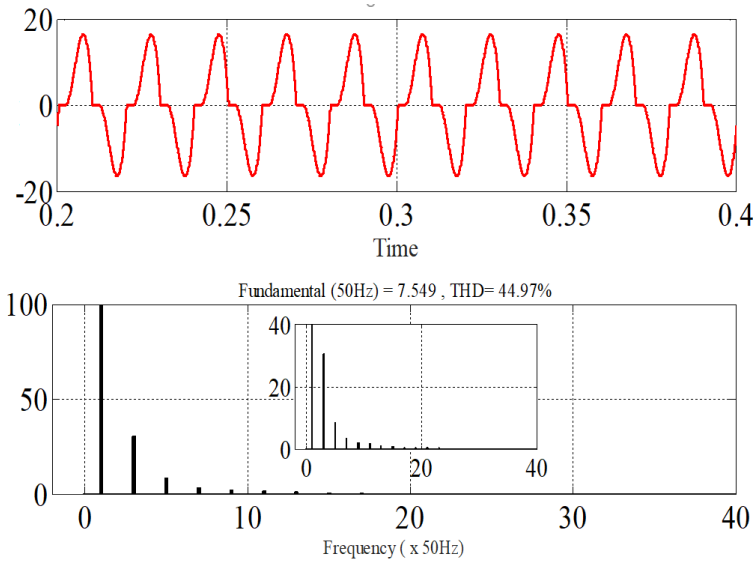

Figure 4.4: The current waveform of phase "a" and its harmonics spectrum under the first scenario.

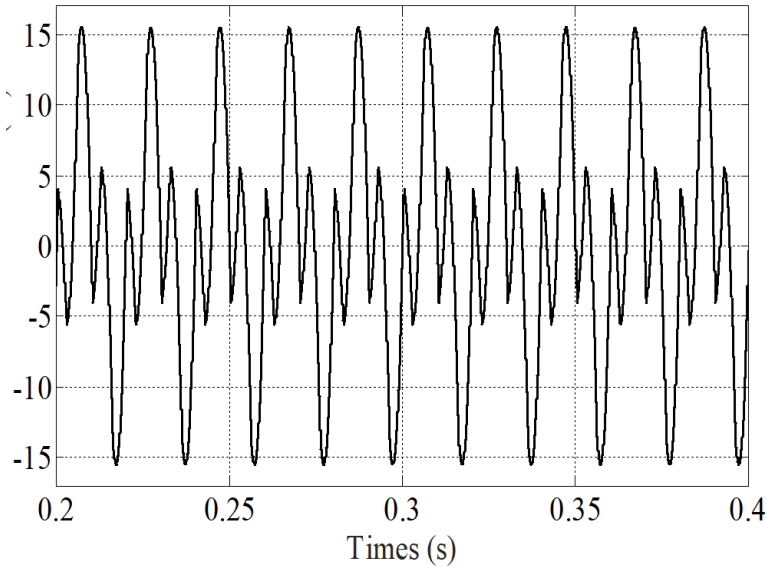

Figure 4.5: The neutral current waveform under the first case.

V.2 Second case: The proposed shunt active power filter is used.

In this scenario, the power supply voltages system behaves differently within the three intervals. As it can be observed clearly from the waveform presented in **Figure 4.6**, the first interval takes place before the instant 0.6s, where the system voltages is unbalanced with pure sine waveform which mean that there are no harmonics content, this unbalance is due to the decrease of the maximum voltage values in phases “b” and “c” to 140 V and 100 V respectively, whereas the voltage at phase “a” is kept at its rated value as shown in Figure 4.6. The second interval takes place within the interval of [0.6s 1.0s], where the voltage waveform of phase ”a” contains a third harmonics component which leads to the deformation of its waveform. Finally, the third interval that takes place after the instant 1.0s, where furthermore the voltage of phase ”a” contains the third and the fifth harmonics components which leads to more deformation of its waveform. The unbalance in the two phases of “b” and “c” remains the same along the three intervals as shown in Figure 4.6.

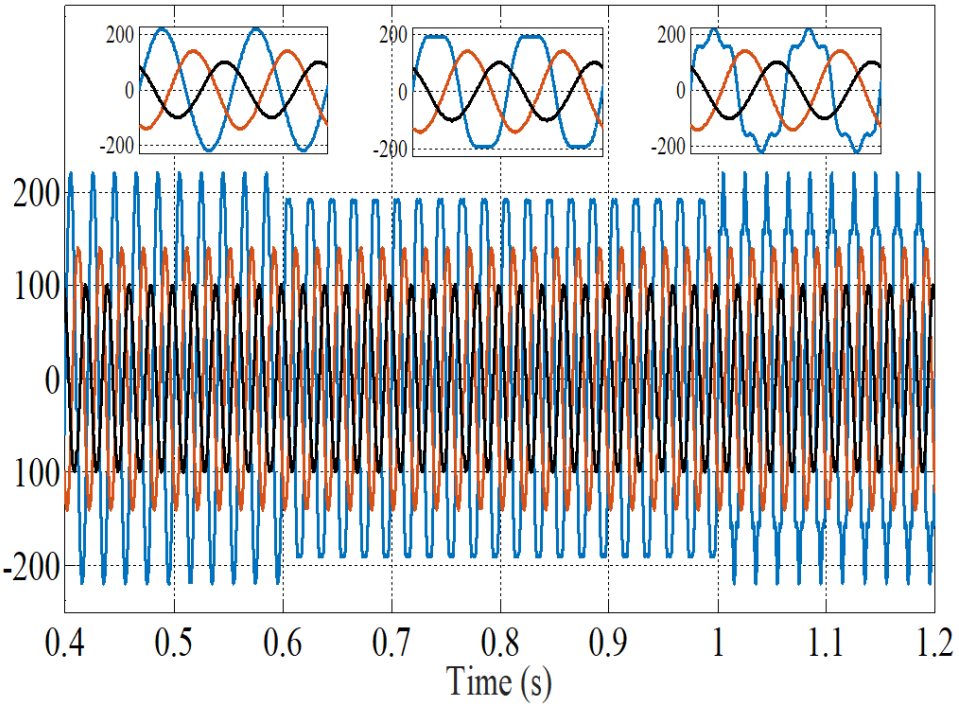

Figure 4.6: The different scenarios of the power supply voltages system.

The simulation has been carried out under the three aforementioned scenarios respectively. **Figure 4.7** presents the waveforms of the power supply current after compensation within the three intervals of power system voltage variation as shown in Figure 4.6. It can be clearly noted that the currents of the power supply during the three intervals are keeping nearly their balanced sinusoidal waveforms with a THD less than 5%, in the same time the current circulating in the neutral wire is nearly equal to zero with very limited ripples as shown in Figure 4.7, especially within the zoom windows. These simulation results prove that the use of the APF allows the compensation of the load current harmonics, the load current unbalance and the neutral current simultaneously. Where it has been proved that the source current obtained after the use of the proposed multilevel SAPF possesses nearly a sinusoidal waveform with a THD which falls within the limits of the standards.

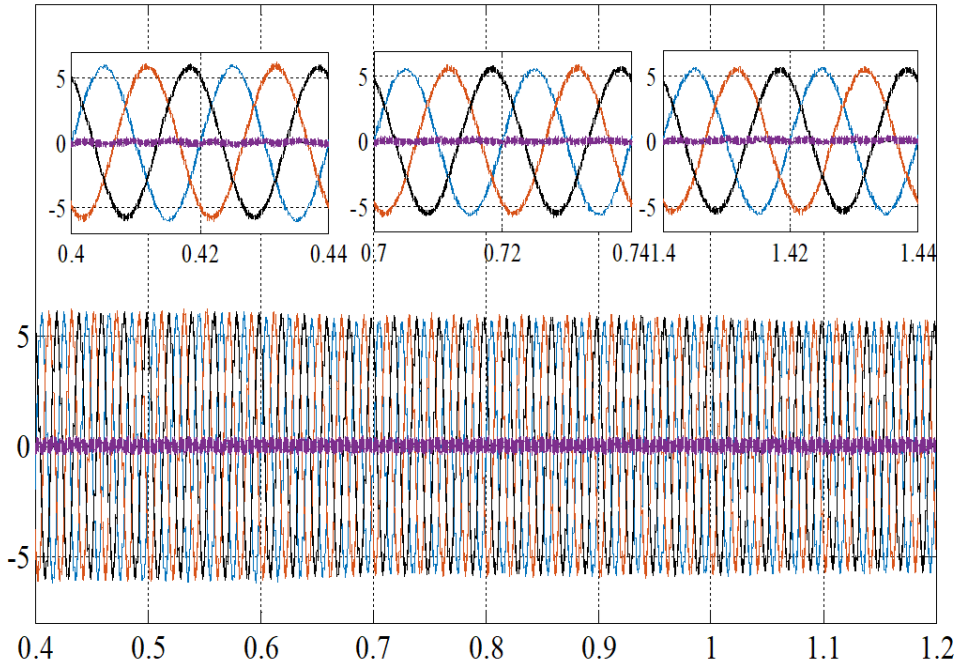

Figure 4.7: The power system currents in the three-phases and in the neutral under the use of the proposed active power filter.

Indeed, the observation on phase "a" which is deeply contaminated by the harmonics proves the effectiveness of the used of the proposed SAPF. It can be clearly seen in **Figure 4.8** that the current in phase "a" has a sinusoidal waveform with constant amplitude along the three intervals. On the other side the presentation of the frequency spectrum of this current to obtain the following THDs along the three intervals such as 2.72%, 1.68 and 2.34 as shown in Figure 4.8 (a), (b) and (c) respectively. These values are very acceptable in comparison with the IEC norms. These results confirms the performance and the dynamic of the APF compensation in such situation.

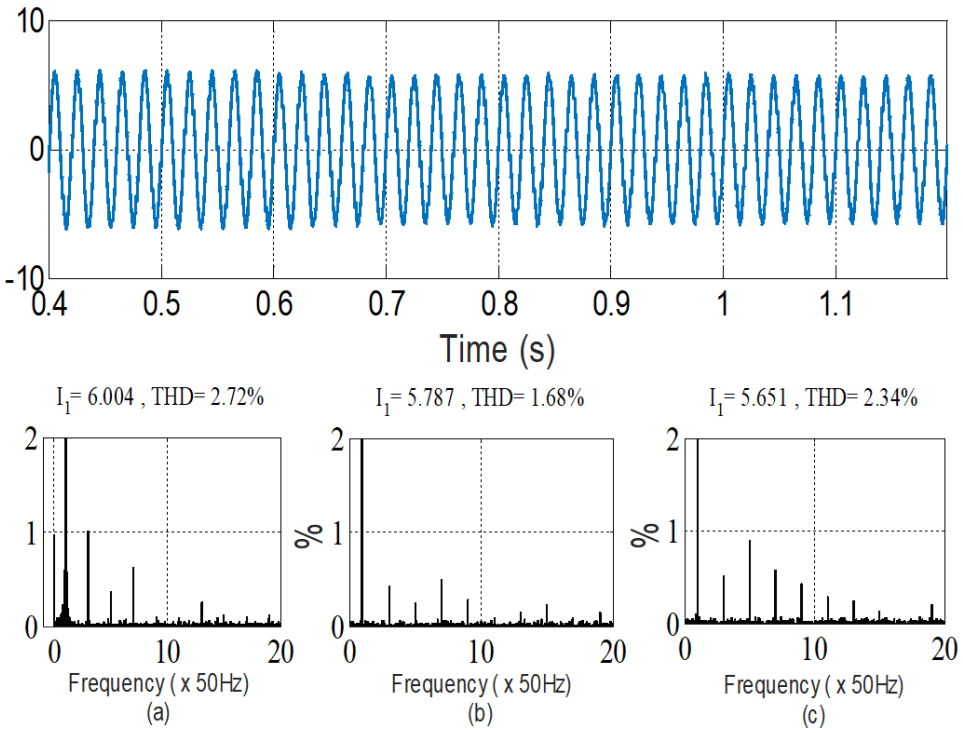

Figure 4.8: The current waveform of phase "a" in the second case under the use of the proposed shunt APF. The first scenario [0.2 0.4s], The second scenario [0.8 1s], The third scenario [1.1 1.3s].

On the other side, it can be remarked that the phase current in phase "a" is practically in phase with its corresponding voltage at the PCC which means that the power factor seen at the source side is nearly increased to the unity as shown in **Figure 4.9**

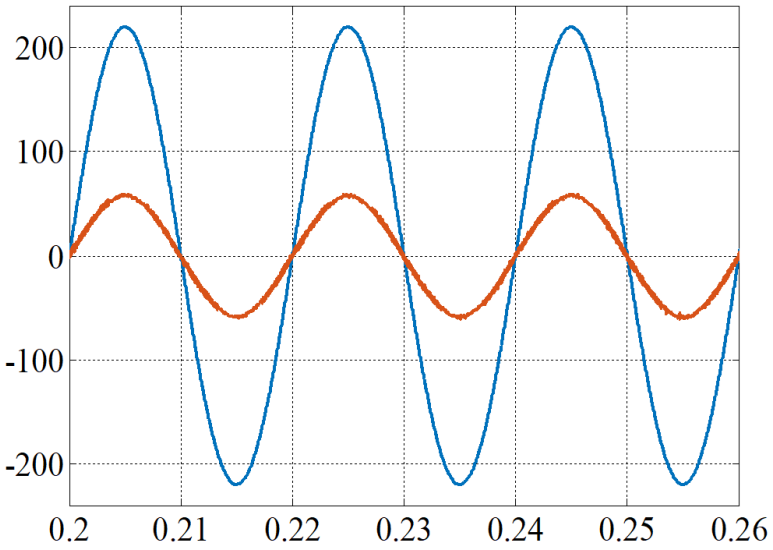

Figure 4.9: Power factor correction (v_s, $10 * i_s$).

Figure 4.10 illustrates a Zoom of the evolution of active power filter current (the reference current and the APF injected current). It can be seen clearly that the active power filter follows the current reference with neglected error between i_{ref} and i_f and with a fast dynamic response.

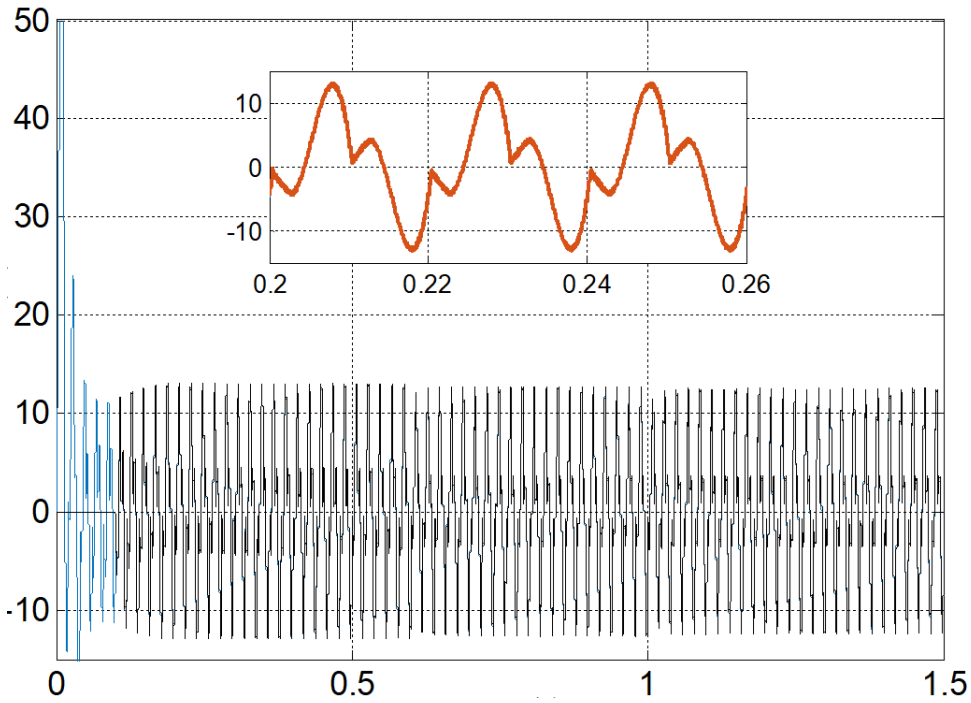

Figure 4.10: The proposed Active power filter current (the reference current and the APF injected current)

Figure 4.11 shows the output voltage waveform of the proposed active power filter. It is clear that it is rich of harmonics components, but due to the use of the low-pass output filter, the used proposed topology of the VSC can be seen as a current source and the high order harmonics that are due specially to the high switching frequency of the VSC are eliminated. However, it is obvious that this source current have to inject the required harmonics to achieve the desired compensation function.

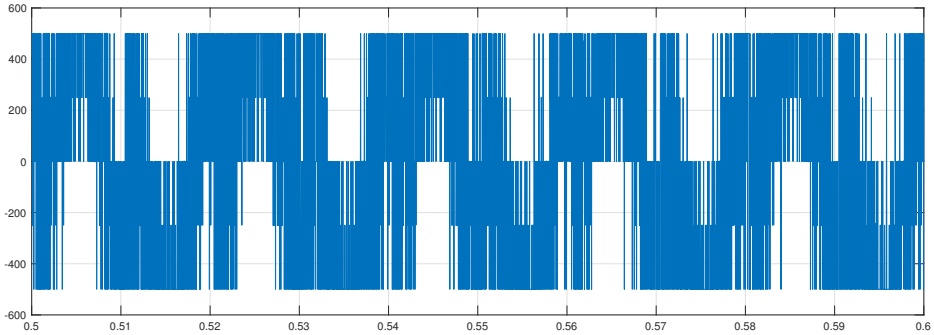

Figure 4.11: APF output voltage v_{fan}.

VI Summary:

The present chapter deals with the study of the performances of a proposed four-leg three-level inverter based on an active power filter, which can be used for high-power applications to ensure the elimination of current harmonics under severe power supply voltages conditions. The use of the proposed shunt active filter has allowed successfully to compensate the harmonics during balanced and unbalanced conditions of the power supply voltages system under the existence of the 3rd and 5th Harmonics voltage components.

The application to determine the set current of the APF pqr power theory provides the balancing of currents and powers, and the decrease of the current in the neutral wire. The obtained results through simulation prove clearly that the proposed active power filter with a control strategy can achieve the function of compensation under severe constraints of the power supply voltages system and the severe dynamics load behaviors constraints and ensuring the current source to be sinusoidal and balanced to maintain the power factor near equals to the unity.

Chapter 5

Conclusion and Future Work

In this chapter conclusion of the research work is presented. Furthermore, some future recommendations are also stated to extend the present work.

I Conclusion

In recent years, there is an increased demand for power electronics devices due to their inherent advantages in several domestic and industrial applications such as; electrical power conversion, adjustable speed drives (ASDs), arc furnaces, bulk rectifiers, power supplies, low power lamps, large air conditioning systems, compressors, etc. Unfortunately, the proliferation of these devices is considered to be among the main causes that are leading to several power quality problems, especially the generation of different harmonics components that are contributing in several serious problems, such as:

- An important current in the neutral wire. This current magnitude can be up to the sum of all 3 phases magnitudes. therefore, it can be a very serious problem causing overheating of the neutral wires. Hence, and an over sizing of the neutral wire is required to solve this problem.
- Overheating of electrical supply transformers which leads to the declassification of their capacities, and the shortening of their lifespan.
- High voltage and current distortions exceeding the standards limits. this can cause the malfunction and the performance degradation of more sensitive equipment and devices, and even the destruction of some sensitive equipment.
- Poor power factor less than 0.9 which results in monthly penalty fees for major users (factories, manufacturing, and industrial).
- Resonances that lead to over-current surges. This results in destroying capacitors and their fuses and damaging the surge suppressors which can cause an electrical power system breakdown.
- High frequency harmonics cause the appearance of the interference phenomena which can be induced into phone lines and data cabling.

Power quality improvement has motivated the development of harmonics compensation schemes such as shunt Active Power Filters (APFs). These devices estimate the harmonic terms and re-inject them phase-opposite in the power distribution system. For optimal performances, APFs should be able to track the changing harmonics and should

be able to adapt their parameters to take into account the time-varying behavior of the power system. Indeed, the power quality issue has become an important concern which is nowadays attracting more attention from the electrical energy producer and the customers, as well as from the researchers. Where, there is a great evident necessity to develop solutions that are able to mitigate such disturbances in the electrical power systems within the main aim to improve the power quality at all levels.

The design and use of three-phase four-wire systems for transmission and distribution of electricity has increased significantly in recent years. The wide use of semiconductor converters for controlling electric machines or industrial plants has led to the presence of higher harmonics of voltage and current in the grid, as well as to the fluctuations of reactive power. The consequences of this are fluctuations and distortions of the supply voltage and the deterioration of the electrical energy quality in general.
In this context, the present thesis proposes the use of the Four-Legged Active Power Filter (FL-APF) in four-wires power distribution system to solve the problems related to the harmonics, the low power factor and the harmful neutral current. Indeed, the three phase four wire system is now being widely used in different areas including industrial facilities, service facilities, office buildings, power generation, distributed energy systems, uninterruptible power supplies, special control motors configurations, medical equipment, rural electrification based on renewable energy sources. and even in our homes. Actually, there are several four-wires APF topologies based on four-leg voltage source inverter (FL-VSI) such as; a single phase VSI topology for each leg, a three-leg topology and a special four leg topology. the four-wires VSI topology used is based on the classical three-level NPC inverter; where a similar leg to the original three legs is added to be as a four leg.
The use of the 4-Leg 3L-NPC topology when associated with an adapted control strategy in a microgrid context presents itself as a promising solution due to its ability to combine the following characteristics.

- Increase the efficiency of renewable energy sources (RES) and a hybrid energy storage system (HESS) integration to the microgrid through a unique power electronics interface acting as an active power compensator able to smooth the RES by acting on the HESS.
- Reduce ac-side current harmonics (for the same switching frequency and ac filter components when compared to a two-level inverter).
- Reduce HESS current harmonics caused by the floating middle point inherent to the NPC topology and move the ripples involved by unbalanced ac loads to the high specific power energy storage system (ESS).
- Compensation of ac-side microgrid disturbances produced by unbalanced/nonlinear loads thanks to the fourth leg.

The use of the proposed shunt active filter has allowed successfully to compensate the harmonics during balanced and unbalanced conditions of the power supply voltages system under the existence of the 3rd and 5th Harmonics voltage components. The application to determine the set current of the APF pqr power theory provides the balancing of currents and powers, and the decrease of the current in the neutral wire. The obtained results through simulation prove clearly that the proposed active power filter with a control strategy can achieve the function of compensation under severe constraints of the power supply voltages system and the severe dynamics load behaviors constraints and ensuring

the current source to be sinusoidal and balanced to maintain the power factor near equals to the unity.

The most significant conclusions of this research work are briefly summarized as follow:

- A thorough literature review of the past and the most recent research works in the development of Smart Grids and the area of power quality compensation using Shunt active filter was conducted. Reported literatures on these topics are briefly discussed. The concepts on the power quality and application of active power filtering in smart grids were also evaluated. Various type of nonlinear loads based on the power quality compensation objective were presented and analyzed. A brief review on conventional harmonic compensation technique such as passive compensators was conducted. A shorten briefing on the active power filtering principles and the state of the art in active compensation was presented. Furthermore, basics of power quality including key concepts and theoretical backgrounds were explained;

- The new technology associated with smart grids offers the opportunity to improve the quality and reliability as experience by the customers. It will however also result in the increase of disturbance levels in several cases and thereby introduce a number of new challenges. But these new challenges should definitely not be used as arguments against the development of smart grids. However they should attract attention to the importance of power quality for the successful and reliable operation of smart grids. New developments need new approaches and perspectives from all parties involved (network operators, equipment manufacturers, customers, regulators, standardization bodies, and others).

II Suggestions for Future Work

The research work presented in this thesis has given a new perspective for future research in the field of shunt active power filtering. The following issues have been detected during this research work and are listed here as possible topics for future work in this area.

- The application of the proposed shunt active power filter system to diminish other power quality problems such as sags, swells and flickering may be investigated.

- This research focuses on the fundamental theoretical problems rather than the hardware implementation. The proposed active filter could be experimentally verified by developing prototype.

- The proposed work can be applied in applications that contain interharmonics, such as speed drives of shipboard power systems and grid connected PV inverters.

- The proposed work can also be applied for ripple factor reduction in HVDC systems with higher current and voltage ratings.

Appendix A

TITLE OF APPENDIX

AC or ac	Alternating Current
APF	Active Power Filter
APLC	Active Power Line Conditioner
ADC	Analog to Digital Converter
ANN	Artificial Neural Network
ASD	Adjustable Speed Drives
CCS	Code Composer Studio
CC-VSI	Current Controlled Voltage Source Inverter
CDSC	Cascaded Delayed Signal Cancellation
CSI	Current Source Inverter
DBHCC	Double Band Hysteresis Curent Control
DC or dc	Direct Current
DFT	Discrete Fourier Transform
DG	Distributed Generation
DSC	Delayed Signal Cancellation
DSP	Digital Signal Processor
EMI	Electro Magnetic Interference
FLC	Fuzzy Logic Controller
FFT	Fast Fourier Transform
GTO	Gate Tune-off Thyristor
HCC	Hysteresis Current Control
HCR	Harmonics Compensation Ratio
HF	Harmonic distortion Factor
HV	High Voltage
HPF	High Pass Filter
HVDC	High Voltage Direct Current
IEC	International Electrotechnical Commission
IEEE	Institute of Electrical & Electronics Engineers
IGBT	Insulated Gate Bipolar Transistor
IRP	Instantaneous Reactive Power
IRPT	Instantaneous Reactive Power Theory
kV	Kilo Volt
kVA	Kilo Volt Ampere
kVAR	kilo Volt Ampere Reactive
KVL	Kirchhoffs voltage law
kW	Kilo Watt
LPF	Low Pass Filter

LV	Low Voltage
MLI	Multilevel Inverter
MV	Medium Voltage
MVA	Mega Volt Ampere
MW	Mega Watt
OCC	One Cycle Control
PCC	Point of Common Coupling
PI	Proportional and Integral
PFC	Power Factor Correction
PHC	Perfect Harmonic Cancellation
PLL	Phase Lock Loop
PQ	Power Quality
PSO	Particle Swarm Optimization
PV	Photovoltaic
PWM	Pulse Width Modulation
RMS	Root Mean Square
SAPF	Shunt Active Power Filter
SBHCC	Single Band Hysteresis Curent Control
SCC	Short Circuit Current
SMPS	Switch Mode Power Supplies
SPWM	Sinusoidal Pulse Width Modulation
SRF	Synchronous Reference Frame
STATCOM	Static Synchronous Compensator
SVC	Static VAR Compensators
TDD	Total Demand Distortion
THD	Total Harmonic Distortion
RTW	Real time workshop
UPQC	Unified Power Quality Conditioner
UPS	Uninterruptible Power Supplies
UPF	Unity Power Factor
VAR	Volt ampere reactive
VCO	Voltage Controlled Oscilator
VLLMS	Variable Leaky Least Mean Square
VSD	Variable Speed Drives
VSI	Voltage source Inverter

Bibliography

[1] X.-P. Zhang and Z. Yan, "Energy quality: A definition," *IEEE Open Access Journal of Power and Energy*, vol. 7, pp. 430–440, 2020.

[2] F. Harirchi and M. G. Simões, "Enhanced instantaneous power theory decomposition for power quality smart converter applications," *IEEE Transactions on Power Electronics*, vol. 33, no. 11, pp. 9344–9359, 2018.

[3] J. Liu, S. Taghizadeh, J. Lu, M. J. Hossain, S. Stegen, and H. Li, "Three-phase four-wire interlinking converter with enhanced power quality improvement in microgrid systems," *CSEE Journal of Power and Energy Systems*, vol. 7, no. 5, pp. 1064–1077, 2021.

[4] M. G. Simes and F. A. Farret, *POWER QUALITY ANALYSIS*, pp. 227–253. 2017.

[5] S. K. Sharma, A. Chandra, M. Saad, S. Lefebvre, D. Asber, and L. Lenoir, "Voltage flicker mitigation employing smart loads with high penetration of renewable energy in distribution systems," *IEEE Transactions on Sustainable Energy*, vol. 8, no. 1, pp. 414–424, 2017.

[6] Y. Hu, T. Siriburanon, and R. B. Staszewski, "Oscillator flicker phase noise: A tutorial," *IEEE Transactions on Circuits and Systems II: Express Briefs*, vol. 68, no. 2, pp. 538–544, 2021.

[7] J. Zuo, B. Zhang, M. Xiang, Y. Shen, and Y. Chen, "Study of transient voltage stability with transient stability probing method in hunan power grid," in *2017 4th International Conference on Systems and Informatics (ICSAI)*, pp. 252–256, 2017.

[8] "Ieee recommended practice for preferred ratings for high-voltage(gt;1000 volts) ac circuit breakers designated definite purpose for fast transient recovery voltage rise times," *IEEE Std C37.06.1-2017*, pp. 1–26, 2018.

[9] Y. Ma, Q. Li, H. Chen, H. Li, and Y. Lei, "Voltage transient disturbance detection based on the rms values of segmented differential waveforms," *IEEE Access*, vol. 9, pp. 144514–144529, 2021.

[10] J. Jiao, Z. Liu, L. Li, and X. Nie, "Threshold dynamics of a stage-structured single population model with non-transient and transient impulsive effects," *Applied Mathematics Letters*, vol. 97, pp. 88–92, 2019.

[11] A. B. Hoffmann, C. H. Beuter, A. L. Pessoa, L. R. Ferreira, and M. Oleskovicz, "Techniques for the diagnosis of oscillatory transients resulting from capacitor bank switching in medium voltage distribution systems," *International Journal of Electrical Power & Energy Systems*, vol. 133, p. 107198, 2021.

[12] G. R. S. Reddy and R. Rao, "Oscillatory-plus-transient signal decomposition using tqwt and mca," *Journal of Electronic Science and Technology*, vol. 17, no. 2, pp. 135–151, 2019.

[13] Y. Yu, P. Ju, Y. Peng, B. Lou, and H. Huang, "Analysis of dynamic voltage fluctuation mechanism in interconnected power grid with stochastic power disturbances," *Journal of Modern Power Systems and Clean Energy*, vol. 8, no. 1, pp. 38–45, 2020.

[14] S. Q. Sun and Q. R. Xiang, "Waveform distortion and distortion power," *IEE Proc. B Electr. Power Appl.*, vol. 139, no. 4, pp. 303–306, 1992.

[15] Q. N. Trinh, P. Wang, Y. Tang, L. H. Koh, and F. H. Choo, "Compensation of dc offset and scaling errors in voltage and current measurements of three-phase ac/dc converters," *IEEE Transactions on Power Electronics*, vol. 33, no. 6, pp. 5401–5414, 2018.

[16] S. Rechka, É. Ngandui, J. Xu, and P. Sicard, "Performance evaluation of harmonics detection methods applied to harmonics compensation in presence of common power quality problems," *Math. Comput. Simul.*, vol. 63, pp. 363–375, nov 2003.

[17] C. Boonseng and K. Kularbphettong, "The harmonic and power quality improvement of office building using hybrid power filter," in *2019 International Conference on Power, Energy and Innovations (ICPEI)*, pp. 146–149, 2019.

[18] H. Zhang, Y. Li, J. Ai, and W. Huang, "Harmonic power flow calculation method based on general model of harmonic source," in *The 10th Renewable Power Generation Conference (RPG 2021)*, vol. 2021, pp. 232–238, 2021.

[19] J. Subjak and J. McQuilkin, "Harmonics-causes, effects, measurements, and analysis: an update," *IEEE Transactions on Industry Applications*, vol. 26, no. 6, pp. 1034–1042, 1990.

[20] R. Robinson, "Harmonics in a.c. rotating machines," *Proc. IEE Part C Monogr.*, vol. 109, no. 16, p. 380, 1962.

[21] A. N. Widyanto and H. Hirsch, "The effect of harmonic distortion voltage to partial discharge characteristics in epoxy insulation," *Lect. Notes Electr. Eng.*, vol. 599 LNEE, pp. 877–884, aug 2020.

[22] S. Adak, H. Cangi, B. Eid, and A. S. Yilmaz, "Developed analytical expression for current harmonic distortion of the PV system's inverter in relation to the solar irradiance and temperature," *Electr. Eng.*, vol. 103, no. 1, pp. 697–704, 2021.

[23] J. Balakrishna, T. Bramhananda Reddy, and M. Vijaya Kumar, "Implementation of Random Pulse Width Modulation Techniques for the Open-End Winding Five-Phase Motor Drives to Reduce Acoustic Noise and Harmonic Distortion," *Lect. Notes Electr. Eng.*, vol. 703, pp. 429–457, 2021.

[24] M. Amir and S. K. Srivastava, "Analysis of Harmonic Distortion in PV–Wind-Battery Based Hybrid Renewable Energy System for Microgrid Development," in *Lect. Notes Electr. Eng.*, vol. 553, pp. 1223–1231, Springer, Singapore, 2019.

[25] A. C. Moreira, L. C. P. da Silva, and H. K. M. Paredes, "Power Quality Study and Analysis of Different Arc Welding Machines," *J. Control. Autom. Electr. Syst.*, vol. 29, no. 2, pp. 163–176, 2018.

[26] O. Lennerhag and M. Bollen, "Power Quality," in *Springer Handbooks*, vol. 17, pp. 1171–1203, Springer, Singapore, 2021.

[27] J. Bartman, "Evaluating the level of waveform distortion," in *Lect. Notes Electr. Eng.*, vol. 452, pp. 305–317, Springer, Cham, 2018.

[28] J. Barros, M. de Apraiz, and R. I. Diego, "Voltage notch detection and analysis using wavelets," in *2008 IEEE Conference on Virtual Environments, Human-Computer Interfaces and Measurement Systems*, pp. 151–155, 2008.

[29] G. Scandurra, G. Cannatà, G. Giusi, and C. Ciofi, "Configurable low noise amplifier for voltage noise measurements," in *2013 22nd International Conference on Noise and Fluctuations (ICNF)*, pp. 1–4, 2013.

[30] F. Milano and Á. O. Manjavacas, *Frequency Variations in Power Systems: Modeling, State Estimation and Control*. 2020.

[31] A. Vicenzutti, M. Chiandone, V. Arcidiacono, and G. Sulligoi, "Enhanced partial frequency variation starting of hydroelectric pumping units: Model based design and experimental validation," *Int. J. Electr. Power Energy Syst.*, vol. 131, p. 107083, oct 2021.

[32] N. Mahdavi Tabatabaei, A. Jafari Aghbolaghi, N. Bizon, and F. Blaabjerg, eds., *Reactive Power Control in AC Power Systems*. Power Systems, Cham: Springer International Publishing, 2017.

[33] W. H. Tang, Y. C. Gu, Y. L. Xin, Q. H. Liang, and T. Qian, "Classification for transient overvoltages in offshore wind farms based on multi-scale mathematical morphology," *Int. J. Electr. Power Energy Syst.*, vol. 136, p. 107157, mar 2022.

[34] P. Schegner, "Power System Protection," in *Springer Handbooks*, pp. 975–1014, Springer, Singapore, 2021.

[35] T. K. Jappe and S. A. Mussa, "Discrete-time current control techniques applied in pfc boost converter at instantaneous power interruption," in *2009 Brazilian Power Electronics Conference*, pp. 1118–1123, 2009.

[36] R. Bayindir, M. Yesilbudak, and S. Ermis, "Standards-based investigation of voltage dips and voltage imbalances in an organized industrial zone," in *2016 IEEE International Power Electronics and Motion Control Conference (PEMC)*, pp. 476–481, 2016.

[37] V. C. Cunha, F. C. Trindade, and B. Venkatesh, "A practical method to assess the potential of energy storage systems to mitigate voltage sags," *Electr. Power Syst. Res.*, vol. 201, p. 107525, dec 2021.

[38] Z. Hanzelka, "Voltage Dips and Short Supply Interruptions," in *Handb. Power Qual.*, pp. 79–134, John Wiley & Sons, Ltd, jun 2008.

[39] S. Patil, S. Pawar, A. Mulla, and D. Patil, "FC-TBSR compensator for reactive power compensation and voltage swell mitigation," in *Lect. Notes Electr. Eng.*, vol. 661, pp. 19–28, Springer, Singapore, 2021.

[40] S.-Y. Yun, J.-C. Kim, J.-C. Bae, Y.-J. Jeon, S.-M. Park, and C.-H. Park, "Reliability Evaluation of Power Distribution Systems Considering the Momentary Interruptions," *IFAC Proc. Vol.*, vol. 36, pp. 761–766, sep 2003.

[41] Q. Huang, S. Jing, J. Yi, and W. Zhen, "Measurement of Energy, Power Quality and Efficiency in Smart Grid," in *Innov. Test. Meas. Solut. Smart Grid*, pp. 147–182, John Wiley & Sons, Ltd, may 2015.

[42] M. Hentea, "Smart Power Grid," in *Build. an Eff. Secur. Progr. Distrib. Energy Resour. Syst.*, pp. 289–324, John Wiley & Sons, Ltd, apr 2021.

[43] B. K. Bose and F. F. Wang, "ENERGY, ENVIRONMENT, POWER ELECTRONICS, RENEWABLE ENERGY SYSTEMS, AND SMART GRID," in *Power Electron. Renew. Energy Syst. Smart Grid*, pp. 1–83, John Wiley & Sons, Ltd, jul 2019.

[44] M. Sathiyanathan, S. Jaganathan, and R. L. Josephine, "Multi-Mode Power Converter Topology for Renewable Energy Integration With Smart Grid," in *Integr. Renew. Energy Sources with Smart Grid*, pp. 141–169, Wiley, oct 2021.

[45] *Power Electronics in Renewable Energy Systems and Smart Grid: Technology and Applications | IEEE eBooks | IEEE Xplore*. Wiley, jul 2019.

[46] A. A. Filimonova, T. A. Barbasova, and D. A. Shnayder, "Outdoor Lighting System Upgrading Based on Smart Grid Concept," in *Energy Procedia*, vol. 111, pp. 678–688, Elsevier, mar 2017.

[47] J. R. Aguero, "Applications of smart grid technologies on power distribution systems," pp. 1–1, Institute of Electrical and Electronics Engineers (IEEE), apr 2012.

[48] L. Martini, "Trends of smart grids development as fostered by European research coordination: The contribution by the EERA JP on smart grids and the ELECTRA IRP," in *Int. Conf. Power Eng. Energy Electr. Drives*, vol. 2015-Septe, pp. 23–30, IEEE Computer Society, sep 2015.

[49] D. Fan, Y. Ren, Q. Feng, Y. Liu, Z. Wang, and J. Lin, "Restoration of smart grids: Current status, challenges, and opportunities," jun 2021.

[50] J. I. Leon, S. Vazquez, and L. G. Franquelo, "MULTILEVEL CONVERTERS – CONTROL AND OPERATION IN INDUSTRIAL SYSTEMS," in *Power Electron. Renew. Energy Syst. Smart Grid*, pp. 219–270, John Wiley & Sons, Ltd, jul 2019.

[51] Z. Shi, W. Yao, Z. Li, L. Zeng, Y. Zhao, R. Zhang, Y. Tang, and J. Wen, "Artificial intelligence techniques for stability analysis and control in smart grids: Methodologies, applications, challenges and future directions," *Appl. Energy*, vol. 278, p. 115733, nov 2020.

[52] F. Blaabjerg and K. Ma, "RENEWABLE ENERGY SYSTEMS WITH WIND POWER," in *Power Electron. Renew. Energy Syst. Smart Grid*, pp. 315–345, John Wiley & Sons, Ltd, jul 2019.

[53] C. Yapa, C. de Alwis, M. Liyanage, and J. Ekanayake, "Survey on blockchain for future smart grids: Technical aspects, applications, integration challenges and future research," *Energy Reports*, vol. 7, pp. 6530–6564, nov 2021.

[54] M. G. Molina, "GRID ENERGY STORAGE SYSTEMS," in *Power Electron. Renew. Energy Syst. Smart Grid*, pp. 495–583, John Wiley & Sons, Ltd, jul 2019.

[55] "Advances in clean energy technologies," in *Advances in Clean Energy Technologies* (A. K. Azad, ed.), p. xiii, Academic Press, 2021.

[56] A. Moeini, H. Zhao, and S. Wang, "A current-reference-based selective harmonic current mitigation pwm technique to improve the performance of cascaded h-bridge multilevel active rectifiers," *IEEE Transactions on Industrial Electronics*, vol. 65, no. 1, pp. 727–737, 2018.

[57] A. Moeini, S. Wang, B. Zhang, and L. Yang, "A hybrid phase shift-pulsewidth modulation and asymmetric selective harmonic current mitigation-pulsewidth modulation technique to reduce harmonics and inductance of single-phase grid-tied cascaded multilevel converters," *IEEE Transactions on Industrial Electronics*, vol. 67, no. 12, pp. 10388–10398, 2020.

[58] C. May, "Passive filters," in *Passive Circuit Analysis with LTspice®: An Interactive Approach* (C. May, ed.), pp. 683–752, Springer International Publishing.

[59] J. Das, "Passive filters - potentialities and limitations," *IEEE Transactions on Industry Applications*, vol. 40, no. 1, pp. 232–241, 2004.

[60] F. Zare, H. Soltani, D. Kumar, P. Davari, H. A. M. Delpino, and F. Blaabjerg, "Harmonic emissions of three-phase diode rectifiers in distribution networks," *IEEE Access*, vol. 5, pp. 2819–2833, 2017.

[61] T. S. Amorim and L. F. Encarnação, "Low rating hybrid power filter for application in distribution systems," in *2015 IEEE 13th Brazilian Power Electronics Conference and 1st Southern Power Electronics Conference (COBEP/SPEC)*, pp. 1–6, 2015.

[62] E. E. Chaplygin, "An active filter with inductive storage for compensation of inactive power of a rectifier with a capacitive filter," *Russian Electrical Engineering*, vol. 88, pp. 1–6, Jan. 2017.

[63] M. H. Antchev, "Chapter 9 - classical and recent aspects of active power filters for power quality improvement," in *Classical and Recent Aspects of Power System Optimization* (A. F. Zobaa, S. H. Abdel Aleem, and A. Y. Abdelaziz, eds.), pp. 219–254, Academic Press, 2018.

[64] V. Nakade and S. Patil, "Implementation of Power Quality Enhancement using Hybrid Series Active Filter," in *2019 International Conference on Communication and Electronics Systems (ICCES)*, pp. 238–241, July 2019.

[65] R. Lakra, I. Kasireddy, and A. K. Singh, "Harmonic mitigation in three phase three wire system using shunt active power filter," in *2018 International Conference on Recent Innovations in Electrical, Electronics Communication Engineering (ICRIEECE)*, pp. 2753–2756, July 2018.

[66] M. Jalil and A. Amiri, "An Effective Structure of Three-Phase Parallel Hybrid Active Power Filter to Accurate Harmonic Elimination," in *2020 15th International Conference on Protection and Automation of Power Systems (IPAPS)*, pp. 123–129, Dec. 2020.

[67] P. Salmerón Revuelta, S. Pérez Litrán, and J. Prieto Thomas, "6 - hybrid filters: Series active power filters and shunt passive filters," in *Active Power Line Conditioners* (P. Salmerón Revuelta, S. Pérez Litrán, and J. Prieto Thomas, eds.), pp. 189–229, San Diego: Academic Press, 2016.

[68] S. Parmar, N. Prajapati, and A. Panchbhai, "Optimum Solution for Power Conditioning in DC Motor Drives Using Shunt Active Power Filter," in *2018 4th International Conference on Electrical Energy Systems (ICEES)*, pp. 203–207, Feb. 2018.

[69] M. Sharanya, B. Banakara, and M. Sasikala, "Power quality improvement using a combination of hybrid active power filter and thyristorised controlled reactor," in *2017 International Conference on Energy, Communication, Data Analytics and Soft Computing (ICECDS)*, pp. 1364–1369, Aug. 2017.

[70] C. Madtharad and S. Premrudeepreechacharn, "Active power filter for three-phase four-wire electric systems using neural networks," *Electric Power Systems Research*, vol. 60, pp. 179–192, Jan. 2002.

[71] A. A. Chihab, H. Ouadi, F. Giri, and T. Ahmed-Ali, "Adaptive non-linear control of three-phase four-wire Shunt active power filters for unbalanced and nonlinear loads.," *IFAC Proceedings Volumes*, vol. 47, pp. 5061–5066, Jan. 2014.

[72] W. U. Tareen and S. Mekhilef, "Transformer-less 3P3W SAPF (three-phase three-wire shunt active power filter) with line-interactive UPS (uninterruptible power supply) and battery energy storage stage," *Energy*, vol. 109, pp. 525–536, Aug. 2016.

[73] S. S. Patnaik and A. K. Panda, "Three-level H-bridge and three H-bridges-based three-phase four-wire shunt active power filter topologies for high voltage applications," *International Journal of Electrical Power & Energy Systems*, vol. 51, pp. 298–306, Oct. 2013.

[74] P. Chittora, A. Singh, and M. Singh, "Application of self tuning filter for power quality improvement in three-phase-three-wire distorted grid system," in *2017 7th International Conference on Power Systems (ICPS)*, pp. 313–318, Dec. 2017.

[75] T.-F. Wu, H.-C. Hsieh, C.-W. Hsu, and Y.-R. Chang, "Three-Phase Three-Wire Active Power Filter With D–$\sum$ Digital Control to Accommodate Filter-Inductance Variation," *IEEE Journal of Emerging and Selected Topics in Power Electronics*, vol. 4, pp. 44–53, Mar. 2016.

[76] N. K. Bett, C. C. Maina, and P. K. Hinga, "New Approach for Design of Shunt Active Power Filter for Power Quality Improvement in a Three Phase Three Wire System," in *2020 IEEE PES/IAS PowerAfrica*, pp. 1–4, Aug. 2020.

[77] L. Zhang, H. Yang, K. Wang, Y. Yuan, Y. Tang, and W. K. Loh, "Design methodology for three-phase four-wire T-type inverter with neutral inductor," *CPSS Transactions on Power Electronics and Applications*, vol. 6, pp. 93–105, Mar. 2021.

[78] Y. Hoon, M. A. A. M. Zainuri, A. S. Al-Ogaili, A. N. Al-Masri, and J. Teh, "Active Power Filtering Under Unbalanced and Distorted Grid Conditions Using Modular Fundamental Element Detection Technique," *IEEE Access*, vol. 9, pp. 107502–107518, 2021.

[79] S. Jiao, K. Rajashekara, R. K. Potti, L. Ben-Brahim, and A. Gastli, "A Double Reduced Order Generalized Integrator based Algorithm for Control of Four-leg Converter to Enhance Power Quality," in *2019 IEEE Energy Conversion Congress and Exposition (ECCE)*, pp. 4293–4298, Sept. 2019. ISSN: 2329-3748.

[80] S. Jiao, K. R. Ramachandran Potti, K. Rajashekara, and S. K. Pramanick, "A Novel DROGI-Based Detection Scheme for Power Quality Improvement Using Four-Leg Converter Under Unbalanced Loads," *IEEE Transactions on Industry Applications*, vol. 56, pp. 815–825, Jan. 2020.

[81] A. Viatkin, M. Hammami, G. Grandi, and M. Ricco, "Analysis of a Three-Phase Four-Leg Front-End Converter for EV Chargers with Balanced and Unbalanced Grid Currents," in *IECON 2019 - 45th Annual Conference of the IEEE Industrial Electronics Society*, vol. 1, pp. 3442–3449, Oct. 2019. ISSN: 2577-1647.

[82] D. Daftary and M. T. Shah, "Design and Analysis of Hybrid Active Power Filter for Current Harmonics Mitigation," in *2019 IEEE 16th India Council International Conference (INDICON)*, pp. 1–4, Dec. 2019. ISSN: 2325-9418.

[83] N. C. Sai Sarita, S. Suresh Reddy, and P. Sujatha, "Control strategies for power quality enrichment in Distribution network using UPQC," *Materials Today: Proceedings*, July 2021.

[84] V. D. Bacon, S. A. O. da Silva, and J. M. Guerrero, "Multifunctional UPQC operating as an interface converter between hybrid AC-DC microgrids and utility grids," *International Journal of Electrical Power & Energy Systems*, vol. 136, p. 107638, Mar. 2022.

[85] R. Wankar and N. T. Pathan, "Power quality improvement by using active power filter and STATCOM of renewable power distribution system," in *ICDSMLA 2019* (A. Kumar, M. Paprzycki, and V. K. Gunjan, eds.), Lecture Notes in Electrical Engineering, pp. 1523–1538, Springer.

[86] B. Bhattacharya and A. K. Chakraborty, "Mathematical vector quantity modulated three phase four leg inverter," in *Information Systems Design and Intelligent Applications* (S. C. Satapathy, J. K. Mandal, S. K. Udgata, and V. Bhateja, eds.), Advances in Intelligent Systems and Computing, pp. 383–393, Springer India.

[87] S. Shamshul Haq, D. Lenine, and S. V. N. L. Lalitha, "Performance analysis of shunt and hybrid active power filter using different control strategies for power quality improvement," in *Emerging Trends in Electrical, Communications and Information Technologies* (K. R. Attele, A. Kumar, V. Sankar, N. V. Rao, and T. H. Sarma, eds.), Lecture Notes in Electrical Engineering, pp. 405–413, Springer.

[88] S. Das, D. Chatterjee, and S. K. Goswami, "An improved reactive power compensation scheme for unbalanced four wire system with low harmonic injection using SVC," in *Modelling and Simulation in Science, Technology and Engineering Mathematics* (S. Chattopadhyay, T. Roy, S. Sengupta, and C. Berger-Vachon, eds.), Advances in Intelligent Systems and Computing, pp. 119–131, Springer International Publishing.

[89] R. K. Chauhan, J. P. Pandey, and M. Hasan, "Comparative performance of the various control techniques to mitigate the power quality events using UPQC," in *Advanced Computational and Communication Paradigms* (S. Bhattacharyya, T. Gandhi, K. Sharma, and P. Dutta, eds.), Lecture Notes in Electrical Engineering, pp. 31–40, Springer.

[90] K. Sozański, "Selected active power filter control algorithms," in *Digital Signal Processing in Power Electronics Control Circuits* (K. Sozański, ed.), Power Systems, pp. 199–275, Springer.

[91] S. Echalih, A. Abouloifa, I. Lachkar, J. M. Guerrero, Z. Hekss, and F. Giri, "Hybrid automaton-fuzzy control of single phase dual buck half bridge shunt active power filter for shoot through elimination and power quality improvement," *International Journal of Electrical Power & Energy Systems*, vol. 131, p. 106986, 10 2021.

[92] A. Ghamri, T. Mahni, M. Benchouia, K. Srairi, and A. Golea, "Comparative study between different controllers used in three-phase four-wire shunt active filter," *Energy Procedia*, vol. 74, pp. 807–816, 8 2015.

[93] M. Ucar and E. Ozdemir, "Control of a 3-phase 4-leg active power filter under non-ideal mains voltage condition," *Electric Power Systems Research*, vol. 78, pp. 58–73, 1 2008.

[94] T. Mahni, M. T. Benchouia, k. Srairi, A. Ghamri, and A. Golea, "Three-phase For-wire Shunt Active Filter with Unbalanced Loads," *Energy Procedia*, vol. 50, pp. 528–535, Jan. 2014.

[95] P. Poure, P. Weber, D. Theilliol, and S. Saadate, "Fault tolerant control of a three-phase three-wire shunt active filter system based on reliability analysis," *Electric Power Systems Research*, vol. 79, pp. 325–334, Feb. 2009.

[96] M. S. Hassan, A. Abdelhakim, M. Shoyama, and G. M. Dousoky, "On-the-analysis and reduction of common-mode voltage of a single-stage inverter through control of a four-leg-based topology," *International Journal of Electrical Power & Energy Systems*, vol. 127, p. 106710, May 2021.

[97] D. Li, T. Wang, W. Pan, X. Ding, and J. Gong, "A comprehensive review of improving power quality using active power filters," *Electric Power Systems Research*, vol. 199, p. 107389, Oct. 2021.

[98] M. Dellahi, H. Maker, G. Botella, E. Alameda-Hernandez, and A. Mouhsen, "Three-phase four-wire shunt active power filter based on the SOGI filter and Lyapunov function for DC bus control," *International Journal of Circuit Theory and Applications*, vol. 48, no. 6, pp. 887–905, 2020.

[99] L. Bin and T. Minyong, "Control Method of the Three-Phase Four-Leg Shunt Active Power Filter," *Energy Procedia*, vol. 14, pp. 1825–1830, Jan. 2012.

[100] A. K. Mishra, P. K. Ray, A. K. Patra, R. K. Mallick, S. R. Das, and R. Agrawal, "Harmonic and reactive power compensation using hybrid shunt active power filter with fuzzy controller," in *Intelligent and Cloud Computing* (D. Mishra, R. Buyya, P. Mohapatra, and S. Patnaik, eds.), Smart Innovation, Systems and Technologies, pp. 533–545, Springer.

[101] R. Sinha and R. Raman, "High frequency resonant inverter with shunt active power filter for harmonic compensation," in *Electronic Systems and Intelligent Computing* (P. K. Mallick, P. Meher, A. Majumder, and S. K. Das, eds.), Lecture Notes in Electrical Engineering, pp. 317–327, Springer.

[102] A. S. Kumar and K. Prakash, "SRF control algorithm for five-level cascaded h-bridge d-STATCOM in single-phase distribution system," in *Artificial Intelligence and Evolutionary Computations in Engineering Systems* (S. S. Dash, C. Lakshmi, S. Das, and B. K. Panigrahi, eds.), Advances in Intelligent Systems and Computing, pp. 229–238, Springer.

[103] M. Stork and D. Mayer, "Reactive power compensation in energy transmission systems with sinusoidal and nonsinusoidal currents," in *Reactive Power Control in AC Power Systems: Fundamentals and Current Issues* (N. Mahdavi Tabatabaei, A. Jafari Aghbolaghi, N. Bizon, and F. Blaabjerg, eds.), Power Systems, pp. 137–190, Springer International Publishing.

[104] J. Jayachandran and R. Murali Sachithanandam, "ANN based controller for three phase four leg shunt active filter for power quality improvement," *Ain Shams Engineering Journal*, vol. 7, pp. 275–292, Mar. 2016.

[105] A. Tamer, L. Zellouma, M. T. Benchouia, and A. Krama, "Adaptive linear neuron control of three-phase shunt active power filter with anti-windup PI controller optimized by particle swarm optimization," *Computers & Electrical Engineering*, vol. 96, p. 107471, Dec. 2021.

[106] E. M. Suhara and M. Nandakumar, "Analysis of hysteresis current control techniques for three phase pwm rectifiers," in *2015 IEEE International Conference on Signal Processing, Informatics, Communication and Energy Systems (SPICES)*, pp. 1–5, 2015.

[107] O. Lopez-Santos, D. S. Dantonio, F. Flores-Bahamonde, and C. A. Torres-Pinzón, "Chapter 2 - Hysteresis control methods," in *Multilevel Inverters* (E. Kabalcı, ed.), pp. 35–60, Academic Press, Jan. 2021.

[108] M. Elbar, K. Aliouane, and I. Merzouk, "3 Dimensional hysteresis PWM techniques for 3-Phase 4-Wire SAPFs under unbalanced conditions by using p-q-r theory," *The International Conference on Electrical Engineering*, vol. 6, pp. 1–12, May 2008. Publisher: Military Technical College.

[109] J. Zhou, X.-j. Wu, Y.-w. Geng, and P. Dai, "Simulation Research on a SVPWM Control Algorithm for a Four-Leg Active Power Filter," *Journal of China University of Mining and Technology*, vol. 17, pp. 590–594, Dec. 2007.

[110] M. Elbar, I. Merzouk, M. M. Rezaoui, and N. Bessous, "Three-Dimensional Pulse Width Modulation Techniques for Three-Phase Four Leg Voltage Source Converters," *Algerian Journal of Signals and Systems*, vol. 5, pp. 153–158, Sept. 2020.

[111] A. Chebabhi, M. K. Fellah, A. Kessal, and M. F. Benkhoris, "A new balancing three level three dimensional space vector modulation strategy for three level neutral point clamped four leg inverter based shunt active power filter controlling by nonlinear back stepping controllers," *ISA Transactions*, vol. 63, pp. 328–342, July 2016.

[112] M.-C. Wong, N.-Y. Dai, J. Tang, and Y.-D. Han, "Theoretical study of 3 dimensional hysteresis PWM techniques," in *The 4th International Power Electronics and Motion Control Conference, 2004. IPEMC 2004.*, vol. 3, pp. 1635–1640 Vol.3, Aug. 2004.